



First-Row Transition Metal-Catalyzed Carbon-Carbon Bond Formation

Buendia, Mikkel Burggraaf

Publication date:
2021

Document Version
Publisher's PDF, also known as Version of record

[Link back to DTU Orbit](#)

Citation (APA):
Buendia, M. B. (2021). *First-Row Transition Metal-Catalyzed Carbon-Carbon Bond Formation*. DTU Chemistry.

General rights

Copyright and moral rights for the publications made accessible in the public portal are retained by the authors and/or other copyright owners and it is a condition of accessing publications that users recognise and abide by the legal requirements associated with these rights.

- Users may download and print one copy of any publication from the public portal for the purpose of private study or research.
- You may not further distribute the material or use it for any profit-making activity or commercial gain
- You may freely distribute the URL identifying the publication in the public portal

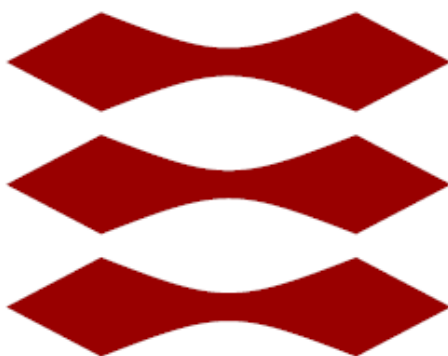
If you believe that this document breaches copyright please contact us providing details, and we will remove access to the work immediately and investigate your claim.

First-Row Transition Metal-Catalyzed Carbon-Carbon Bond Formation

PhD Thesis 2021

Mikkel Burggraaf Buendia

DTU



Supervisors:

Professor Søren Kegnæs

Assistant Professor Søren Kramer

Preface

This thesis represents the work carried out during my PhD studies at the department of chemistry at the Technical University of Denmark (DTU) from August 2018 to August 2021. The work was carried out under the supervision of Professor Søren Kegnæs and Assistant Professor Søren Kramer. A four month external stay at Institut Català d'Investigació Química (ICIQ), Tarragona, Spain was carried out from September 2020 to December 2020 under supervision of Professor Ruben Martin.

The thesis consists of three projects described in four chapters. The first chapter, **1) Introduction**, covers the basic principles of catalysis relevant for the thesis and an introduction to porous organic polymers (POPs). The second chapter, **2) Asymmetric Michael Addition of Malonates to Aliphatic Nitroalkenes**, describes the synthesis of heterogeneous POP catalysts for the asymmetric Michael addition of malonates to aliphatic nitroalkenes. This chapter is based on the publication: **M. B. Buendia**, S. Kegnæs, S. Kramer, *Adv. Synth. Catal.* **2020**, 362, 5506. Experimental details can be found at: DOI: 10.1002/adsc.202000875 under Supporting Information. The third chapter, **3) Copper-Catalyzed Alkynylation of Benzylic C-H Bonds with Alkynyl Boronic Esters**, describes the development of a methodology for the direct C-H alkynylation of 1-alkyl naphthalenes. The work of this project was carried out in collaboration with Jan-Georges J. Balin (former Master student) and Mette E. Andersen (former Master student). The chapter is based on the publication: **M. B. Buendia**, J.-G. J. Balin, M. E. Andersen, Z. Lian, S. Kramer, *Synlett* **2021**, 32, A-E. Experimental details can be found at: DOI: 10.1055/s-0040-1720474 under Supplementary Material. The fourth chapter, **4) Combined Nickel- and Photoredox-Catalyzed Direct C-H Allylic Alkylation**, describes the development of a novel methodology for the direct alkylation of allylic C-H bonds from terminal olefins and alkyl bromides. The concept of the project was developed and initiated at ICIQ, but the experimental work was carried out at DTU with intellectual input from both ICIQ and DTU. This project is in the process towards publication.

Acknowledgment

First and foremost, I would like to thank my supervisor Professor Søren Kegnæs for giving me the opportunity to join his research group and pursue a PhD degree. A special thanks for always ensuring an excellent working environment and giving me the freedom to pursue my own ideas and projects. Additionally, I would like to express my deepest gratitude to my co-supervisor Assistant Professor Søren Kramer for his guidance, sharing his laboratory expertise and always showing an immense interest in my projects. He has made me strive for excellence within chemistry and because of him I have become a much better chemist.

I would like to thank everyone at the center for sustainable chemistry and catalysis (CSC) and especially all the present and former members of Kegnæs's group for making all the time spent at DTU very enjoyable. A special thanks to Niklas R. Bennedsen and Faliu Yang for all the good discussions both scientific and non-scientific and in general, for making all those hours spent in the laboratory so entertaining. I would like to acknowledge everyone helping me with specialized techniques and instruments: Dr. David B. Christensen for doing transmission electron microscopy, Dr. Farnoosh Goodarzi for doing scanning electron microscopy, Dr. Mariusz Kubus for doing single crystal X-ray analysis and analyzing the data and Dr. Kasper Enemark-Rasmussen for measuring solid state NMR and helping with data interpretation.

I would like to thank Professor Ruben Martin for allowing me to join his laboratories at ICIQ despite the strange circumstances caused by COVID-19. I would like to thank everyone in the Martin group for making it an excellent external stay and especially Hongfei Yin, Jessica Giacoboni and Craig Day for making me feel so welcome from the first day.

Lastly, I would like to thank my friends, family and girlfriend for always being good company and for cheering me up when chemistry have been frustrating.

Abstract

Chemistry is fundamental in our society and plays a key role in every aspect of our lives, from our basic needs of food and clothing to life-saving medicine. The essence of organic chemistry and the synthesis of organic molecules like pharmaceuticals lies in the coupling of carbon atoms. The development of metal-catalyzed carbon-carbon bond forming cross-coupling reactions have been an immense advancement within chemistry invaluable for the pharmaceutical industry and society. This was acknowledged in 2010 where the Nobel Prize in chemistry was awarded for the work on cross-coupling reactions. Upgrading existing carbon-carbon bond forming protocols and developing new methodologies are an imperative endeavor for the chemical industry and for the betterment of mankind. This thesis contains three projects. The first project aims at improving an existing catalytic C-C bond forming system by making the catalyst reusable and suitable for continuous flow setups. The last two projects are focused on developing novel C-C forging methodologies via direct C-H functionalization.

In the first project, a chiral nickel(II) bis(diamine) complex was incorporated into a polystyrene matrix without compromising the catalytic properties of the nickel complex. The catalyst effectively catalyzed the asymmetric Michael addition of malonates to nitroalkenes and was easily reused. The catalyst showed good tolerance towards sensitive functional groups, was suitable for a continuous flow setup and obtained a TON almost five times higher than previous reports. To illustrate the relevance of the catalytic system, the protocol was used to synthesize the blockbuster drug Pregabalin in 88% overall yield.

In the second project, a novel methodology for the alkynylation of benzylic C-H bonds was developed. Using copper catalysis in combination with NFSI it was possible to develop a coupling protocol between alkynyl boronic esters and 1-alkyl naphthalenes, with the C-H substrate as the limiting reagent. The protocol showed a good functional group tolerance, however, the C-H source was limited to 1-alkyl naphthalenes. Preliminary mechanistic experiments in combinations with literature points towards a mechanism resembling a radical relay process.

In the third project, a novel methodology for the direct alkylation of allylic C-H bonds was developed. Using a combination of a nickel catalyst and a photocatalyst a protocol for the coupling of alkyl bromides with terminal olefins was developed. The methodology proceeds at benign conditions and exclusively yields the linear product. The protocol is robust towards functional groups and even densely functionalized biological derivatives could be utilized. A preliminary mechanistic investigation indicated that the photocatalyst function as a SET species which catalytic cycle is intertwined with the catalytic cycle of nickel.

Resumé

I det moderne samfund er kemi fundamentalt. Det spiller en essentiel rolle i alle aspekter af vores liv, fra basale nødvendigheder som tøj og mad til livsvigtigt medicin. Essensen af organisk kemi og syntese af organiske molekyler som medicin er baseret på koblingen af karbon atomer. Opfindelsen af metal katalyseret karbon krydskoblings reaktioner har været en enorm fremgang inden for kemien som har været uvurderlig for den farmaceutiske industri og samfundet. I 2010 blev dette anerkendt da Nobel Prisen for kemi netop blev uddelt på baggrund af udviklingen af metal katalyseret krydskoblings reaktioner. Udviklingen af nye katalytiske protokoller til at lave C-C bindinger og opgraderingen af eksisterende metoder er ekstremt vigtige projekter der vil medføre forbedringer til den kemiske industri og til menneskeligheden som helhed. Denne afhandling indeholder tre projekter. Det første projekter bestræber sig på at forbedre en eksisterende katalytisk C-C bindingsdannende metode ved at gøre katalysatoren genanvendelig samt at gøre den egnet til kontinuerligt flow. De sidste to projekter omhandler udviklingen af nye katalytiske protokoller til C-C dannelse ved at funktionalisere C-H bindinger direkte.

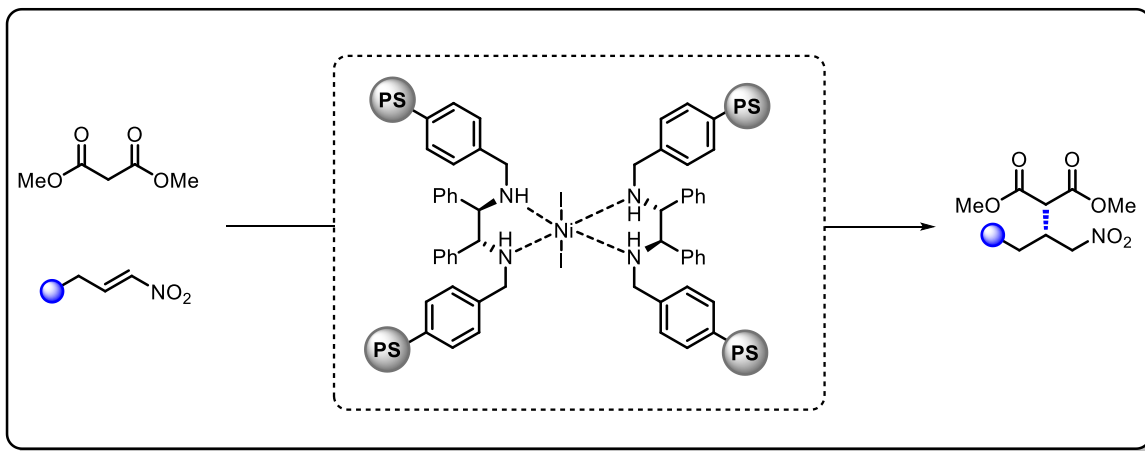
I det første projekt er et nikkel(II) bis(diamine) kompleks blevet inkorporeret i en polystyren matrix uden at påvirke nikkel kompleksets katalytiske egenskaber. Katalysatoren katalyserede den asymmetriske Michael addition af malonater til alifatiske nitroalkener meget effektivt og kunne nemt genanvendes. Katalysatoren var robust overfor sensitive funktionelle grupper, den kunne anvendes i et kontinuerligt flow system og et TON næsten fem gange højere end tidligere rapporter var opnået. For at illustrere systemets relevans blev det brugt til at syntetisere blokbuster medicinen Pregabalin i 88% overordnet udbytte.

I det andet projekt er en ny metode for alkynyleringer af benzylliske C-H bindinger blevet udviklet. Ved at benytte kopper katalyse i kombination med NFSI har det været muligt at udvikle en protokol der kan koble alkynyl borestere og 1-alkyl naphthalener med C-H kilden som den begrænsende kilde. Proceduren er tolerant overfor mange funktionelle grupper, men desværre kunne kun 1-alkyl naphthalener benyttes som C-H kilde. Indledende mekanistiske studier i kombinationer med litteraturen antyder at mekanismen følger en radikal-relay proces.

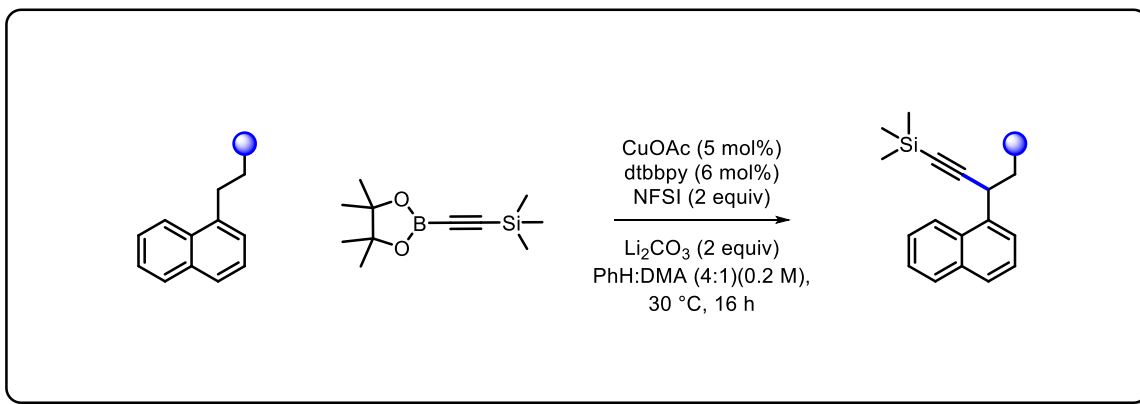
I det sidste projekt er en ny metode for alkyleringen af allylliske C-H bindinger blevet udviklet. Ved at bruge en kombination af nikkel og fotokatalyse er det lykkedes at udvikle en metode til at koble alkyl bromider og terminale alkener. Metoden foregår under milde betingelser og giver udelukkende det lineære produkt. Proceduren er robust overfor funktionelle grupper og kan benyttes på derivater af biologiske molekyler der indeholder mange funktionelle grupper. En indledende mekanistisk undersøgelse indikerer at fotokatalysatoren fungerer som en én elektron overførsel specie hvis katalytiske cyklus er forbundet med nikkels katalytiske cyklus.

Graphical Abstract

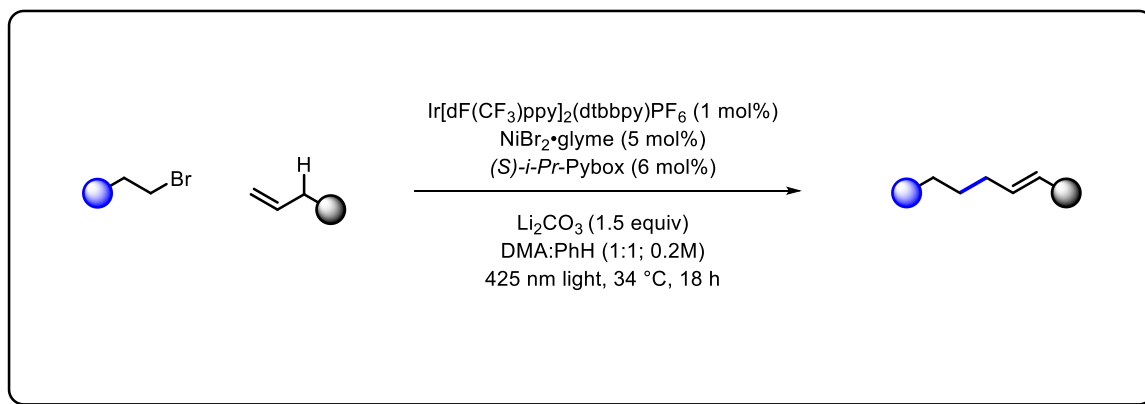
Chapter 2: Asymmetric Michael Addition of Malonates to Aliphatic Nitroalkenes.



Chapter 3: Copper-Catalyzed Alkynylation of Benzylic C-H bonds with Alkynyl Boronic Esters.



Chapter 4: Combined Nickel- and Photoredox-Catalyzed Direct C-H Allylic Alkylation.



Abbreviations

18-crown-6	1,4,7,10,13,16-Hexaoxacyclooctadecane	GC	Gas chromatography
acac	Acetylacetone	HAT	Hydrogen atom transfer
AIBN	Azobisisobutyronitrile	HPLC	High-performance liquid chromatography
BDE	Bond dissociation energy	ICP	Inductively coupled plasma
BINAP	(2,2'-Bis(diphenylphosphino)-1,1'-binaphthyl)	SPS	Solvent purification system
COD	1,5-Cyclooctadiene	MS	Mass spectrometry
BIOX	2,2'-Bis(2-oxazoline)	NFSI	<i>N</i> -Fluorobenzenesulfonimide
BOX	2,2'-Alkylbis(2-oxazoline)	NMR	Nuclear magnetic resonance
Bpy	2,2'-Bipyridine	Phen	Phenanthroline
CFL	Compact fluorescent lamp	POPs	Porous organic polymers
DCE	1,2-Dichloroethane	Pybox	2,6-Bis(4,5-dihydrooxazol-2-yl)pyridine
DIPEA	<i>N,N</i> -Diisopropylethylamine	SCE	Saturated calomel electrode
DMA	Dimethylacetamide	TBAB	Tetrabutylammonium bromide
DMF	Dimethylformamide	mCPBA	<i>meta</i> -Chloroperoxybenzoic acid
DMSO	Dimethyl sulfoxide	TEM	Transmission electron microscopy
DPEN	1,2-Diphenylethylenediamine	SEM	Scanning electron microscopy
dppe	1,2-Bis(diphenylphosphino)ethane	TEMPO	2,2,6,6-Tetramethylpiperidine 1-oxyl
dtbbpy	4,4'-Di- <i>tert</i> -butyl-2,2'-dipyridyl	Terpy	Terpyridine
DVB	Divinylbenzene	TES	Triethylsilyl
E _a	Activation energy	THF	Tetrahydrofuran
<i>ee</i>	Enantiomeric excess	TIPS	Triisopropylsilyl
EPR	Electron paramagnetic resonance	DMPS	Dimethylphenylsilyl
equiv	Equivalent	TMS	Trimethylsilyl
FID	Flame ionization detector	TBDMS	<i>tert</i> -Butyldimethylsilyl
		TOF	Turnover frequency

TON	Turnover number
XPS	X-ray photoelectron spectroscopy
ΔG	Gibbs free energy

Table of Contents

Preface	i
Acknowledgment	iii
Abstract.....	v
Resumé	vii
Graphical Abstract	ix
Abbreviations	xi
Table of Contents.....	xiii
1) Introduction	1
1.1 Introduction to Catalysis.....	1
1.2 Transition Metal Catalysis in Organic Chemistry	3
1.3 Direct C-H functionalization	9
1.4 Asymmetric Catalysis	10
1.5 Porous Organic Polymers.....	12
1.6 Continuous Flow Chemistry	16
1.7 References	18
2) Asymmetric Michael Addition of Malonates to Aliphatic Nitroalkenes	21
2.1 Background	21
2.2 Synthesis of NiL ₂ -POPs	25
2.3 Optimization	29
2.4 Characterization of NiL ₁ -POP	31
2.5 Recycling	34
2.6 Scope.....	36
2.7 Applications.....	40
2.8 Conclusion.....	40
2.9 Outlook – POPs	41
2.10 References	42
3) Copper-Catalyzed Alkynylation of Benzylic C-H bonds with Alkynyl Boronic Esters	44
3.1 Background	44
3.2 Project Initiation	47
3.3 Optimization	47
3.4 Scope.....	52

3.5	Investigation of the Reaction Mechanism	54
3.6	Applications.....	57
3.7	Conclusion and Outlook.....	58
3.8	References	59
4)	Combined Nickel- and Photoredox-Catalyzed Direct C-H Allylic Alkylation	60
4.1.	Introduction to Photoredox Catalysis in Organic Chemistry	60
4.2.	Background	61
4.3.	Project Initiation and Optimization.....	65
4.4.	Scope.....	69
4.5.	Discussion.....	72
4.6.	Conclusion and Perspective	82
4.7.	Experimental	83
4.8.	References	93
5)	Final Remarks.....	95
6)	Appendix	96
6.1	Publications.....	96
6.2	Co-Author statements.....	97

1) Introduction

1.1 Introduction to Catalysis

The development of catalysis have been one of the most crucial advancements within chemistry necessary for the development of modern society. The most famous example, the Haber-Bosch process for the formation of ammonia, used in the agrochemical industry for fertilizers, helps feed half of the world's population.^[1] Moreover, it is estimated that the chemical industry contributes 10% of the total world trade and 90% of chemicals are produced with the use of a catalyst.^{[2][3]}

The use of catalysis dates back many centuries (in fermentation process for wine and beer), however, at that point the principles of catalysis were most likely not understood. The science of catalysis began 200 years ago, but the first definition of a catalyst, which is still relevant today, came in 1896 by Wilhelm Ostwald: *"a catalyst accelerates a chemical reaction without affecting the position of the equilibrium"*.^[2] Essentially, this means that a catalyst cannot alter the thermodynamics of a reaction, only increase the rate of the reaction. Typically, a catalyst works by altering the chemical mechanism providing an alternative reaction pathway with a decreased activation energy (Figure 1.01). This allows reactions to occur much faster, more importantly it enables countless new reactions, which would never otherwise happen on a reasonable timescale.

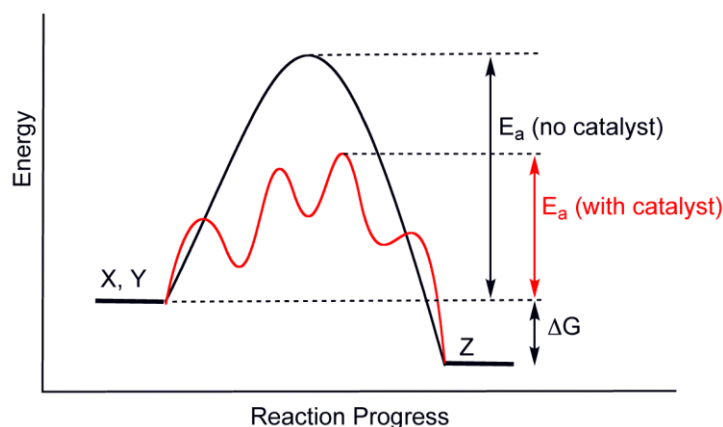


Figure 1.01. Illustration of generic energy profile for a non-catalyzed reaction (black) and a catalyzed reaction (red).^[4]

While Ostwald's definition is still accurate, it does not mention that a catalyst, in principle, is not consumed during the reaction. Although the catalyst itself takes part in the reaction it is regenerated after the desired reaction has taken place. When the catalyst is reformed, it has carried out one catalytic cycle, the amount of catalytic cycles, known as "turnover numbers" (TON), is an important evaluation parameter. A high TON indicates that a very small amount of catalyst can deliver a huge amount of product, meaning little catalyst is required.

As awareness of the anthropogenic consequences of the industrialization grew, chemist turned their attention toward more sustainable practices. Especially during the 1990's a new philosophy flourished, evolving around benign and non-hazardous processes.^[5] With the seminal publication in 1998 "Green Chemistry: Theory and Practice" by Anastas and Warner the discipline became well defined and coined as

“Green Chemistry”.^[6] Within the definition twelve principles of Green Chemistry were formulated. Catalysis plays a crucial role in many of these principles;

- *“It is better to prevent waste than to treat or clean up waste after it is formed.” (1. Prevention)*
- *“Synthetic method should be designed to maximize the incorporation of all materials used in the process into the final product.” (2. Atom Economy)*
- *“Energy requirements should be recognized for their environmental and economic impacts and should be minimized. Synthetic methods should be conducted at ambient temperature and pressure.” (6. Design for Energy Efficiency)*
- *“Catalytic reagents (as selective as possible) are superior to stoichiometric reagents.” (9. Catalysis)*

The importance of Green Chemistry is undeniably still growing and research within the field of catalysis remains imperative.

Catalysis are typically divided into two main fields; heterogeneous catalysis and homogeneous catalysis. In heterogeneous catalysis the active phase of the catalyst is in another phase than the reaction media, the catalyst is typically a solid in a gaseous or liquid reaction media. This inherent property provides one of the key benefits of heterogeneous catalysis, its ease of recovery and recycling. In homogeneous catalysis, the active phase of the catalyst is in the same phase as the reaction media, typically a dissolved transition metal complex in a liquid media.^{[2][7]}

Heterogeneous catalysts typically consist of a metal(s) or a metal oxide(s) immobilized on a support material. Many support materials exist, but common support materials include silica, metal oxides and active carbon. Heterogeneous catalysis is widely applied within the chemical industry especially for the synthesis of bulk chemicals. The conditions are typically extremely harsh and often limited to the production of rather simple molecules. Despite the impressive success of heterogeneous catalysis within industrial chemistry, they typically lack the selectivity required for the synthesis of more complex molecules (fine chemicals).^[7]

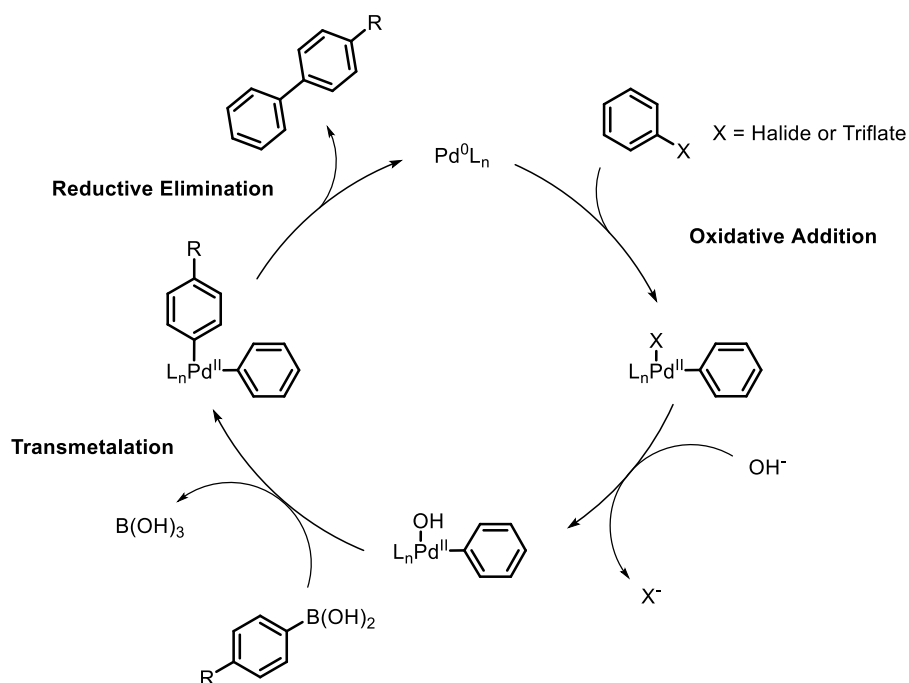
While homogeneous catalysis falls short in stability and recyclability, it shines in selectivity, activity and analyzability. A homogeneous catalyst typically consist of a transition metal and some surrounding ligands forming the active metal complex. As the ligands heavily influence the electronic and sterically nature of the metal complex the activity of the catalysts can be tuned by design of ligands. Another major advantage is that homogeneous catalysts are much easier to observe spectroscopically which can provide crucial mechanistic insights making optimization easier, partly owing to the uniformity of homogeneous catalysts (compared to heterogeneous catalysts).^[8]

Industrially, homogeneous catalysis find some application within the bulk chemical industry, e.g. the production of acetic acid via the Monsanto Process and oxidation of ethene to acetaldehyde via the Wacker process. It finds multiple uses within the fine chemical industry, for the synthesis of specialty polymers, fragrances, agrochemicals and pharmaceuticals. The development of homogeneous catalysis have especially been crucial for the development of asymmetric catalysis.^[8]

1.2 Transition Metal Catalysis in Organic Chemistry

Formation of new C-C bonds is the essence of organic chemistry. One of the first examples of C-C bond formation utilizing transition metals dates back to the beginning of the 20th century, where Ullmann discovered that copper could facilitate the coupling of aryl halides.^[9] Since Ullmann's ground-breaking discovery an immense advancement has been undertaken, and especially within the last 20 years the power of transition metal catalysis has become evident. Since the new millennium the Nobel Prize in chemistry has been awarded for transition metal catalysis; in 2001 when Karl B. Sharpless, Ryoji Noyori and William S. Knowles shared the Nobel Prize for their work in asymmetric transition metal catalysis, in 2005 when Yves Chauvin, Robert H. Grubbs and Richard R. Schrock shared the Prize for their work in olefin metathesis and in 2010 when Richard F. Heck, Ei-Ichi Negishi and Akira Suzuki were awarded the Prize for their work on palladium catalyzed cross-coupling reactions in organic synthesis.^[10]

These reactions have become fundamental in any organic chemist's toolbox, especially the Suzuki-Miyaura cross-coupling reaction has proven effective within medicinal chemistry, where it is the most used carbon-carbon forming reaction.^[11]

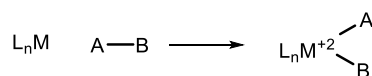


Scheme 1.01. The Suzuki-Miyaura cross-coupling reaction mechanism.

Within metal catalyzed cross-coupling reactions the mechanism mainly consists of three mechanistic steps: oxidative addition, transmetalation and reductive elimination (Scheme 1.01). Another important reaction within transition metal catalysis is “migratory insertion”, however, the work in this thesis do not include any examples of migratory insertion.

Oxidative Addition

Within catalysis, the first substrate-metal constructing step is typically the oxidative addition. The oxidative addition step cleaves a bond from an organic or main group molecule and forms two new metal – ligand bonds, formally oxidizing the metal (Scheme 1.02). One of the most common examples within organic chemistry is the formation of Grignard reagents. In such mononuclear examples the oxidation state of the metal is formally increased by two, however, oxidative addition also occurs with multinuclear metal complexes, in the cases of binuclear examples the oxidation state of each metal center is increased by one. Reagents that undergo oxidative addition ranges from nonpolar molecules like H₂ to highly polar molecules like alkyl halides – and everything in-between.

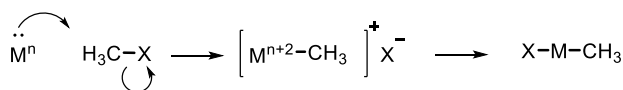


Scheme 1.02. General oxidative addition.

The nature of the oxidative addition makes electron-rich metals more inclined to undergo oxidative addition, this is also true for less-hindered metal centers. Generally, for a metal to undergo oxidative addition, the metal-center must be coordinatively unsaturated and contain a maximum d-electron count of 16. While the product of an oxidative addition is straightforward to predict, the mechanistic route is less trivial. Various mechanistic pathways have been disclosed, however, they can be categorized into three main mechanisms; S_N2, one-electron mechanisms and concerted pathways.^{[12][13]}

S_N2 Pathway

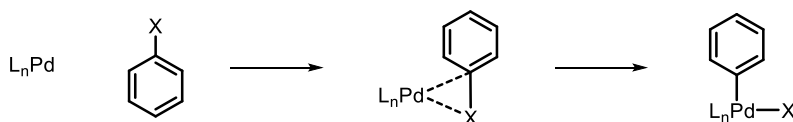
The S_N2 pathway can occur with highly polar substrates like alkyl halides and is similar to a traditional organic S_N2 reaction (Scheme 1.03). Evidence for the oxidative addition S_N2 mechanism follows the same principles of a typical S_N2 mechanism; the carbon configuration is inverted, the reaction is more rapid in polar solvents and the kinetics are of first order with respect to both metal and electrophile (second order overall). Additionally, examples following this pathway yields the trans stereochemistry (of the metal complex) as the kinetic product, which is inconsistent with a concerted pathway, and are unaffected by radical traps. This pathway is typically encountered with palladium(0) and alkyl halides.^[14–16]



Scheme 1.03. Oxidative addition via an S_N2 pathway.

Concerted Oxidative Additions

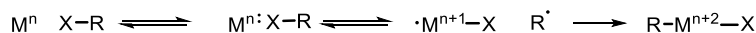
While S_N2 and one-electron pathways typically occurs with very polar substrates; substrates with little polarity and Ar-X substrates unable to undergo S_N2 reactions typically undergo oxidative addition via concerted pathways. One of the most studied cases is the oxidative addition of aryl halides to palladium(0) as it is a crucial step in the cross-coupling reactions. These substrates undergo oxidative addition to palladium(0) via a concerted three-centered transition state (Scheme 1.04).^[13]



Scheme 1.04. Oxidative addition via a concerted pathway.

One-Electron Pathways

The reagents undergoing oxidative addition via the one-electron pathway are similar to those following the S_N2 mechanism. However, metals that are prone to undergo one-electron oxidations are more susceptible towards radical processes. There are multiple types of one-electron pathways; inner-sphere, outers-sphere, radical chain and atom abstraction and combination. The inner-sphere process requires a vacant coordination site and the oxidation potential of the metal needs to be sufficient to reduce the electrophile (Scheme 1.05).

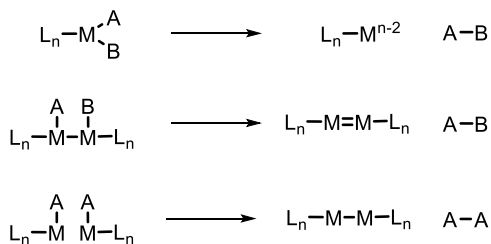


Scheme 1.05. Oxidative addition via an inner-sphere radical pathway.

The outer-sphere pathways resembles the inner-sphere process, however, the initial electron transfer does not require prior coordination. This pathway is more likely with bulky electrophiles and metals without vacant coordination sites. Additionally, radical chain mechanisms and “atom abstraction and combination of the resulting radical with a second metal” have also been reported.^[13,17–19]

Reductive Elimination

In catalytic reactions, reductive elimination is typically the product-forming step. It is, simply put, the opposite process of the oxidative addition step. Here two metal-ligand bonds are broken to form a ligand-ligand bond formally reducing the metal(s) with two electrons (Scheme 1.06).

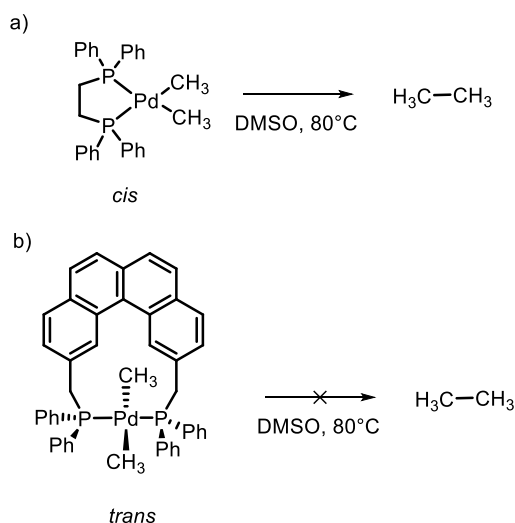


Scheme 1.06. Three types of reductive eliminations.

As the process is similar to the oxidative addition, albeit, in the opposite direction, similar transition states and pathways exist, the process can proceed via stepwise radical and/or ionic species or by concerted three-centered transition states. The predisposition towards reductive elimination is governed by the electronic and sterically nature of the metal complex and is often opposite to those promoting oxidative addition. Thus, reductive elimination is promoted in more electron poor metal complexes. The use of bulky ancillary ligands correspondingly increase the rate of reductive elimination, as more bulky ancillary ligands results in more strain release. In regard to transition metals; first row metals tend to undergo reductive elimination faster than second row metals. This is ascribed to the smaller ionic radius of first row metals leading to more strained complexes, consequently resulting in more strain release upon reductive elimination. Second-row metals react faster than third-row metals due to their, relative to third-row metals, weak metal-ligand bonds.^[20]

The type of bond formed also heavily influences the ease of reductive elimination. Almost all metals undergo reductive elimination to form C-H bonds. However, species undergoing reductive elimination to

forge C-C bonds is less abundant. The challenge does not arise from a smaller thermodynamic driving force, but rather from a higher-energy transition state. This arises, as the M-C bond, in order to obtain appropriate orbital overlap for bond formation, must distort away from the preferred orientation leading to steric repulsion between the alkyl substituents and the ancillary ligands. It has been shown that most reductive eliminations forming C-C bonds proceeds via a concerted pathway, which also points to the need for appropriate orbital overlap. A consequence hereof, is the need for correct geometry, namely the two carbon ligands should be located cis (Scheme 1.07).^[20]

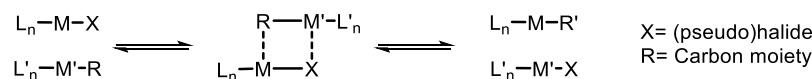


Scheme 1.07. Reductive elimination of palladium species in *cis* (a) and *trans* (b).

Within C-C formation the reductive elimination rates also vary significantly between sp^3 - sp^3 and sp^2 - sp^2 formation. For group 10 metals, reductive elimination tend to be more rapid for sp^2 carbons, as metal (group 10) aryl/vinyl complexes are more stable than the corresponding metal alkyl complex this is not a thermodynamic effect. This could be ascribed to the previously described distortion being more pronounced for sp^3 -carbons as they have more substituents, however, the nature of the different orbital hybridizations could also have an impact. The more “s” character the orbital hybridization has, the less “direction” it will possess resulting in better total overlap in a three-centered concerted transition state.^{[19][20]}

Transmetalation

In most cross-coupling reactions transmetalation plays a vital role. It occurs after the oxidative addition setting up the complex to release the desired product via reductive elimination. In these reactions, the transmetalation typically involves the transfer of an organic moiety (typically aryl, vinyl or alkyl) from a main group metal (and group 12) to the transition metal complex in exchange for a (pseudo)halide (Scheme 1.08).

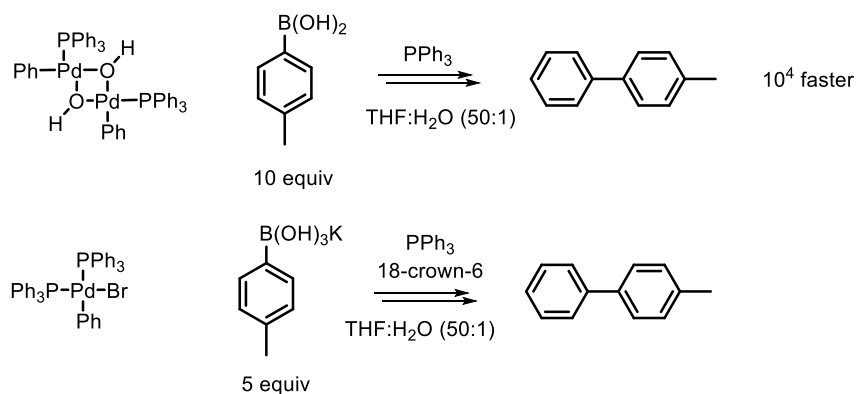


Scheme 1.08. Illustration of a transmetalation reaction.

This process does not involve any change in coordination or oxidation number of either metal and is thought to proceed as a metathesis type reaction. The reaction is an equilibrium, however, this is rarely a

concern in catalytic coupling reactions as the organic fragment bearing species is often used in large quantities relative to the transition metal (the catalyst) pushing the equilibrium to the right. The nature of the catalytic cycles further pushes the equilibrium to the right as reductive elimination follows the transmetalation effectively removing the “product”. Thermodynamically, the equilibrium is dependent on the two metal-(pseudo)halide bonds and the two metal-carbon bonds; a general rule suggest that if the metal transferring the organic moiety is more electropositive than the metal receiving it, the equilibrium is pushed towards product formation. This is generally the case if the transmetalation “metal” is Mg or Zn (e.g. used in Kumada and Negishi couplings, respectively), however, it is generally not the case for boron species, which have become one of the most successful transmetalation species in cross-coupling reactions.^[22]

For boron species, it is often required to add an activator in form of an inorganic base salt (or fluoride salt). In the case of the Suzuki-Miyaura coupling the addition of a weak inorganic base (typically carbonate or phosphate) and the presence of water results in a more activated boronic species, a trihydroxyborate species, and/or a palladium hydroxide species rather than a palladium halide species. Hartwig and co-workers have via stoichiometric experiments illustrated that the transmetalation occurs four orders of magnitudes faster between palladium hydroxide species and a neutral boronic acid than between the corresponding palladium bromide species and a trihydroxy borate species. Suggesting that the transmetalation mainly proceeds via a neutral boronic acid species and a hydroxyl palladium species (Scheme 1.09).^[23]

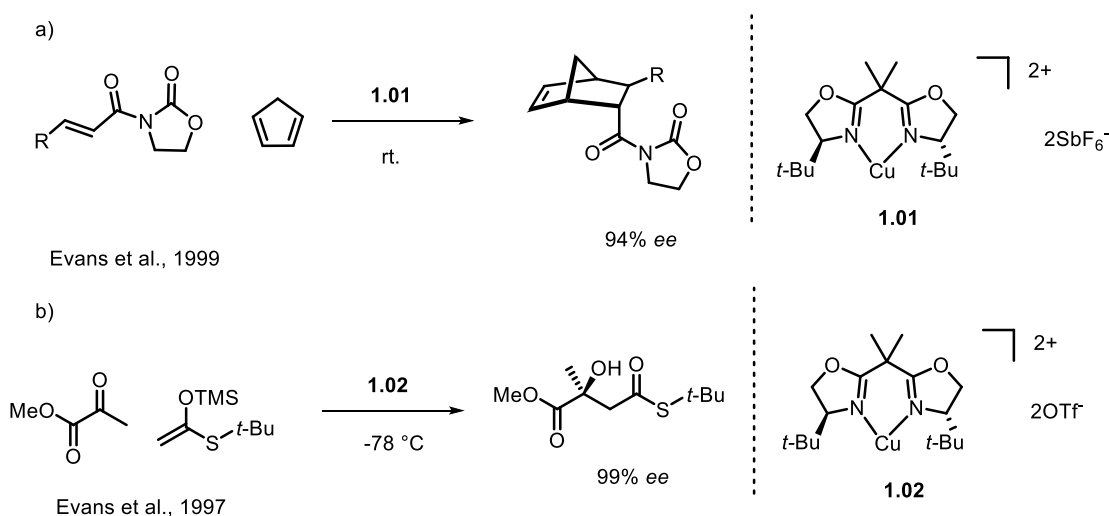


Scheme 1.09. Different transmetalation pathways in the Suzuki-Miyaura cross-coupling.^[23]

Lewis Acid Catalysis

Transition metals also find wide applications as Lewis acid catalysts. Lewis acid catalysis is well known in the chemical industry, especially from the petrochemical industry, which heavily employ Lewis acid catalysts in the form of zeolites. Within organic chemistry Lewis acid catalysts are often used in many common reaction types; Diels-Alder, Friedel-Crafts, Michael additions etc. Common Lewis acids include AlCl_3 , BF_3 , ZnCl_2 etc.^[24]

Transition metals find use as Lewis acid catalysts in combination with chiral ligands where stereogenic control of the product can be achieved (Scheme 1.10).^[25–27]



Scheme 1.10. Examples of asymmetric transition metal Lewis acid catalyzed reactions.

Towards Earth-Abundant Transition Metal Catalysts

The success of transition metal catalysis in organic chemistry have been built on rare and expensive metals; palladium (cross-coupling reactions), iridium and ruthenium (asymmetric hydrogenation and metathesis). With an increasing world population and a limited amount of resources, an interest for more earth-abundant metals have sparked.

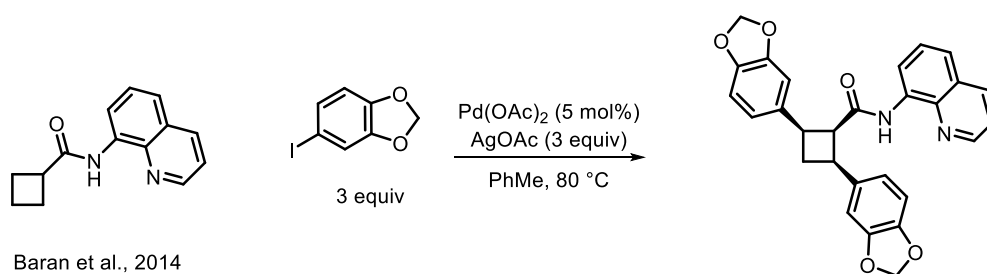
Especially the interest in nickel and copper as catalysts in organic coupling reactions have increased rapidly since the millennium change.^[28] Nickel have proven capable of catalyzing the same type of coupling reactions developed with palladium, however, nickel is more than a cheap abundant substitute for palladium. The chemistry of nickel is very different to that of palladium. Nickel is accessible in oxidation states ranging from 0 to IV, making it susceptible for single electron (radical) pathways. Additionally, it has lower electronegativity, ionic radius and reduction potential. These features contribute to nickel being less prone to β -elimination possibly leading to nickel's greater success in $C(sp^3)$ - $C(sp^3)$ cross-couplings.^[29] Currently, nickel is the main choice of metal in the rapidly developing field of photoredox catalysis, which is the focus of chapter four.

Like nickel, the chemistry of copper is incredibly diverse; it has oxidation states readily available from 0 to III making it prone to both polar and radical pathways (two and one electron pathways). Copper has gained immense success within click-chemistry owing to its efficiency in the azide-alkyne cycloaddition. However, copper has also gained momentum within cross-coupling reactions.^[28] Copper catalyzed coupling reactions have been known since Ullmann's discovery in 1901. With the success of organoboron compounds a new wave of copper catalyzed coupling reactions have emerged, most famous, the Chan-Lam coupling; a reaction complimenting the palladium catalyzed Buchwald-Hartwig coupling. Although the Chan-Lam coupling utilizes aryl boron species instead of aryl halides it can be carried out in air at room temperature, making it extremely robust.^[30] Recently, examples of copper catalyzing the Suzuki-Miyaura-type cross coupling are also appearing, highlighting the potential of copper catalysis.^[30–32] Another area of rapid advancing copper catalysis is its use in direct C-H functionalization, this topic will be subject of chapter three.^[33]

1.3 Direct C-H functionalization

Direct C-H functionalization strategies can be divided into two types. One strategy relies on auxiliary direction groups connected to the substrate. The other strategy relies on utilizing the subtle difference in C-H bond energies within the molecule.

The use of directing group has the advantage of not relying on bond energies, meaning that you can potentially functionalize the most stable C-H bond selectively, even in the presence of weaker C-H bonds. However, one must be able to install a directing group in proximity to the targeted C-H bond, which severely limits the scope of the strategy. Another drawback of the directing group, is the very need of a directing group, which constitutes two additional synthetic steps, which to some extent defeats the purpose of “direct” C-H functionalization. Within this area, palladium in combination with 8-amidoquinoline type directing groups have been extremely successful, especially within formation of carbon-carbon bonds (Scheme 1.11).^[34–37]



Scheme 1.11. Example of a direct C-H arylation reaction using a directing group.^[35]

The utilization of bond–energy differences in organic molecules for direct C-H functionalization has the advantage of actually being direct, meaning that in one synthetic step a C-H bond becomes e.g. a C-C bond. The main drawback is the need for relatively big differences in the C-H bond strength to provide acceptable selectivity leading to a limited scope. Especially copper and nickel (in combination with photoredox chemistry) has shined within this area of chemistry. The two projects in chapter 3 and 4 is a testimony to that.

1.4 Asymmetric Catalysis

Asymmetric catalysis is the practice of producing enantioenriched molecules with the aid of catalytic amount of enantiopure catalysts. This is a highly efficient method of promoting enantioinduction as one molecule can lead to the formation of thousands of enantiopure molecules.^[8,38,39]

Although chirality in chemistry was not discovered until 1819 by Louis Pasteur, it has most likely existed since the beginning of time. Nature has developed chemistry to be chiral; meaning that despite two enantiomeric compounds possess the same physical properties they will interact with nature differently, producing different physiochemical responses. Most people can easily distinguish the smell of oranges from lemons, despite they in fact origin from the same molecule limonene; (*S*)-(-)-limonene produces a lemony and (*R*)-(+)-limonene an orangy smell. Although this example is relatable to many it might not underline the importance. A horrific example, underlying the importance of chirality, is the case of Thalidomide. Thalidomide was extensively prescribed to pregnant women from 1957-1962 against morning sickness. Horrifyingly, when taken in the first trimester of pregnancy it resulted in severe birth defects. It was realized that one enantiomer was highly toxic while the other was helpful. Consequently, chiral drugs have since then increasingly been approved as a single enantiomers (Figure 1.02).^[38]

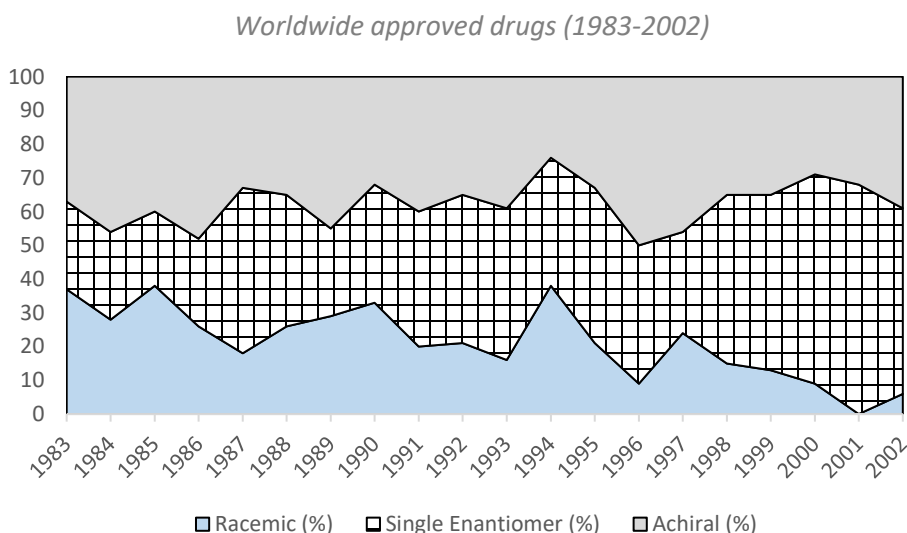
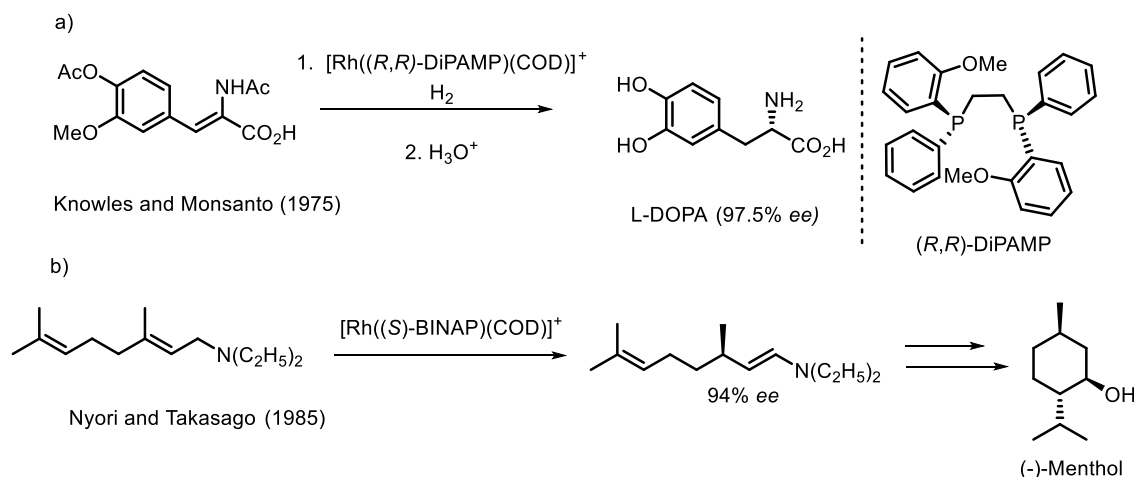


Figure 1.02 The distribution of approved drugs worldwide from 1983-2002.^[40]

Outside the area of pharmaceuticals, asymmetric synthesis is imperative within fragrance, flavors and agrochemistry. Multiple strategies towards synthesis of enantioenriched compounds exist such as the use of chiral auxiliaries, the use of chiral starting materials (from the chiral pool) and resolution of enantiomers. Although each method can be powerful, they have their limitations and are typically more wasteful than asymmetric catalysis.

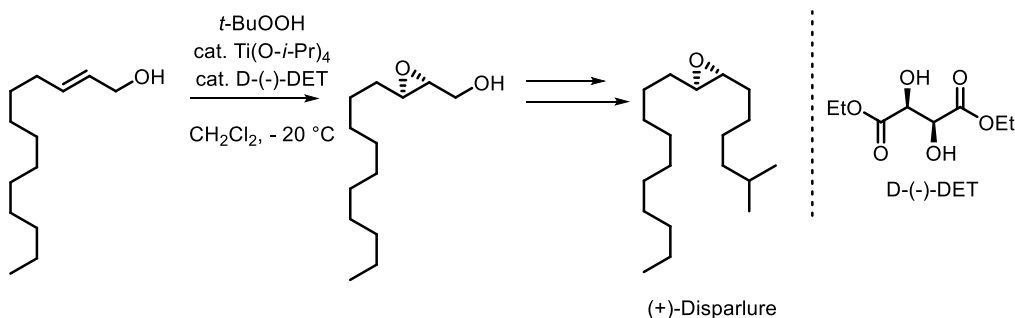
The importance of asymmetric catalysis were underlined in 2001 when Sharpless, Noyori and Knowles shared the Nobel Prize in chemistry for their work in asymmetric catalysis. Knowles and Noyori shared one part of the Nobel Prize for the development of asymmetric hydrogenation, which have had tremendous impact on industrial production of enantiomeric pure compounds. Knowles and Monsanto developed a process for the synthesis of L-DOPA via an asymmetric hydrogenation step patented already

in 1975 (Scheme 1.12a). Approximately ten years later, Noyori and Takasago developed a process for the synthesis of Menthol (Scheme 1.12b). Since then, asymmetric hydrogenation catalysts have been utilized for a multitude of industrial processes.^[41] The success of the asymmetric hydrogenation catalysis is linked with its unprecedented enantioselectivity and activity, enantioselectivities reaching more than 99% *ee* and TONs up to 100,000.^[42]



Scheme 1.12. Examples of asymmetric catalytic reactions. a) Knowles and Monsanto's synthesis of L-DOPA. b) Noyori and Takasago's isomerization of allylic amines for the synthesis of (-)-Menthol.

The other part of the Nobel Prize was given to Sharpless for his work on asymmetric epoxidation and asymmetric dihydroxylation. These reactions have found less industrial relevance possibly due to the use of toxic osmium tetroxide (Sharpless asymmetric dihydroxylation) and a less active catalyst (5-10 mol% needed of the $\text{Ti}(\text{iOPr})_4/(-/+)\text{-DET}$) in the Sharpless epoxidation (Scheme 1.13).^[43–45]



Scheme 1.13. Sharpless asymmetric epoxidation used in the synthesis of (+)-Disparlure.^[45]

Since then the development of novel asymmetric catalytic systems have seen an explosion in academia. Unfortunately, it has not seen a corresponding introduction within industrial chemistry outside of the hydrogenation and enzymatic arena. Most of the expansion in asymmetric catalysis is based on homogeneous catalysis, most however, much less selective and active than the hydrogenation catalysts. Further, asymmetric catalysts are typically quite expensive due to their complex ligands, accordingly, recycling of the catalyst might aid to make them feasible in an industrial setting.

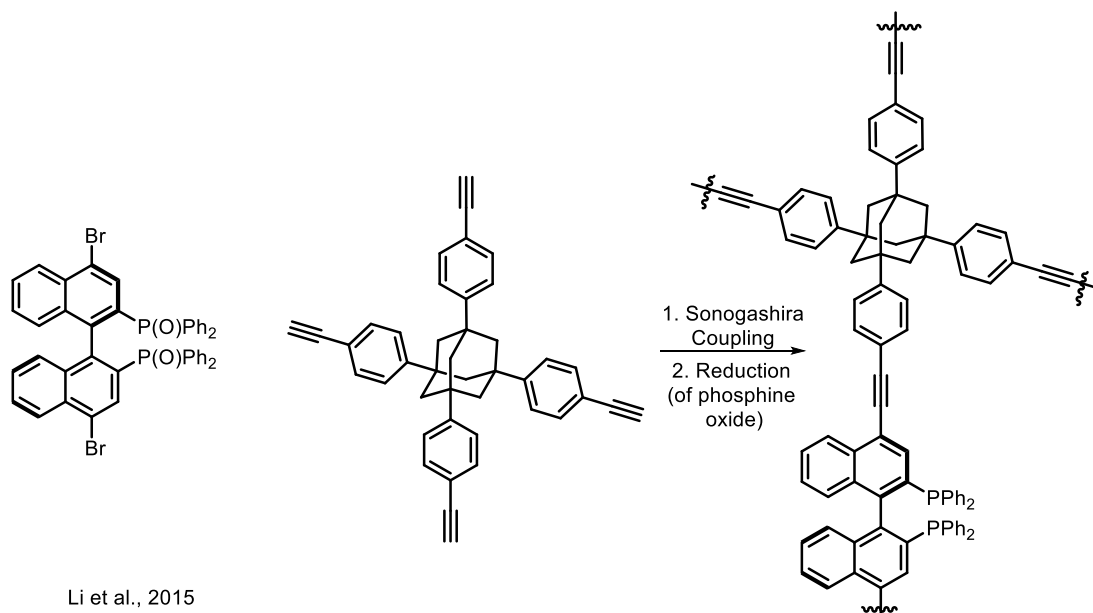
Merging homogeneous and heterogeneous catalysis can potentially lead to catalysts with the inherent recyclability of heterogeneous catalysts while possessing the unique selectivity of homogeneous catalysis required in asymmetric catalysis.

1.5 Porous Organic Polymers

The high selectivity of homogeneous catalysis is mainly owed to its homogeneity of active species and the presence of ligands. A straightforward strategy to obtain heterogeneous catalysts with selectivity on par with the corresponding homogeneous ones is to immobilize the desired metal complex onto a support material. Multiple attachment strategies onto various support materials exist, e.g., immobilizing into porous organic polymers (POPs), integrating in metal-organic frameworks, integrating in covalent organic frameworks, attaching to inorganic oxides and so forth.^[46–50]

The concept of using polymer supports in organic chemistry originated already in the 1960s initially developed for solid-state peptide synthesis and similar sequential synthesis. However, already in the beginning of 1970s the first examples of metal immobilized POPs were reported.^[51] Since then, it has been an active field of research; however, around the new millennium, the area saw a renaissance, possibly linked to the advances within the field of asymmetric homogeneous catalysis, and the field remains very active.

Various types of POPs exist but in general they can be categorized into two types; POPs with sp^2 - sp^2 or sp^2 - sp^3 backbones and POPs with sp^3 - sp^3 backbones. The first type is typically synthesized via cross-coupling reactions like Suzuki and Sonogashira cross-coupling reactions, which provides controlled ABA type polymers (Scheme 1.14). The main drawback of metal catalyzed polymerizations is the remaining metal catalyst in the polymer, which has to be removed. These types of polymers are rigid and like typical heterogeneous catalysts relies on their porosity and surface area to provide good activity. The porosity can be tuned by cleverly designing the geometry and size of the building blocks and very impressive porosities can be obtained.^[52–57]



Scheme 1.14. A BINAP immobilized POP synthesized via Sonogashira cross-coupling.^[58]

Polymers with sp^3 - sp^3 carbon backbones are typically polymerized via radical polymerization and provides polymers with a random monomer distribution. These polymers do typically not possess any porosity, however, they possess the ability to “swell” when dissolved in a solvent.

Among the many strategies, “swellable” POPs provide a rather unique alternative as its amorphous nature gives it distinctively different properties from more typical heterogeneous support materials. Typically, in heterogeneous catalysis, pore volume and surface area are key parameters and high values are essential for good activity. Polymer supports capable of swelling, most polymers with sp^3-sp^3 carbon backbones, do not possess any noteworthy surface area or pore volume, however, when dispersed in some solvents they get pseudo dissolved, or “swelled”, exposing the active sites.^{[55][56]} Moreover, this property has been suggested to provide a chemical environment very similar to homogeneous catalysts. This was nicely illustrated by Xiao and co-workers by carrying out solid-state ^{31}P NMR of their dppe-POP in dried state and in swollen state. They found that the swollen polymer provided a sharp ^{31}P NMR signal similar to that of the homogeneous ligand while the dry sample provided a broad signal (Figure 1.03).^[59]

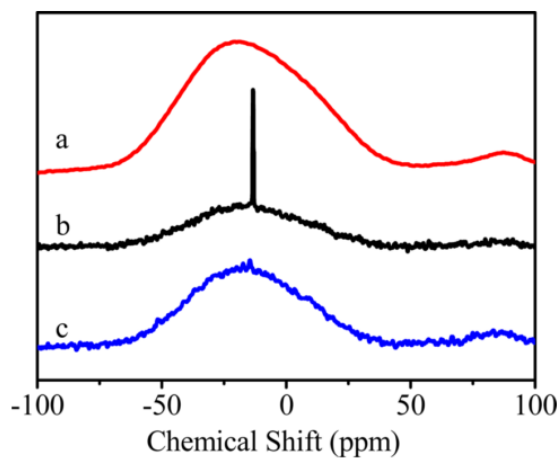
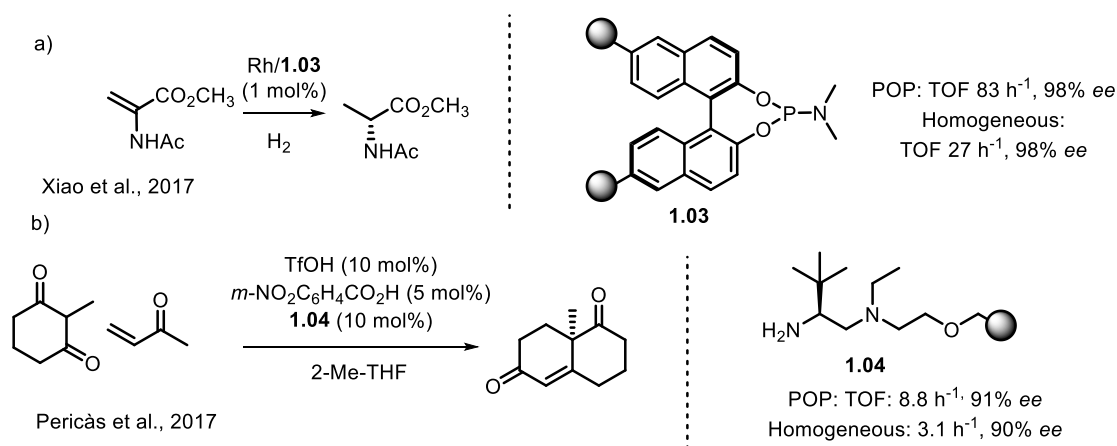


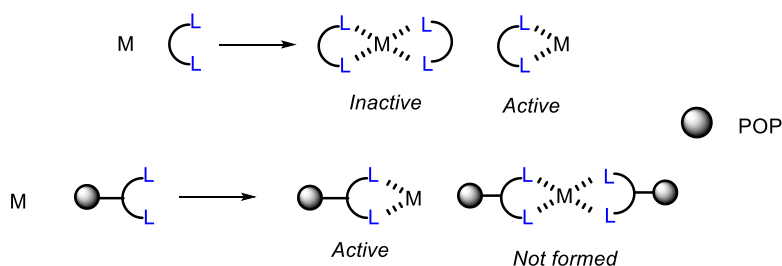
Figure 1.03. ^{31}P NMR adapted from the work of Xiao et al. on their dppe-POP.^[59] The red curve (a) shows the spectrum of their dried POP, the black curve (b) of a swollen POP. The blue curve (c) is an example of a non-swelling POP.

This ability to mimic a homogeneous environment might be one of the key factors in swelling POPs success within asymmetric catalysis where immobilization rarely results in enantioselectivity erosion (Scheme 1.15).^[60–62] However, the ability to swell also constitutes a drawback, as swelling is required to provide decent activity, but it is only caused by limited solvents. Although, the polymers ability to swell is dependent on the solvent, it is also possible to design the polymer to swell in a certain solvent.



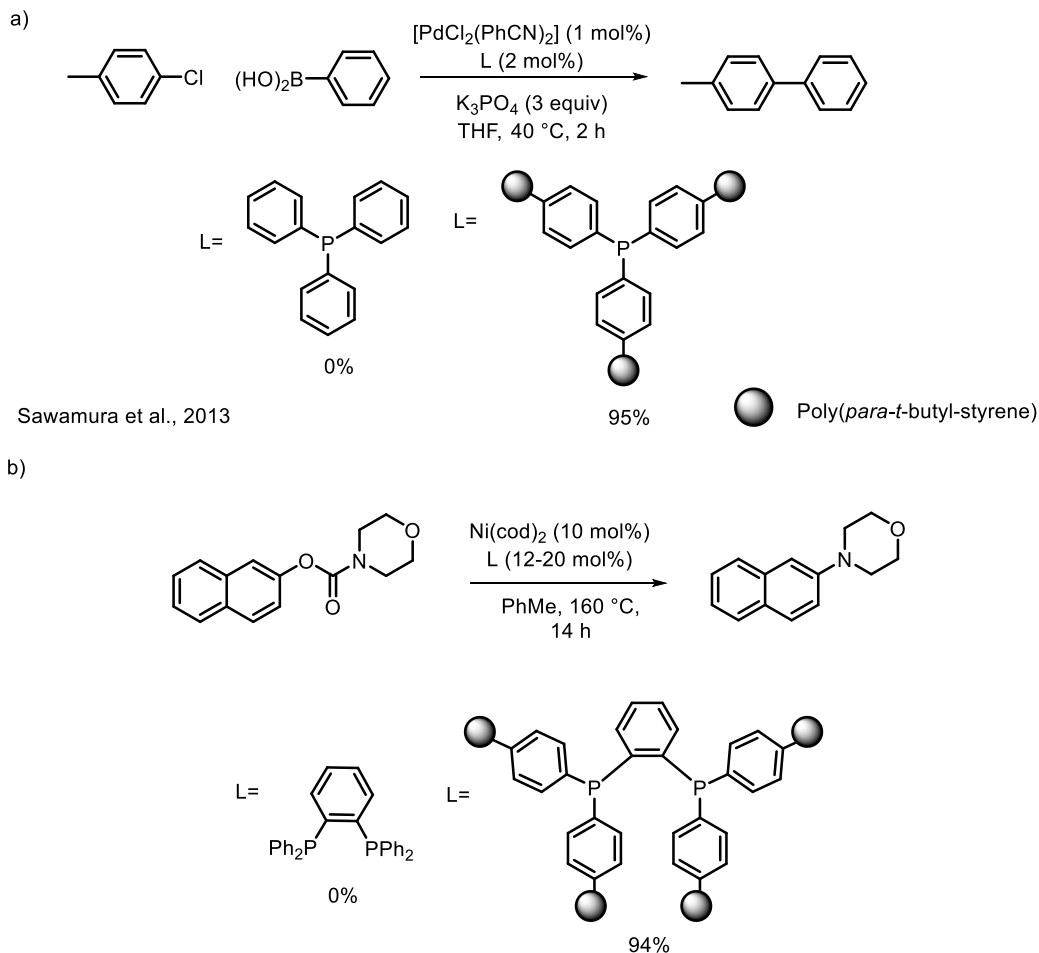
Scheme 1.15. Two examples where a polystyrene-based POP outperforms the corresponding homogeneous catalyst.^{[61][62]}

Another more niche-based approach is the ability of preventing ligand saturation providing a much higher activity. In some cases when mixing ligands and transition metals, it can be difficult to control the amount of ligands attaching to the metal site. In cases where addition of multiple ligands to a metal center leads to an inactive species this can lead to a much lower concentration of active catalyst than anticipated (Scheme 1.16). The immobilization of ligands into polymeric backbones can prevent this, possibly due to the increased bulk around the ligand and limited mobility.



Scheme 1.16. Illustration of how POPs can help control metal chelation.

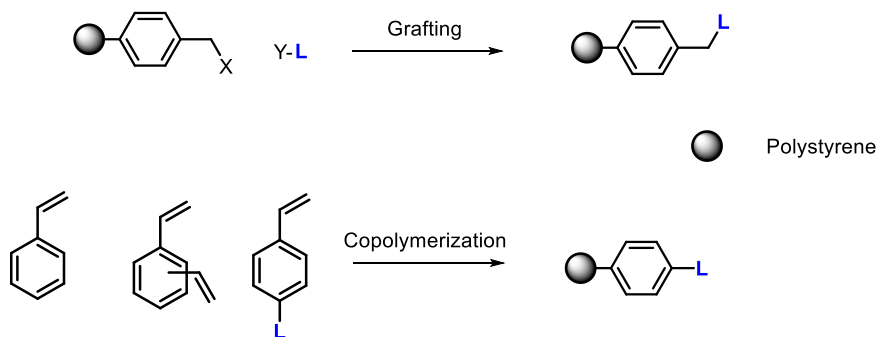
Especially Sawamura and co-workers have elegantly demonstrated the potential of controlling the metal chelation.^[63] The introduction of triphenylphosphine into a bulky poly(*para*-*t*-butyl)styrene allowed for the Suzuki cross-coupling of chlorotoluene at 40 °C with phenylboronic acid in almost quantitative yields after just two hours.^[64] Carrying out the reaction with triphenylphosphine as ligand yielded no product (Scheme 1.17a). Interestingly, they also found that using triple cross-linked triphenylphosphine was significantly more active than “mono” cross-linked triphenylphosphine, presumably owing to same effect more pronounced in a more rigid system. Later, his team in collaboration with Tobisu, Chatani and Iwai developed a nickel catalyzed protocol for the decarboxylation of aryl carbamates. The protocol utilizes a polystyrene immobilized 1,2-bis(diphenylphosphino)benzene, notably, the corresponding homogeneous ligand provides no product (Scheme 1.17b).^[65]



Scheme 1.17. Two examples that illustrates the potential of preventing ligand saturation by immobilizing into a polystyrene matrix.^{[64][65]}

Immobilization Strategies of Polystyrene POPs

For the synthesis of polystyrene-based POPs two main strategies exist. The ligand can either be grafted onto a functionalized polystyrene resin or the ligand can be copolymerized with styrene and the desired cross-linker (Scheme 1.18).^[55] The grafting strategy is typically based on commercially available polystyrene resins with a functional group like alkyl chloride, carboxylic acid or azide as grafting handle. Multiple commercial resins are available e.g. Merrifield, TentaGel and ArgoGel. The commercial resins offers a much better control over the polymer properties, such as cross-linking degree, swellability and size. However, one must carefully choose the grafting connection to ensure it is stable and non-coordinating within the desired catalytic system.^[66]



Scheme 1.18. Two approaches to obtain polystyrene immobilized POPs.

Introducing the ligand via copolymerization provides one major advantages in an academic setting; the ease of tuning. For instance, the ligand to styrene and cross-linker ratio is much easier (and faster) evaluated, incorporation of other (co)monomers is possible etc. At the current state the research mainly evolves around the catalysis and the properties of the polymer support seems less important. This might become equally crucial when the area matures and projects moves closer to an industrial setting.

1.6 Continuous Flow Chemistry

Within organic chemistry, especially in academic laboratory settings, reactions are carried out in batch mode as default. However, in recent years, the development of continuous flow chemistry have flourished. Continuous flow chemistry have multiple advantages over batch reactions especially with regard to safety, efficiency and environmental factors. The low-volume reaction space offers much more efficient temperature control. Additionally, it suppresses consequences of hazardous chemicals and “run-away” reactions as a much smaller volume of chemicals is present at any time. However, it also introduces several limitations; formation of insoluble solids is disastrous as they clog the system, low yields and formation of by-products becomes troublesome downstream in multistep synthesis.^[67]

Within flow chemistry, the types of reaction can be categorized into four different types (Figure 1.04):

Type 1: Two substrates (A & B) are passed through the hollow reaction tube and if carried out efficiently only the product is eluted with the solvent.

Type 2: A substrate (A) is passed through a column containing a supported substrate (B), if carried out smoothly only the product is eluted with the solvent, however the column resin must be recharged over time.

Type 3: Two substrates (A & B) and a homogeneous catalyst are passed through a hollow column, if carried out efficiently, only the product and the catalyst is co-eluted with the solvent.

Type 4: Two substrates (A & B) is passed through a column containing a supported catalyst, if carried out smoothly, only the desired product is eluted with the solvent.

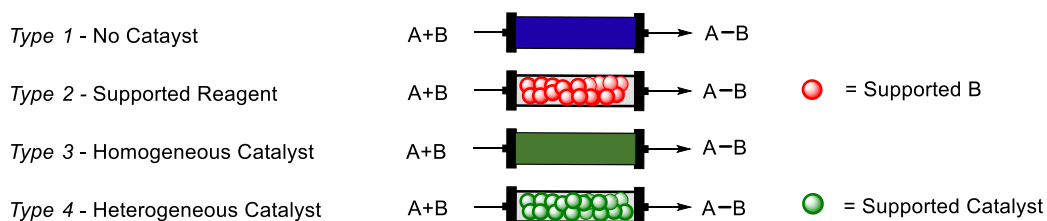


Figure 1.04. Illustration of different continuous flow systems.

All the types find purpose and have been utilized to carry out extremely elegant chemistry. Particularly, the research group of Jamison have highlighted the potential of continuous flow chemistry in organic synthesis, especially utilizing type 1-3. In 2015 Jamison et al. reported a continuous flow synthesis of Ibuprofen capable of providing pure ibuprofen in just three minutes.^[68] He has since developed multiple continuous flow synthesis of multiple pharmaceuticals e.g. Fluoxetine hydrochloride and Diazepam in big scale (up to 4500 doses/day).^[69–73]

Despite the inherent previously mentioned advantages of flow chemistry, the type 4 reactions provides additional advantages. The catalysts does not need to be recovered and dried prior to reuse and the purification of the product is not complicated by presence of catalyst. In multiple steps this becomes increasingly valuable as less by-products (e.g. catalysts) are co-eluted which is troublesome downstream. In this regard, POPs can play an important role for carrying out asymmetric catalytic reactions in flow systems. Especially, Kobayashi and co-workers have excelled at utilizing type 4 flow reactions. The potential was underlined in 2015 when Kobayashi and co-workers demonstrated a continuous flow multistep synthesis of (*R*) and (*S*)-Rolipram using only type 4 reactions. The key step, the asymmetric catalytic step, was carried out by a Pybox-CaCl₂ – polystyrene POP catalyst.^[74] More recently, they developed a polystyrene-based POP catalyst for the important asymmetric reductive amination reaction, operating in flow with only 6 bars of H₂, providing higher enantioselectivity and yield under flow condition.^[75]

In industrial settings, when suitable, continuous flow conditions are often highly preferred over batch conditions, especially on large scale. The compatibility of POPs with continuous flow conditions provides an additional driver for developing asymmetric heterogeneous POP catalysts.

1.7 References

- [1] J. W. Erisman, M. A. Sutton, J. Galloway, Z. Klimont, W. Winiwarter, *Nat. Geosci.* **2008**, *1*, 636–639.
- [2] J. Hagen, “1. Introduction” *Industrial Catalysis: A Practical Approach*, Wiley-VCH, **2015**.
- [3] S. Bhaduri, D. Mukesh, “1. Chemical Industry and Homogeneous Catalysis” *Homogeneous Catalysis: Mechanism and Industrial Applications*, Wiley-VCH, **2014**.
- [4] “Catalysis,” can be found under <https://en.wikipedia.org/wiki/Catalysis>, (accessed 30/07/2021).
- [5] G. Rothenberg, “1 Introduction” *Catalysis: Conceptions and Green Applications*, Wiley-VCH, **2008**.
- [6] P. T. Anastas, J. C. Warner, *Green Chemistry, Theory and Practise*, Oxford University Press, **1998**.
- [7] J. Hagen, *Industrial Catalysis: A Practical Approach*, Wiley-VCH, **2015**.
- [8] S. Bhaduri, D. Mukesh, *Homogeneous Catalysis: Mechanism and Industrial Applications*, Wiley-VCH, **2014**.
- [9] F. Ullmann, J. Bielecki, *Ber. Dtsch. Chem. Ges.* **1901**, *34*, 2174–2185.
- [10] “THE NOBEL PRIZE,” can be found under <https://www.nobelprize.org/prizes/chemistry/>, (accessed 12/07/2021).
- [11] D. Blakemore, “Chapter 1 Suzuki–Miyaura Coupling” *Synthetic Methods in Drug Discovery: Volume 1*, The Royal Society Of Chemistry, **2016**.
- [12] J. F. Hartwig, “Chapter 6 Oxidative Addition of Nonpolar Reagents” *Organotransition Metal Chemistry: From Bonding to Catalysis*, University Science Books, **2009**.
- [13] J. F. Hartwig, “Chapter 7 Oxidative Addition of Polar Reagents” *Organotransition Metal Chemistry: From Bonding to Catalysis*, University Science Books, **2009**.
- [14] M. R. Netherton, G. C. Fu, *Angew. Chem., Int. Ed.* **2002**, *41*, 3910–3912.
- [15] I. D. Hills, M. R. Netherton, G. C. Fu, *Angew. Chem., Int. Ed.* **2003**, *42*, 5749–5752.
- [16] P. K. Wong, K. S. Y. Lau, J. K. Stille, *J. Am. Chem. Soc.* **1974**, *96*, 5956–5957.
- [17] J. Halpern, J. P. Maher, *J. Am. Chem. Soc.* **1965**, *87*, 5361–5366.
- [18] R. H. Hill, R. J. Puddephatt, *J. Am. Chem. Soc.* **1985**, *107*, 1218–1225.
- [19] N. D. Schley, G. C. Fu, *J. Am. Chem. Soc.* **2014**, *136*, 16588–16593.
- [20] J. F. Hartwig, “Chapter 8 Reductive Elimination” *Organotransition Metal Chemistry: From Bonding to Catalysis*, University Science Books, **2009**.
- [21] J. J. Low, W. A. Goddard, *J. Am. Chem. Soc.* **1986**, *108*, 6115–6128.
- [22] S. C. Rasmussen, *ChemTexts* **2020**, *7*, 1.
- [23] B. P. Carrow, J. F. Hartwig, *J. Am. Chem. Soc.* **2011**, *133*, 2116–2119.
- [24] A. Corma, H. García, *Chem. Rev.* **2003**, *103*, 4307–4366.

- [25] J. S. Johnson, D. A. Evans, *Acc. Chem. Res.* **2000**, *33*, 325–335.
- [26] D. A. Evans, M. C. Kozlowski, C. S. Burgey, D. W. C. MacMillan, *J. Am. Chem. Soc.* **1997**, *119*, 7893–7894.
- [27] D. A. Evans, D. M. Barnes, J. S. Johnson, T. Lectka, P. von Matt, S. J. Miller, J. A. Murry, R. D. Norcross, E. A. Shaughnessy, K. R. Campos, *J. Am. Chem. Soc.* **1999**, *121*, 7582–7594.
- [28] S. Saranya, G. Anilkumar, J. Nekvinda, W. L. Santos, N. A. Harry, R. V Jagadeesh, X.-X. Guo, *“Copper Catalysis: An Introduction” Copper Catalysis in Organic Synthesis*, Wiley-VCH, **2020**.
- [29] J. B. Diccianni, T. Diao, *Trends Chem.* **2019**, *1*, 830–844.
- [30] J. Nekvinda, W. L. Santos, X.-X. Guo, *“Copper-Catalyzed Cross-Coupling Reactions of Organoboron Compounds” Copper Catalysis in Organic Synthesis*, Wiley-VCH, **2020**.
- [31] Y. P. Budiman, A. Friedrich, U. Radius, T. B. Marder, *ChemCatChem* **2019**, *11*, 5387–5396.
- [32] S. K. Gurung, S. Thapa, A. Kafle, D. A. Dickie, R. Giri, *Org. Lett.* **2014**, *16*, 1264–1267.
- [33] Z. Ni, Q. Zhang, T. Xiong, Y. Zheng, Y. Li, H. Zhang, J. Zhang, Q. Liu, *Angew. Chem., Int. Ed.* **2012**, *51*, 1244–1247.
- [34] H. M. L. Davies, D. Morton, *J. Org. Chem.* **2016**, *81*, 343–350.
- [35] W. R. Gutekunst, P. S. Baran, *J. Org. Chem.* **2014**, *79*, 2430–2452.
- [36] D. Shabashov, O. Daugulis, *J. Am. Chem. Soc.* **2010**, *132*, 3965–3972.
- [37] Y. Feng, Y. Wang, B. Landgraf, S. Liu, G. Chen, *Org. Lett.* **2010**, *12*, 3414–3417.
- [38] J. Clayden, N. Greeves, S. Warren, *“Asymmetric Synthesis” Organic Chemistry*, Oxford University Press, **2012**.
- [39] M. Gruttadauria, F. Giacalone, Eds. , *Catalytic Methods in Asymmetric Synthesis*, Wiley-VCH, **2012**.
- [40] H. Caner, E. Groner, L. Levy, I. Agranat, *Drug Discov. Today* **2004**, *9*, 105–110.
- [41] P. A. Dub, J. C. Gordon, *Nat. Rev. Chem.* **2018**, *2*, 396–408.
- [42] W. S. Knowles, *J. Chem. Educ.* **1986**, *63*, 222.
- [43] H. C. Kolb, M. S. VanNieuwenhze, K. B. Sharpless, *Chem. Rev.* **1994**, *94*, 2483–2547.
- [44] K. B. Sharpless, *Angew. Chem., Int. Ed.* **2002**, *41*, 2024–2032.
- [45] R. A. Fernandes, N. Chandra, A. J. Gangani, *New J. Chem.* **2020**, *44*, 17616–17636.
- [46] K. Ding, Y. Uozumi, Eds. , *Handbook of Asymmetric Heterogeneous Catalysis*, Wiley-VCH, **2008**.
- [47] M. Yoon, R. Srirambalaji, K. Kim, *Chem. Rev.* **2012**, *112*, 1196–1231.
- [48] H. Zhang, L.-L. Lou, K. Yu, S. Liu, *Small* **2021**, *17*, 2005686.
- [49] F. Meemken, A. Baiker, *Chem. Rev.* **2017**, *117*, 11522–11569.
- [50] S. Roy, M. A. Pericàs, *Org. Biomol. Chem.* **2009**, *7*, 2669–2677.

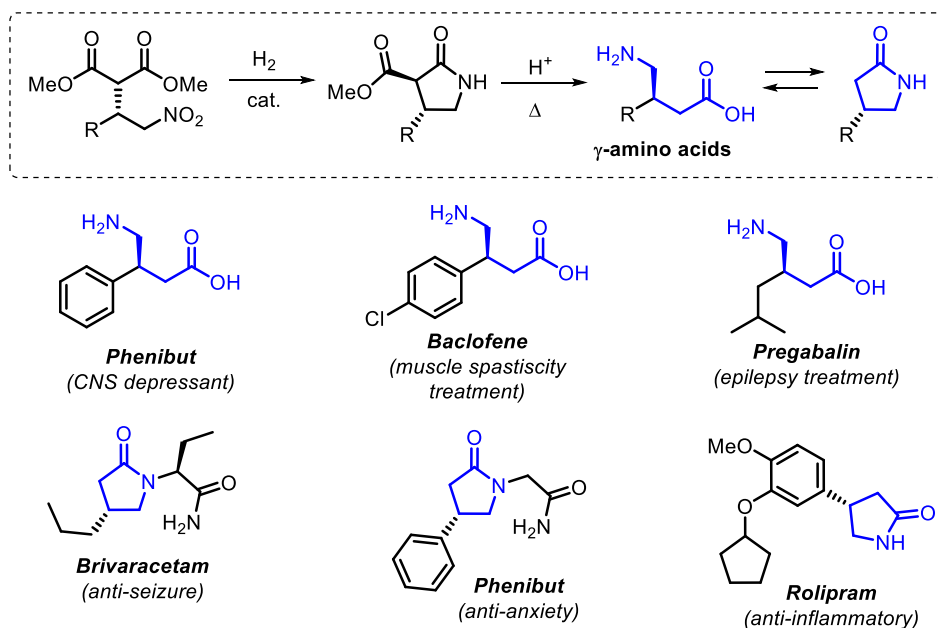
- [51] C. C. Leznoff, *Chem. Soc. Rev.* **1974**, 3, 65–85.
- [52] P. Kaur, J. T. Hupp, S. T. Nguyen, *ACS Catal.* **2011**, 1, 819–835.
- [53] L. Tan, B. Tan, *Chem. Soc. Rev.* **2017**, 46, 3322–3356.
- [54] Q. Sun, Z. Dai, X. Meng, F. S. Xiao, *Chem. Soc. Rev.* **2015**, 44, 6018–6034.
- [55] C. A. McNamara, M. J. Dixon, M. Bradley, *Chem. Rev.* **2002**, 102, 3275–3300.
- [56] S. Kramer, N. R. Bennedsen, S. Kegnæs, *ACS Catal.* **2018**, 8, 6961–6982.
- [57] X. Wang, S. Lu, J. Li, Y. Liu, C. Li, *Catal. Sci. Technol.* **2015**, 5, 2585–2589.
- [58] K. Wilckens, M.-A. Duhs, D. Lentz, C. Czekelius, *Eur. J. Org. Chem.* **2011**, 2011, 5441–5446.
- [59] Q. Sun, Z. Dai, X. Liu, N. Sheng, F. Deng, X. Meng, F.-S. Xiao, *J. Am. Chem. Soc.* **2015**, 137, 5204–5209.
- [60] B. Altava, M. I. Burguete, E. García-Verdugo, S. V Luis, *Chem. Soc. Rev.* **2018**, 47, 2722–2771.
- [61] S. Cañellas, C. Ayats, A. H. Henseler, M. A. Pericàs, *ACS Catal.* **2017**, 7, 1383–1391.
- [62] Q. Sun, Z. Dai, X. Meng, F.-S. Xiao, *Chem. Mater.* **2017**, 29, 5720–5726.
- [63] T. Iwai, T. Harada, H. Shimada, K. Asano, M. Sawamura, *ACS Catal.* **2017**, 7, 1681–1692.
- [64] T. Iwai, T. Harada, K. Hara, M. Sawamura, *Angew. Chem., Int. Ed.* **2013**, 52, 12322–12326.
- [65] A. Nishizawa, T. Takahira, K. Yasui, H. Fujimoto, T. Iwai, M. Sawamura, N. Chatani, M. Tobisu, *J. Am. Chem. Soc.* **2019**, 141, 7261–7265.
- [66] “RAPP POLYMERE,” can be found under <http://www.rapp-polymere.com/index.php?id=73¤cy=eur>, (accessed 30/06/2021).
- [67] S. Kobayashi, *Chem. – An Asian J.* **2016**, 11, 425–436.
- [68] D. R. Snead, T. F. Jamison, *Angew. Chem., Int. Ed.* **2015**, 54, 983–987.
- [69] A. Adamo, R. L. Beingessner, M. Behnam, J. Chen, T. F. Jamison, K. F. Jensen, J.-C. M. Monbaliu, A. S. Myerson, E. M. Revalor, D. R. Snead, et al., *Science* **2016**, 352, 61–67.
- [70] C. W. Coley, D. A. Thomas, J. A. M. Lummiss, J. N. Jaworski, C. P. Breen, V. Schultz, T. Hart, J. S. Fishman, L. Rogers, H. Gao, et al., *Science* **2019**, 365, eaax1566.
- [71] R. E. Ziegler, B. K. Desai, J.-A. Jee, B. F. Gupton, T. D. Roper, T. F. Jamison, *Angew. Chem., Int. Ed.* **2018**, 57, 7181–7185.
- [72] M. G. Russell, T. F. Jamison, *Angew. Chem., Int. Ed.* **2019**, 58, 7678–7681.
- [73] C. P. Breen, T. F. Jamison, *Chem. – A Eur. J.* **2019**, 25, 14527–14531.
- [74] T. Tsubogo, H. Oyamada, S. Kobayashi, *Nature* **2015**, 520, 329–332.
- [75] T. Yasukawa, R. Masuda, S. Kobayashi, *Nat. Catal.* **2019**, 2, 1088–1092.

2) Asymmetric Michael Addition of Malonates to Aliphatic Nitroalkenes

This chapter describes the work carried out to develop a polystyrene-based POP catalyst for the asymmetric Michael addition of malonates to aliphatic nitroalkenes. The work was published in "Advanced Synthesis & Catalysis".^[1]

2.1 Background

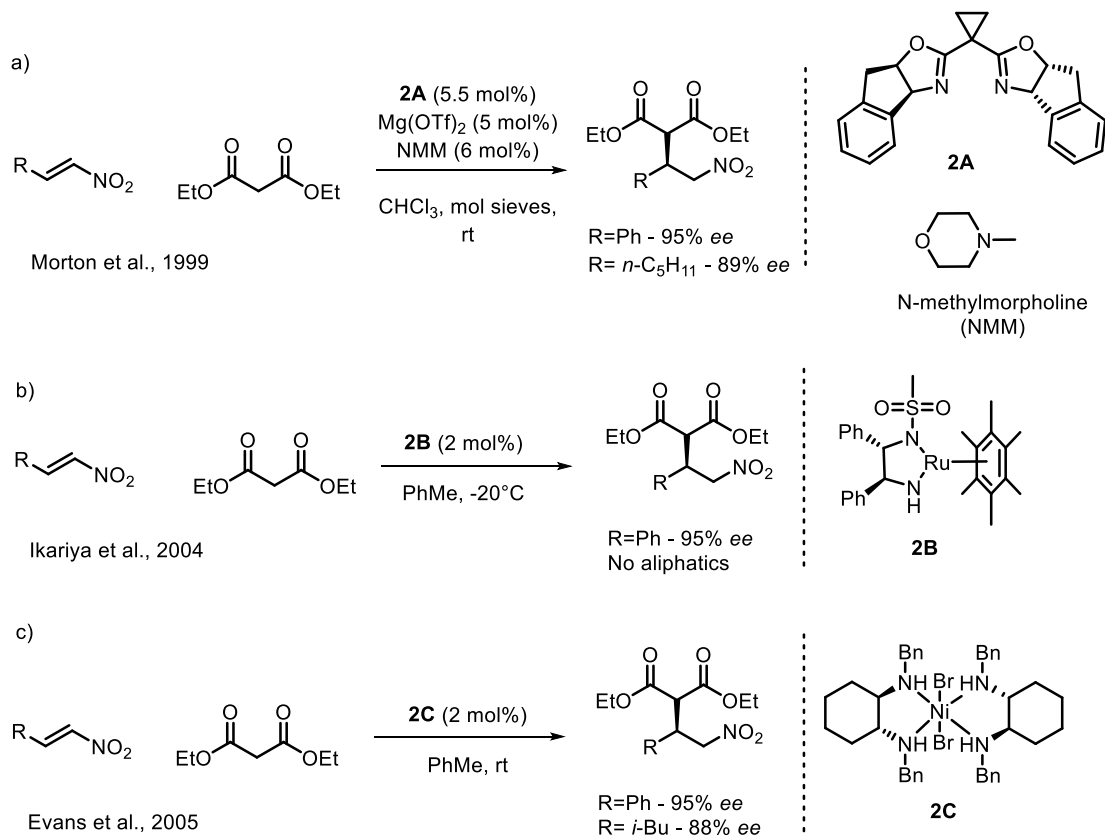
The asymmetric Michael addition of carbon-based nucleophiles to nitroalkene acceptors is a powerful transformation yielding very functional dense molecules containing up to three stereogenic centers.^[2] The addition of malonate esters to nitroalkenes is especially advantageous, as the products are easily transformed into γ -amino acids. A class of chemicals with a big array of biological activity; evident by the numerous γ -amino acid based pharmaceuticals, including the blockbuster drug Pregabalin (Scheme 2.01).^[3]



Scheme 2.01. Synthesis of γ -amino acids and pharmaceuticals based on γ -amino acids.

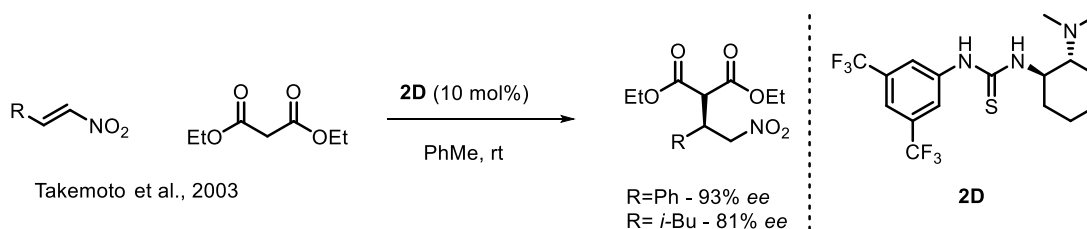
In 1999 Morton and co-workers reported the first successful asymmetric Michael addition of a malonate ester to a nitroalkene. They reported a system utilizing $\text{Mg}(\text{OTf})_2$ in combination with a BOX ligand (**2A**) and *N*-methylmorpholine as a co-catalyst in chloroform which provided almost quantitative yields and enantiomeric excess up to 95 % for the addition of dimethyl malonate to β -*trans*-nitrostyrene and even an aliphatic nitroalkene was included (Scheme 2.02a).^[4] A few years later, in 2004, Ikariya et al. reported a sulfonated DPEN (1,2-diphenylethylenediamine) ruthenium catalyst (**2B**) which provided good to excellent yield and enantioselectivity for aromatic nitroalkenes, with low catalyst loading (2 mol%) and without the presence of a base (Scheme 2.02b).^[5] A year later, Evans et al. reported a nickel(II) bis(*N,N'*-dibenzylcyclohexane-1,2-diamine) catalyst (**2C**) which performed similarly well using same conditions

(room temperature, 2 mol% catalyst and no co-catalyst), however, they also included a few aliphatic nitroalkenes (Scheme 2.02c).^[6] This remains the *state of art* organometallic homogeneous catalyst for this reaction.



Scheme 2.02. Previous work on the asymmetric Michael addition of malonates to nitroalkenes with organometallic catalysis.

A range of organocatalysts has also been reported to efficiently catalyze the transformation. The first organocatalyst was reported in 2003 by Takemoto et al. They reported a thiourea catalyst based on a chiral diamine scaffold (**2D**) (Scheme 2.03).^[7] Good results were obtained for aromatic nitroalkenes, but only moderate enantiomeric excess was obtained for aliphatic alkenes. Since then, a range of organocatalysts have been reported, however, most systems rely on high catalyst loadings (10 mol%) and examples of aliphatic nitroalkenes are scarce.^[2,7-11]

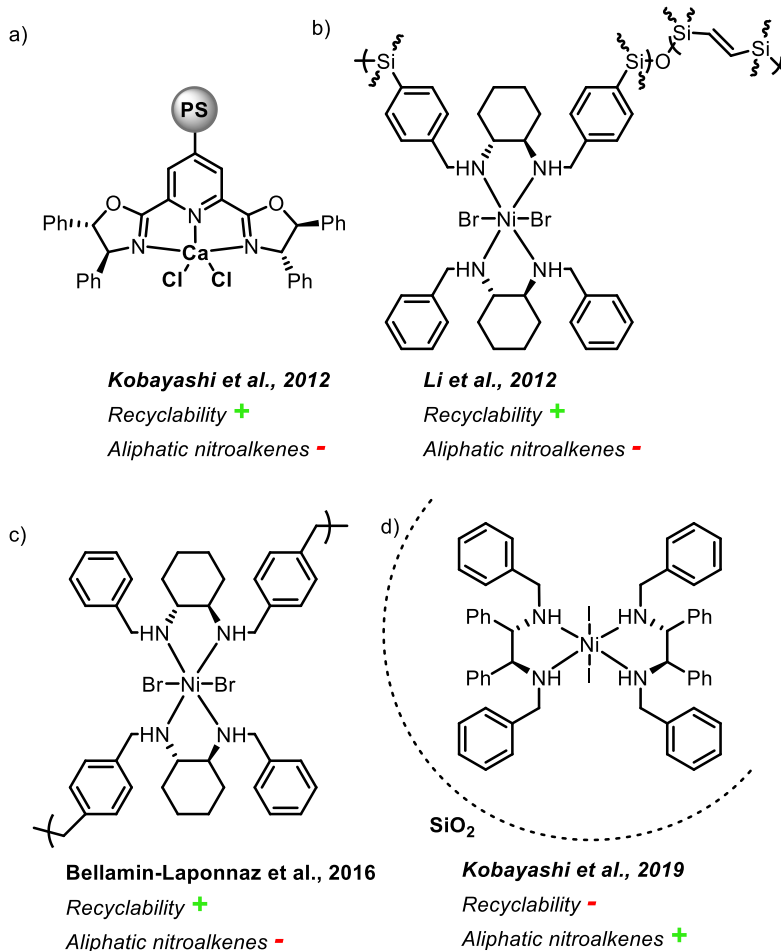


Scheme 2.03. Previous work on the asymmetric Michael addition of malonates to nitroalkenes with organocatalysis.

Despite the many excellent homogeneous catalytic systems for this transformation, the use of heterogeneous catalysis is sparse. Two groups independently reported the first examples of an organometallic heterogeneous catalyst for this transformation in 2012. Kobayashi et al. reported a

polystyrene immobilized CaCl_2 Pybox system which showed good results for aromatic nitroalkenes but fell short with aliphatic nitroalkenes (Scheme 2.04a).^[12] The system proved quite resilient and was operated in a continuous flow system for 9 days without noticeable deactivation. The group of Kobayashi later used this system to design the first multistep continuous flow synthesis of enantioenriched Rolipram which was published in the high impact journal Nature, demonstrating the importance of heterogenizing asymmetric homogeneous catalysts.^[3]

Li and co-workers reported the first immobilization of the catalytic system developed by Evans.^[13] They heterogenized the nickel bis(diamine) complex by incorporating the ligand within a ethylene-bridged periodic mesoporous organosilica and subsequently forming the active nickel complex (Scheme 2.04b). The catalyst yielded good enantioselectivity and decent activity (required 40 °C) while being very robust; carrying out 8th consecutive reactions without losing any noteworthy activity or selectivity. Unfortunately, no examples of aliphatic nitroalkenes were included in the scope. In 2016 Bellamin-Lopez et al. reported a self-supported chiral nickel bis(diamine) polymer (scheme 2.04c).^[14] They synthesized a ditopic cyclohexyldiamine-based ligand, which forms a self-supported polymeric catalyst with the complexation of NiBr_2 . The catalyst showed good activity and decent enantioselectivity (required 4 °C) for aromatic nitroalkenes, however, no aliphatic nitroalkenes were included. The catalyst was recycled thirteen times without any noticeable conversion erosion, however activity was not measured and the enantioselectivity started dropping after the 5th recycling. Finally, in 2019 Kobayashi reported the first heterogeneous catalysts that provided good enantioselectivity for aliphatic nitroalkenes.^[15] The catalyst consisted of a chiral nickel(II) bis(diamine) complex impregnated into silica (Scheme 2.04d). Unfortunately, the reusability of the catalyst was rather poor, losing activity already at second run (1st recycling) caused by leaching of the chiral ligand, possibly a consequence of not having a covalent support attachment.



Scheme 2.04. Previous work on the asymmetric Michael addition of malonates to nitroalkenes with heterogeneous catalysis.

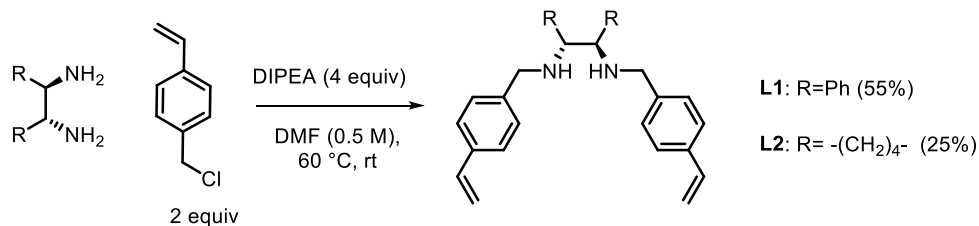
Despite many active organocatalysts there is no examples of an immobilized organocatalysts focusing on the asymmetric Michael addition of malonates to nitroalkenes. A few examples with immobilized organocatalysts exist but mostly focusing on the more reactive 1,3 diketones or β -ketoesters, however, single examples of a malonate esters are included.^[16–20]

Although it has been twenty years since the first efficient example of the asymmetric Michael addition of malonates to nitroalkenes, examples of aliphatic nitroalkenes are still scarce, and none of the previously mentioned heterogeneous systems proved both robust and efficient for aliphatic nitroalkenes (Scheme 2.04). Furthermore, no examples of functionalized aliphatic nitroalkenes have ever been reported.

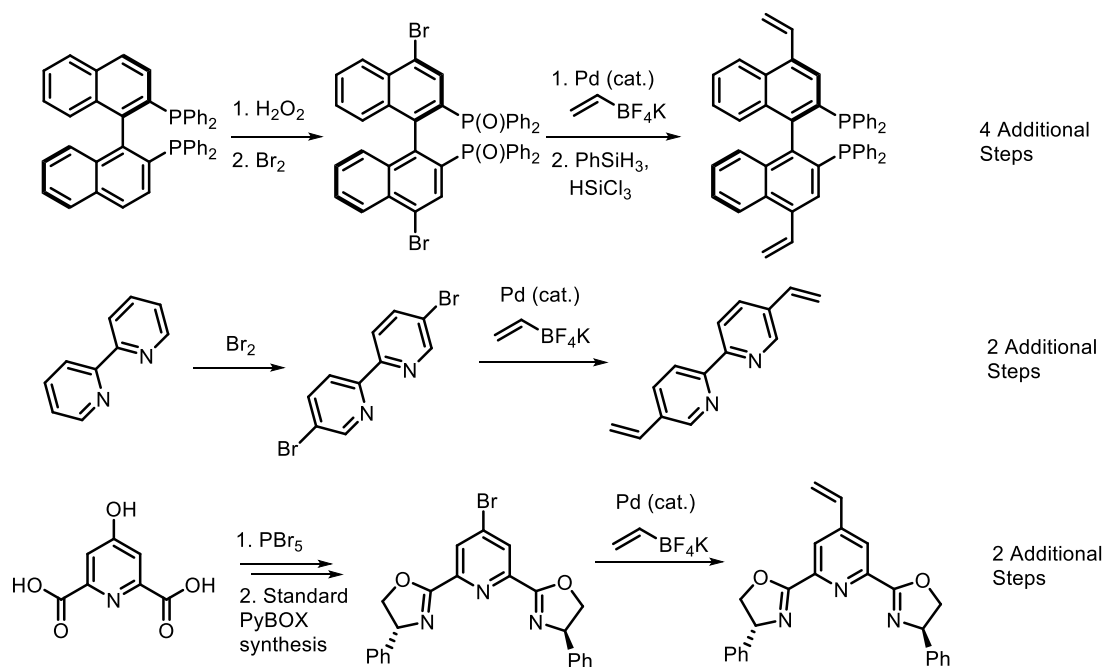
Inspired by the previous work, we hypothesized that if the nickel(II) bis(diamine) ligand complex (which provided good activity and selectivity for the aliphatic nitroalkenes) was covalently immobilized via the ligands into a polystyrene matrix, leaching could be neglected providing good recyclability.

2.2 Synthesis of NiL_2 -POPs

The synthesis of the vinyl-functionalized chiral bis(diamine) ligand was conveniently carried out in a single step from the chiral amine precursor and 4-chloromethylstyrene in the presence of base (Scheme 2.05). The short synthesis route is noteworthy as it induces no additional steps (other than a polymerizing step), which is highly unusual. Typically, the synthesis of ligands with a handle for polymerization requires several additional synthetic steps to already laborious routes; see Scheme 2.06 for examples of three common ligand families (BINAP, bipyridine and Pybox, respectively).^[21–23]



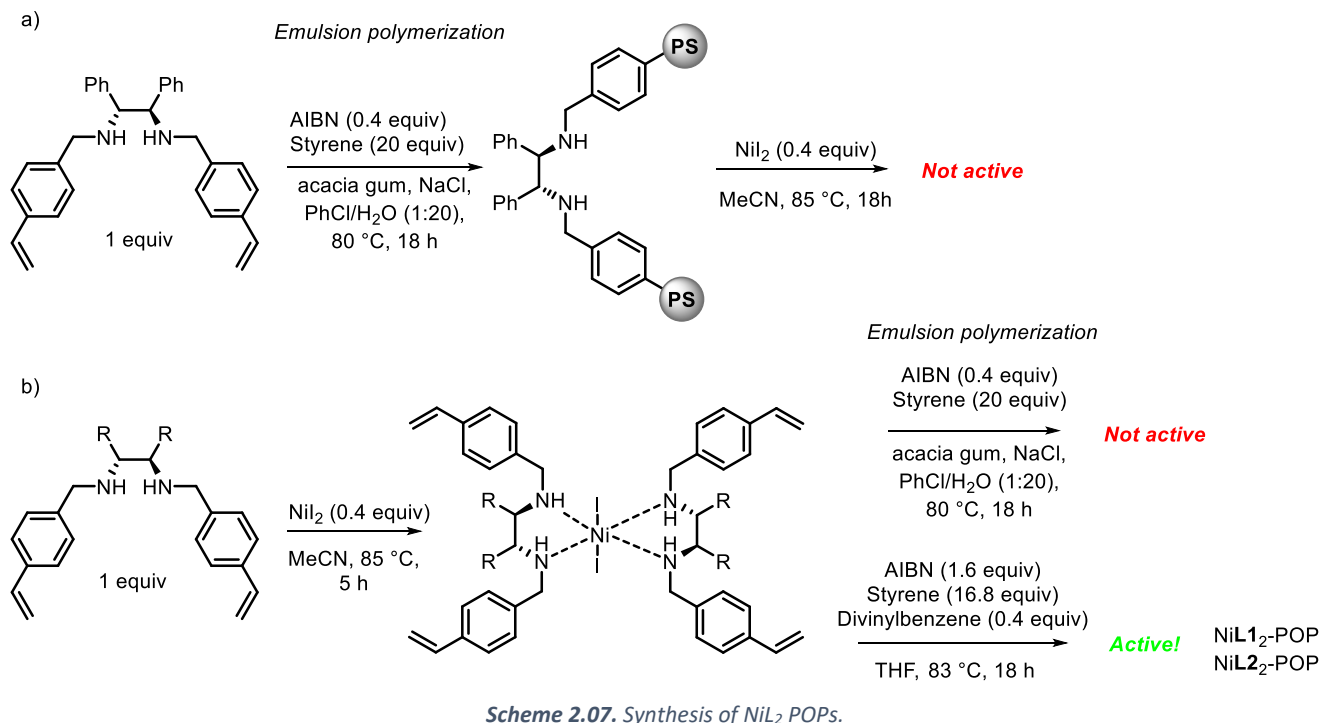
Scheme 2.05. Synthesis route for the vinyl-functionalized ligand.



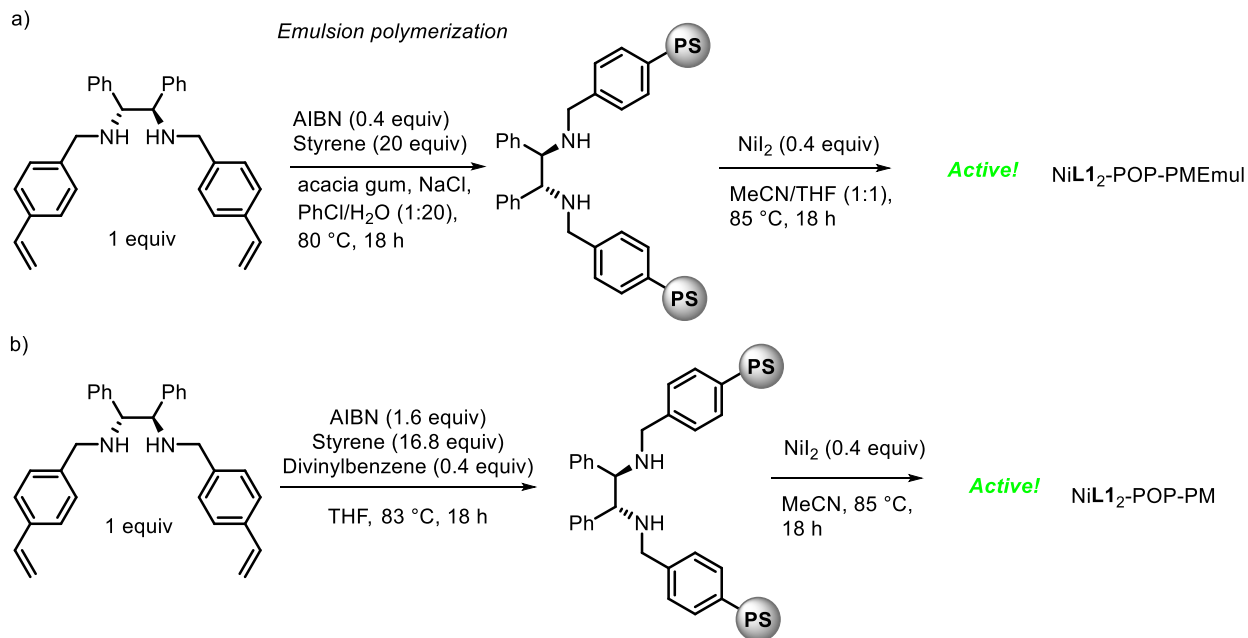
Scheme 2.06. Synthetic routes to vinyl functionalized ligands of three common ligand families.

With the chiral ligands in hand, the desired POP catalyst could be obtained through radical polymerization. Initially, a POP containing **L1** was prepared through emulsion polymerization. However, the first metalation attempt (refluxing the **L1** containing POP and NiL₂ in acetonitrile overnight) was unsuccessful (Scheme 2.07a). It was hypothesized that within the polymer two **L1** ligands would not be in close enough proximity for the nickel bis(diamine) complex to form. Instead, attempts to form the complex prior to polymerization was carried out. The first polymerization of the metal complex was once again carried out via an emulsion polymerization despite the complex is slightly water sensitive. This polymer was, not surprisingly, inactive. To avoid inactivation of the catalyst due to water, the complex was polymerized

directly in THF in a less controlled manner. Gratifyingly this yielded an off-white powder, which showed good selectivity and activity (Scheme 2.07b).

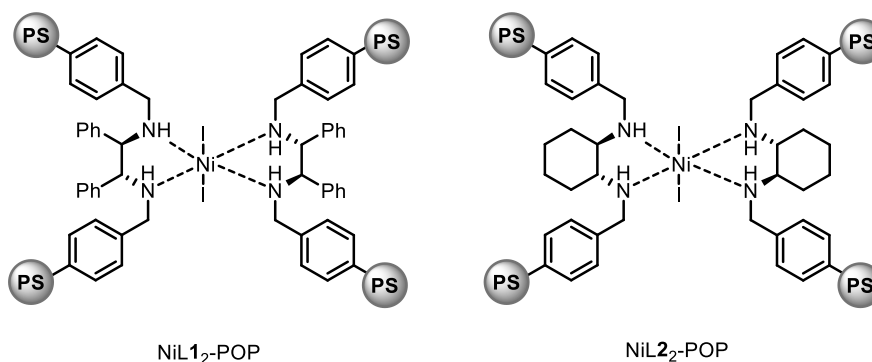


Later, it was found that the POP containing **L1** synthesized by emulsion polymerization could be efficiently metalated if the metalation was carried out in a 1:1 mixture of THF:MeCN, presumably as the polymer requires some degree of swelling in order for the complex to be formed (Scheme 2.08a). This polymer was later used in continuous flow operations. Additionally, it was found that a POP containing **L1** polymerized in THF could be post-metated by simply refluxing it with NiI₂ in MeCN overnight (Scheme 2.08b).



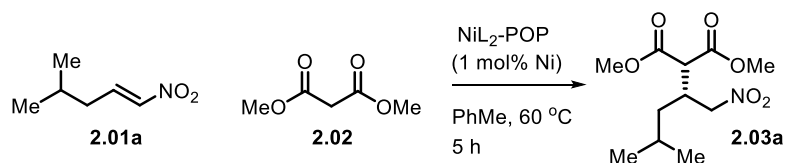
Scheme 2.08. Synthesis of NiL₂ POPs.

We started our investigation by evaluating the nickel-POPs, NiL₁-POP and NiL₂-POP (Scheme 2.09), in the asymmetric Michael addition of the nitroalkene (*E*)-4-methyl-1-nitropent-1-ene (**2.01a**) and dimethyl malonate (Table 2.01). In order to compare activities the reaction was evaluated after just five hours at low catalyst loading (1 mol%) where the reaction was incomplete.



Scheme 2.09. Illustration of NiL₁-POP (left) and of NiL₂-POP (right).

Table 2.01. Evaluation of the nickel-POPs.



Entry	Catalyst	Yield[%] ^[a]	ee [%] ^[b]
1	NiL ₂ L ₁ ₂	69	90
2	NiL ₁ ₂ -POP	69	90
3	NiL ₁ ₂ -POP-PM	65	90
4	NiL ₁ ₂ -POP-PMEmul	59	90
5	NiL ₂ L ₂ ₂	47	88
6	NiL ₂ ₂ -POP	49	89
7	None	0	-

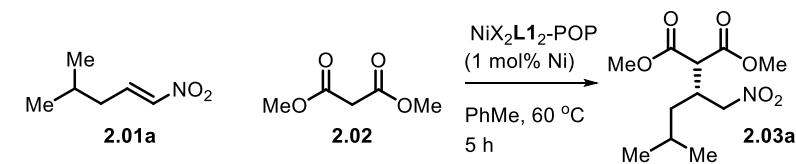
Reaction conditions: **2.01a** (0.25 mmol), **2.02** (0.35 mmol), and 1 mol% catalyst in PhMe (1 mL) at 60 °C for 5 h. [a] Yield determined with ¹H-NMR analysis using dibenzylether as internal standard. [b] Enantiomeric excess determined by chiral-phase HPLC analysis. Adapted from Kramer et al.^[1]

Pleasingly, all the POPs performed as good as the corresponding homogeneous catalysts in regard to both activity and enantioselectivity. The polymer, NiL₁₂-POP, synthesized via an initial metalation followed by polymerization in THF was used for the rest of the project (unless otherwise stated). It showed the highest activity, but more importantly, it was the simplest to prepare, as it could be prepared in a one-pot procedure, allowing for the synthesis of approximately 3 grams pr. batch. With our heterogeneous catalyst in hand, a brief optimization was carried out.

2.3 Optimization

Initially, the effect of the nickel halide precursor was evaluated, as Evans et al. demonstrated that the bromide was 20 % more active than the corresponding chloride or iodide complex.^[24] Strangely, it was found that going down the group the activity increased quite rapidly (Table 2.02). Thus, the study was continued with nickel(II) iodide.

Table 2.02. Effect of the halide.

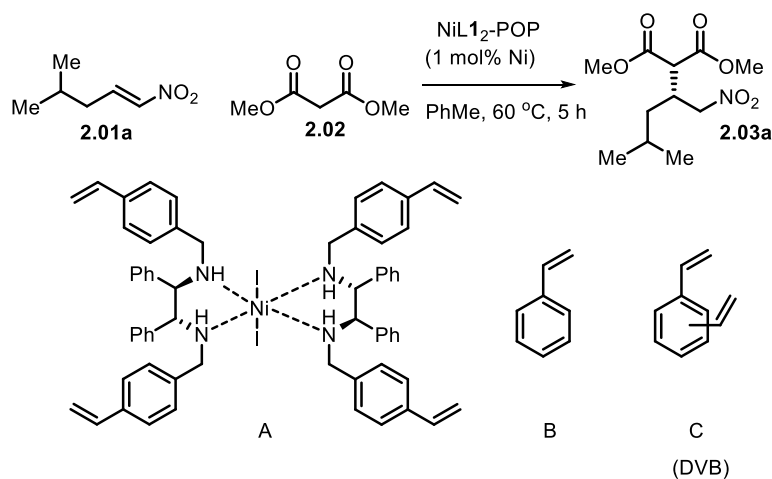


Entry	Halide	Yield[%] ^[a]	ee [%] ^[b]
1	Cl	21	89
2	Br	40	90
3	I	69	90

Reaction conditions: **2.01a** (0.25 mmol), **2.02** (0.35 mmol), and 1 mol% catalyst in PhMe (1 mL) at 60 °C for 5 h. [a] Yield determined with ¹H NMR analysis using dibenzylether as internal standard. [b] Enantiomeric excess determined by chiral-phase HPLC analysis. Adapted from Kramer et al.^[1]

Next, the effect of the polymer flexibility was evaluated (Table 2.03). Simply polymerizing the vinyl functionalized complex, NiL1₂, with itself, provided a catalyst with comparable activity, but with a reduced enantioselectivity. Incorporating styrene and divinylbenzene (DVB) significantly increased the enantioselectivity; however, too much styrene had a negative impact on the activity. Additionally, EtOAc and THF were evaluated as alternative solvents, however, toluene gave superior results (Table 2.04). With the optimum catalyst in hand, the catalyst was characterized.

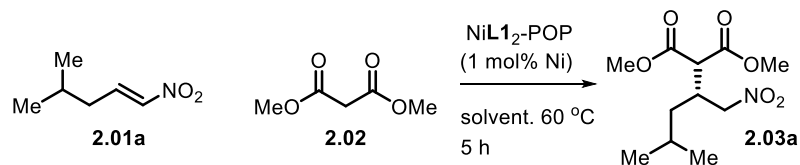
Table 2.03. Effect of styrene equivalents in the POP.



Entry	A:B:C	Yield [%] ^[a]	ee [%] ^[b]
1	1:0:0	66	85
2	1:42:1 ($\text{NiL1}_2\text{-POP}$)	69	90
3	1:84:1	53	90

Reaction conditions: **2.01a** (0.25 mmol), **2.02** (0.35 mmol), and 1 mol% catalyst in toluene (1 mL) at 60 °C for 5 h. [a] Yield determined with ^1H NMR analysis using dibenzylether as internal standard. [b] Enantiomeric excess determined by chiral-phase HPLC analysis. Adapted from Kramer et al.^[1]

Table 2.04. Effect of solvent.



Entry	Solvent	Yield[%] ^[a]	ee [%] ^[b]
1	Toluene	69	90
2	THF	45	81
3	EtOAc	31	89

Reaction conditions: **2.01a** (0.25 mmol), **2.02** (0.35 mmol), and 1 mol% catalyst in solvent (1 mL) at 60 °C for 5 h. [a] Yield determined with ^1H NMR analysis using dibenzylether as internal standard. [b] Enantiomeric excess determined by chiral-phase HPLC analysis.

2.4 Characterization of NiL1₂-POP

The best performing catalyst, NiL1₂-POP, was characterized in detail to determine the origin of its catalytic activity. Thermogravimetric analysis indicated that the catalyst was stable up to 300 °C which is consistent with literature reports for similar materials (Figure 2.01(left)).^[25] It is also a temperature which is much higher than usually required for asymmetric reactions. The porosity and surface area was investigated via N₂-physisorption which indicated the material practically do not possess any inherent porosity: a surface area of 24 m²/g and pore volume of 0.049 cm³/g (Figure 2.01(right)).

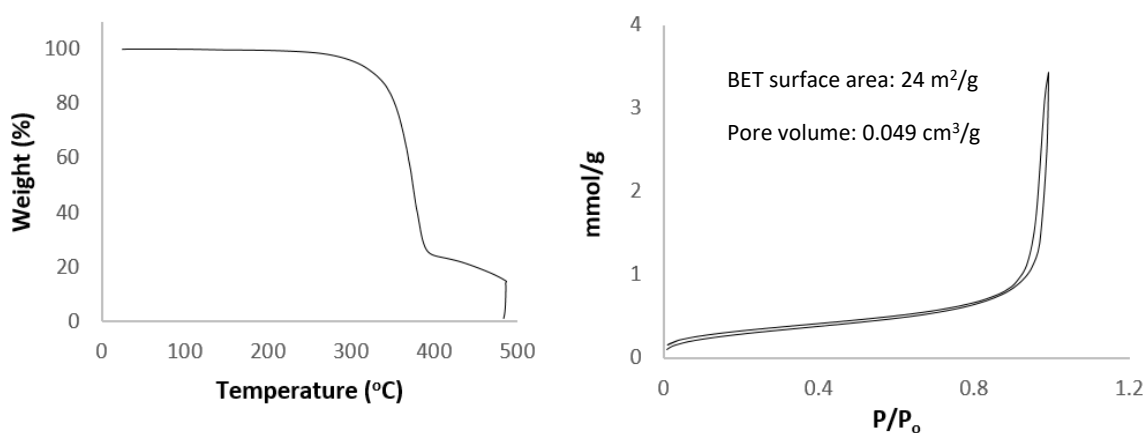


Figure 2.01. Left: Thermogravimetric analysis of NiL1₂-POP. Right: N₂-physisorption analysis of NiL1₂-POP. Adapted from Kramer et al.^[1]

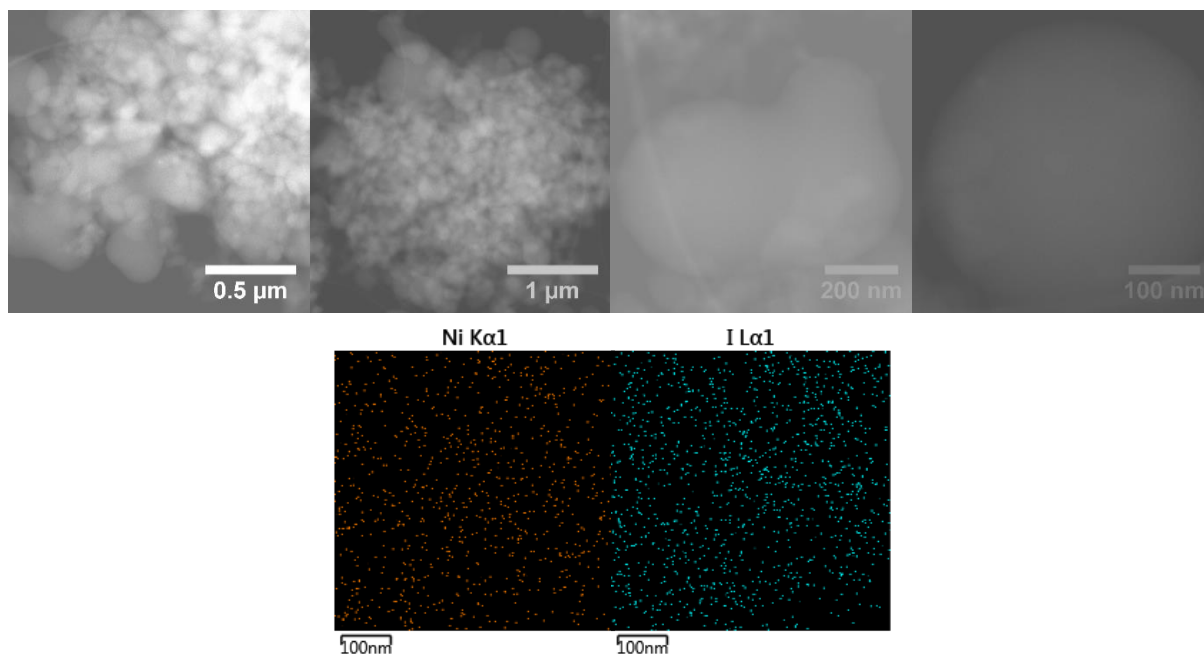


Figure 2.02. Top: Transmission electron microscopy images of NiL1₂-POP. Bottom: Energy-dispersive X-ray analysis of nickel (left) and iodide (right). Adapted from Kramer et al.^[1]

Transmission electron microscopy (TEM) revealed that the material did not contain any nanoparticles (Figure 2.02(top)). The coupled energy-dispersive X-ray spectroscopy analysis confirmed the presence of nickel and iodide (Figure 2.02(bottom)).

Scanning Electron Microscopy (SEM) indicated the NiL1₂-POP consisted of both hollow sheets, in the size range 10 µm to 50 µm, and spheres with a broad size distribution ranging from 50 nm to a 1 µm (Figure 2.03).

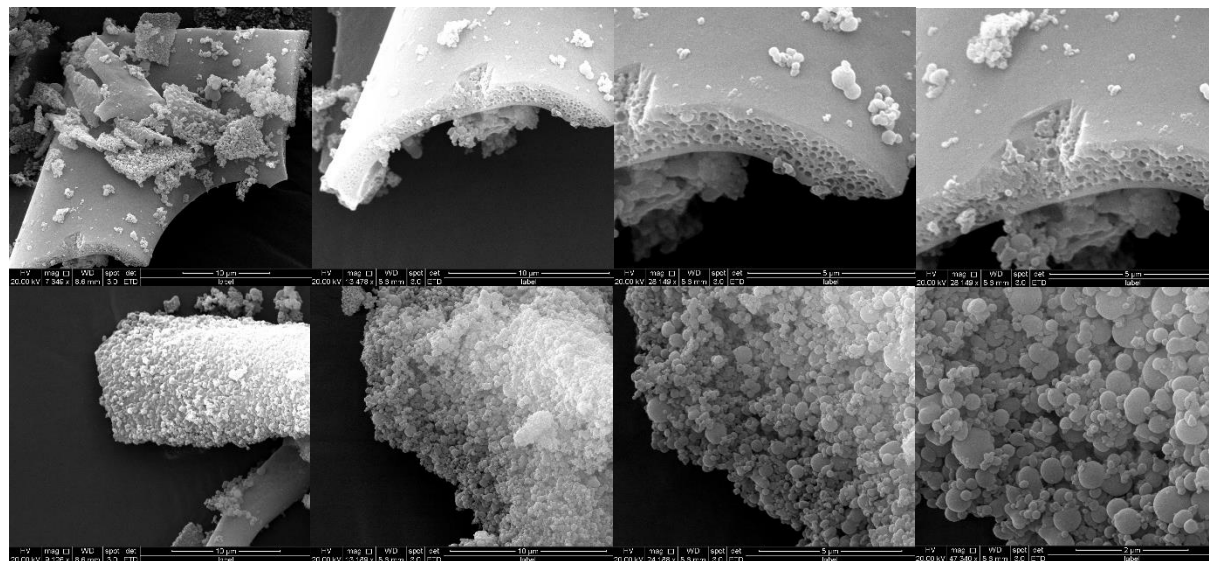


Figure 2.03. Scanning electron microscopy images of NiL1₂-POP. Adapted from Kramer et al.^[1]

To confirm the presence of the ligand, solid ¹³C NMR (¹³C-¹H CP/MAS NMR) of the material was conducted. Unfortunately, it was not possible at the time to obtain a spectrum with 15 kHz spinning which eliminates the spinning bands. The relatively low ligand concentration (relative to styrene) and its proximity to the paramagnetic nickel, broadening the signals even further, made it quite challenging to identify the ligand. One signal in the aromatic area in-between the styrene's two aromatic signals was believed to origin from the ligand (Figure 2.04).

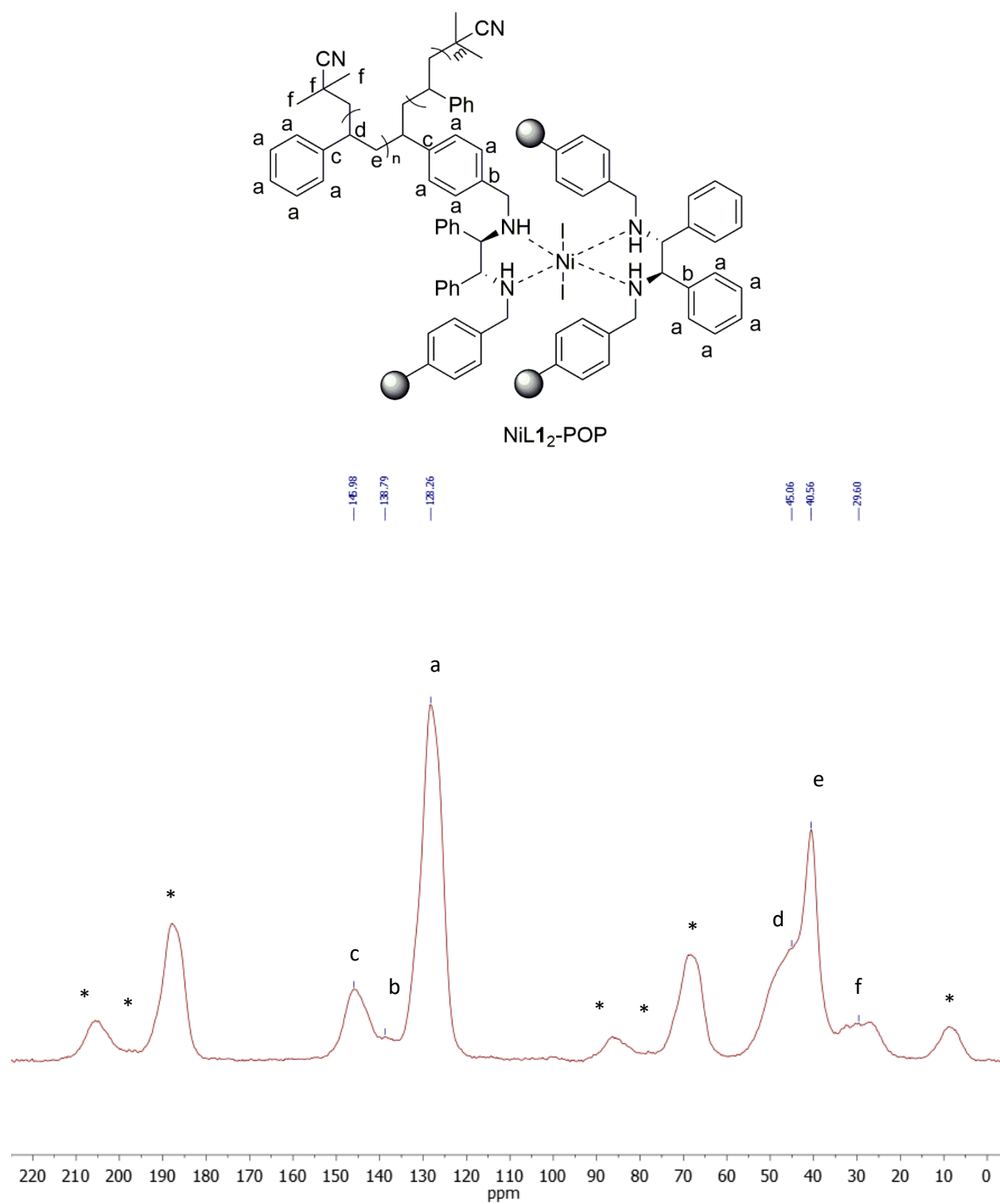


Figure 2.04. ^{13}C - ^1H CP/MAS NMR of the $\text{NiL1}_2\text{-POP}$ at a spinning frequency of 9 kHz, CP contact time 1.5 ms and 5 seconds interscan delay. *= spinning sidebands. Adapted from Kramer et al. ^[1]

Although the presence of nickel, iodide and the ligand were confirmed in the catalyst, it was not possible to obtain conclusive results proving the presence of the active nickel complex. As the nickel complex was paramagnetic, electron paramagnetic resonance (EPR) measurements were carried out, unfortunately the homogeneous nickel complex is silent in the standard EPR regime (9.5 GHz). X-ray photoelectron spectroscopy analysis was also carried out to compare the homogeneous metal complex and the heterogeneous material. However, the concentration of surface nickel was not sufficient to obtain a signal. Lastly, ultraviolet-visible spectroscopy analysis was carried out, but the complex did not have a distinct signal, which could be used to relate the homogeneous and heterogeneous catalyst.

Though it was not possible to obtain evidence for the presence of the nickel complex it seems highly unlikely that the homogeneous complex and three different POPs, based on the homogeneous complex, all have the same enantioselectivity and nearly identical activities, unless the catalysis origins from the same metal complex.

2.5 Recycling

The reusability of the polymer is the most essential feature as it is the main purpose of heterogenization. After a reaction, the polymer was easily isolated from the reaction mixture by centrifugation after addition of hexane: ether (4:1). The addition of ether and hexane “deswells” the polymer which allows it to solidify at the bottom of the centrifuge tube where it can be isolated through decanting. Prior to a new reaction, the catalyst was dried in vacuum overnight. Fortuitously, the NiL1₂-POP was capable of carrying out three consecutive reactions with no loss in selectivity or activity, evident by the yield after five hours, but after the 3rd reaction the activity unfortunately started diminishing (Figure 2.05). Despite the deactivation, the catalyst obtained an impressive TON of 450 after the five reactions, almost five times better than previous reports (95 for batch and 63 for continuous flow).^[15]

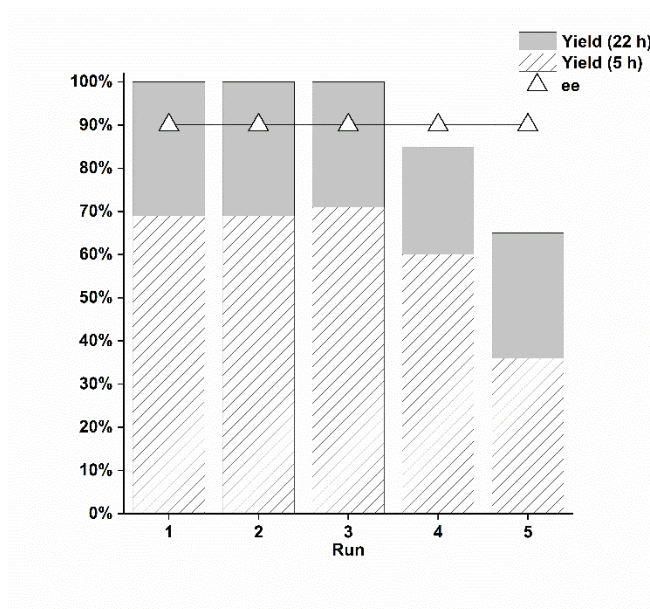
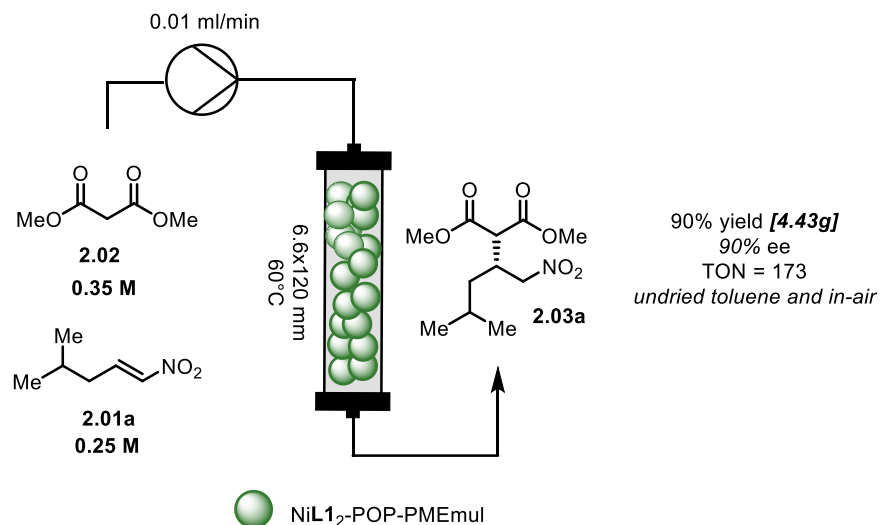


Figure 2.05 – Recycling experiments including activity tests (yields at 5 hours). Reaction conditions **2.01a** (0.25 mmol), **2.02** (0.35 mmol) and 1 mol% NiL1₂-POP in PhMe (1 mL) at 60 °C for 22h. [a] Yield determined with ¹H NMR analysis using dibenzylether as internal standard. [b] Enantiomeric excess determined by chiral-phase HPLC analysis.

To further demonstrate the applicability of the catalyst, it was evaluated in a continuous flow setup (Scheme 2.10). It was found that the polymer prepared by emulsion polymerization, NiL1₂-POP-PMEmul, was better suited for this reaction setup. NiL1₂-POP-PMEmul showed good stability and was operated for five consecutive days before deactivation began. After five days, 4.43 grams of product were isolated, corresponding to a TON of 173. Despite the TON is significantly lower than the one obtained via batch recycling, it is almost three times higher than previous reports.^[15]



Scheme 2.10. – Illustration of the reaction in continuous flow setup. Adapted from Kramer et al.^[1]

Unfortunately, we were not able to elucidate the origin of the deactivation. ICP analysis revealed low amounts of leaching, approximately 0.7 % of the nickel content was found in the liquid after 22 hours of reaction. As filtration tests confirmed activity originated from a heterogeneous species it is highly unlikely that nickel leaching is the main cause of deactivation. From TEM imaging of the spent catalyst it was evident that no nickel nanoparticles had formed. SEM imaging revealed some change in the morphology, however, this is not believed to be influential, as the polymer did not have a well-defined morphology to begin with (Figure 2.06).

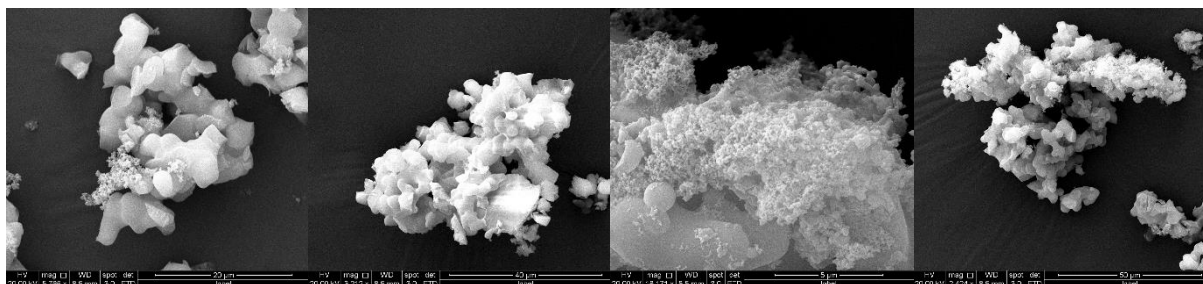


Figure 2.06. Scanning electron microscopy images of NiL1₂-POP after five reactions.

The complex is however, to some extent, sensitive to water. The stability of the metal complex towards water is somewhat unclear at this point. Evans and co-workers claimed the catalyst (nearly same complex) was bench stable for months, whereas Bellamin Lopez claims that after just two days in air, Evans catalyst is almost fully deactivated (38% yield, 0% ee).^{[6][14]} From laboratory experience, the deactivation does not

occur very rapidly even when stored in air. One racemic batch of NiL2_2 was used for multiple months without severe deactivation observed. Nonetheless, the catalyst is definitely not stable in water, and hydrolysis presumably happens much more rapidly in solution. Thus, exposure to water in the polymer's swelled state is a plausible cause of deactivation.

This is consistent with the more rapid deactivation of the catalyst in the continuous flow setup compared to batch recycling. During the recycling experiments, the reaction was carried out with dried toluene (SPS quality), although the hexane and diethyl ether was undried (HPLC grade), they deswell the polymer presumably making it less prone to hydrolysis additionally hexane generally contain less water than toluene. In the continuous flow setup, HPLC grade toluene was used instead of SPS quality. Herein, the polymer is in its swelled state and the reaction takes place at elevated temperatures (60 °C). The flow setup was running continuously for five consecutive days, potentially exposing it to a significant amount of water. This could easily be investigated by integrating a drying column (in combination with SPS grade toluene) prior to the reaction; but due to time limitations, this hypothesis was not further investigated.

2.6 Scope

To evaluate the generality of the system an investigation of the reaction scope was carried out. Initially, the malonate source was evaluated (Table 2.05). Exchanging the methyl groups of the malonate ester to either ethyl or isopropyl had little impact on activity and none on enantioselectivity. The very bulky *tert*-butyl group significantly reduced the activity, but did not affect the enantioinduction.

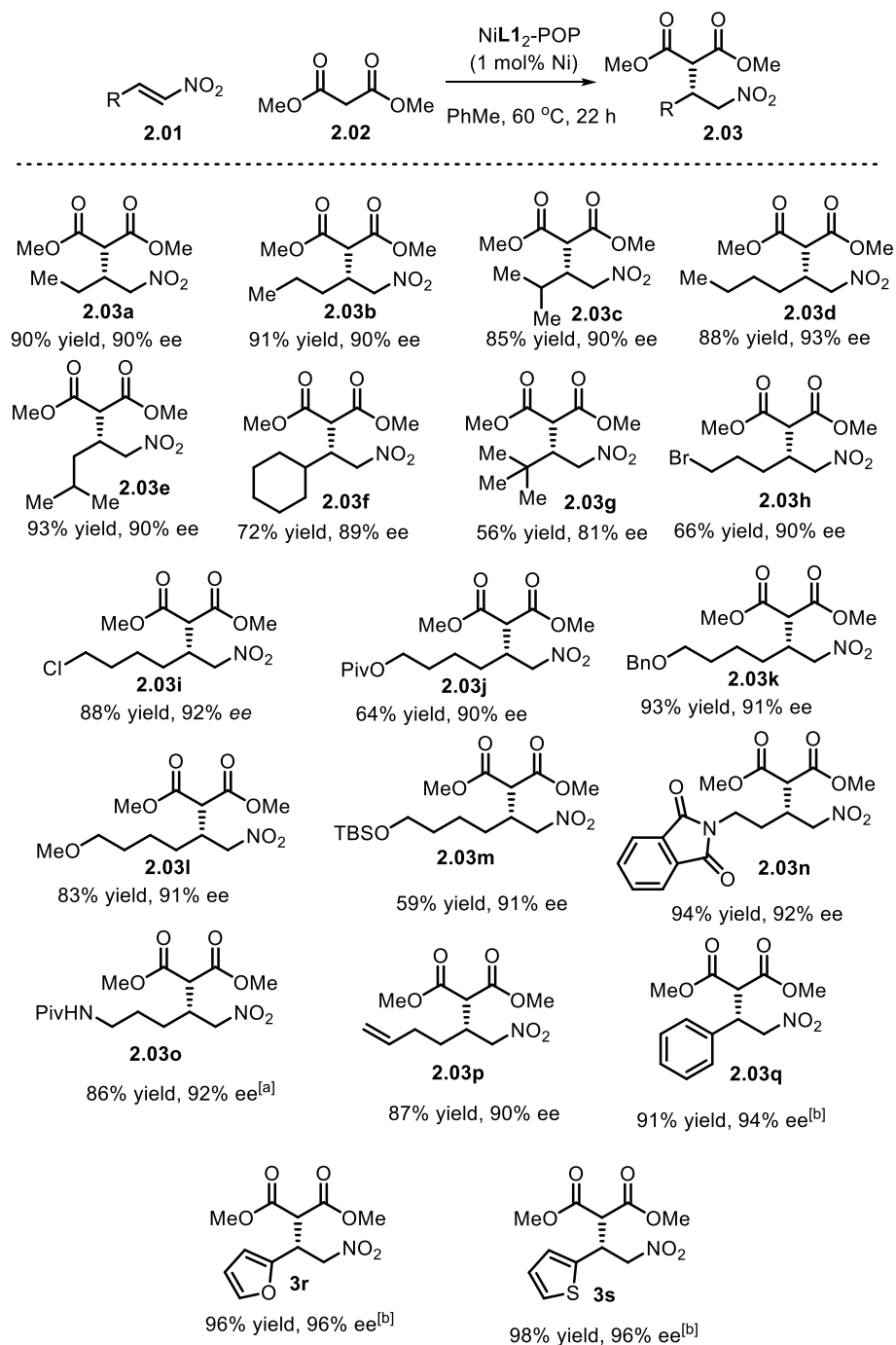
Table 2.04. Malonate Scope.

Entry	R	Yield at 5h [%] ^[a]	Yield at 22h [%] ^[a]	ee [%] ^[b]
1	Me	69	100	90
2	Et	75	100	90
3	<i>i</i> -Pr	65	100	90
4	<i>t</i> -Bu	40	80	90

Reaction conditions: malonate ester (0.35 mmol), **2.01a** (0.25 mmol), and 1 mol% $\text{NiL1}_2\text{-POP}$ in PhMe (1 mL) 60 °C for 22 h. [a] Yield determined with ^1H NMR analysis using dibenzylether as internal standard. [b] Enantiomeric excess determined by chiral-phase HPLC analysis. Adapted from Kramer et al.^[1]

Subsequently, the scope of the nitroalkene was investigated (Scheme 2.11). Generally, examples of aliphatic nitroalkenes are quite scarce in the literature and examples of functionalized aliphatic alkenes non-existing. To broaden the utility of the reaction the sterically influence of the carbon scaffold and the presence of functional groups were investigated. First, the influence of the chain lengths were evaluated; increasing the lengths of the alkyl chain (**2.03a**, **2.03b**, and **2.03d**) had no impact on the yield or enantioselectivity. Next, more bulky substrates were tested, the *iso*-propyl substrate (**2.03c**) proceeded smoothly providing good yields and enantioselectivity. The bigger cyclohexane (**2.03f**) motif also provided good enantioselectivity but with some yield erosion. The extremely bulky *tert*-butyl group (**2.03g**) proved more challenging decreasing both enantioselectivity and yield significantly.

Gratifyingly, the reaction tolerated a broad range of functionalities, even some sensitive functional groups, all providing good enantioselectivity (>90%)(Scheme 2.11). The functional groups included a primary alkyl bromide (**2.03h**), a primary alkyl chloride (**2.03i**), a pivaloyl ester (**2.03j**), a benzyloxy ether (**2.03k**), a methoxy ether (**2.03l**), a silyl ether (**2.03m**), a phtalimido-protected amine (**2.03n**), a pivaloyl amide (**2.03o**) and a terminal alkene (**2.03p**). To illustrate the generality of the scope three (hetero)aromatic substrates (**2.03q-2.03s**) were included all providing good to excellent yield and enantioselectivity at room temperature.



Scheme 2.11. Scope of nitroalkenes Reaction conditions: , **2.01** (0.375 mmol), **2.02** (0.525 mmol) and 1 mol% catalyst in toluene (1.5 mL) 60 °C for 22 h. [a] 2 mol% $\text{NiL1}_2\text{-POP}$, 72h. [b] Room temperature. Yields after isolation. Enantiomeric excess determined by chiral-phase HPLC analysis. Adapted from Kramer et al.^[1]

Most of the products appeared as yellow or colorless oils, but the phthalimido-protected amine (**2.03n**) appeared as a crystalline solid. Fortunately, it was possible to obtain X-ray suitable crystals of the product (Figure 2.07). From single crystal X-ray analysis the absolute stereochemistry of the product was determined as the (*R*) product. The compounds of same class (alkyl products) were tentatively assigned as (*R*) as well.

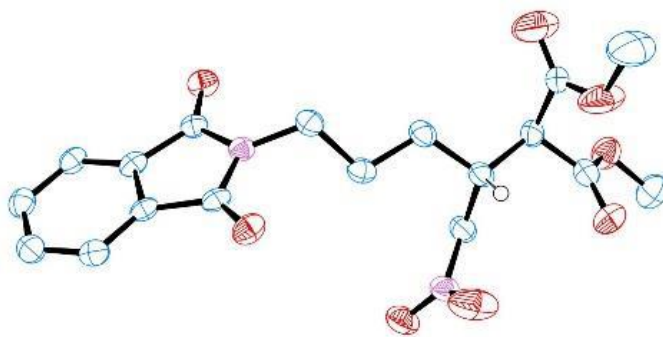
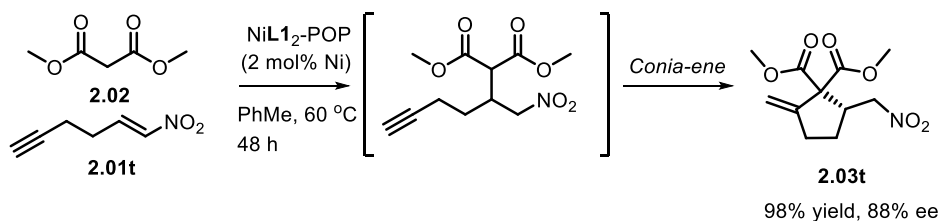


Figure 2.07. X-ray crystal structure of **2.03n** (ellipsoids are shown at 50% probability, and most hydrogens are omitted for clarity). Adapted from Kramer et al.^[1]

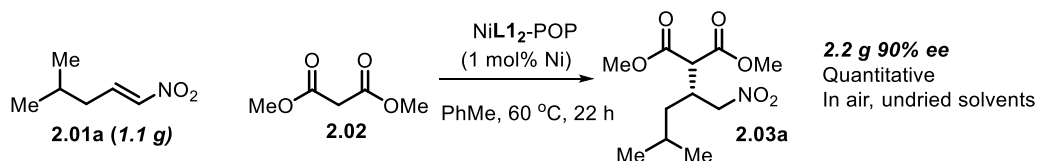
A substrate carrying a terminal alkyne was also synthesized, **2.01t**, but when using it with the standard reaction conditions a mixture of the expected product and a cyclized *exo*-methylenecyclopentane product (**2.03t**) were obtained. Stirring a mix of the two products in toluene for 24 hours at 60 °C without NiL1₂-POP did not alter the ratio of the two products indicating that the catalyst catalyzes both steps. Increasing the catalyst loading to 2 mol% and prolonging the reaction time to 48 hours furnished the cyclized product in quantitative yield and 88% *ee* (Scheme 2.12). There are no previous reports on a Michael addition/conia-ene tandem reaction solely catalyzed by one catalyst. Additionally, there is no previous reports of a [4+1] annulation of a malonate and an alkyne functionalized nitroalkene.^{[26][27]}



Scheme 2.12. A novel tandem reaction, both steps are catalyzed by NiL1₂-POP. Adapted from Kramer et al.^[1]

2.7 Applications

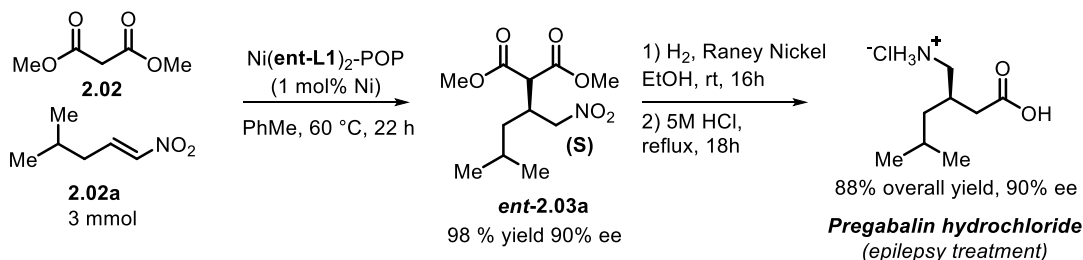
To illustrate the application potential of the methodology, a multigram batch reaction was carried out. Running the reaction in air and with undried solvents on 8.4 mmol scale provided the product in quantitative yields and 90% *ee* (Scheme 2.13).



Scheme 2.13. Gram-scale reaction. Adapted from Kramer et al.^[1]

Additionally, as previously described, the reaction could also be carried out in a continuous flow system also providing the product in gram scale (4.43 grams).

To highlight the relevance of the catalytic system, the blockbuster drug Pregabalin was synthesized. In order to obtain the correct stereoisomer (S), the opposite enantiomer of the catalyst was prepared, $\text{Ni}(\text{ent-L1})_2\text{-POP}$. This was easily carried out using the same procedure. As expected, when carrying out the reaction of substrate **2.01a** with $\text{Ni}(\text{ent-L1})_2\text{-POP}$ in 3mmol scale, the product **ent-2.03a** was furnished in 98% yield and 90% *ee*. In just two steps from **ent-2.03a** Pregabalin was synthesized in 88% overall yield and 90% *ee*, emphasizing the relevance for medicinal chemistry (Scheme 2.14).



Scheme 2.14. Synthesis of Pregabalin. Adapted from Kramer et al.^[1]

2.8 Conclusion

To summarize, a polystyrene-bound chiral nickel(II) bis(diamine) complex have been synthesized. The POP could be used as a heterogeneous catalyst in the asymmetric Michael addition reaction of malonates to aliphatic nitroalkenes, providing high yields and enantioselectivity. It was demonstrated that the catalyst had activity and selectivity on par with the homogeneous catalyst while showing good recyclability. The catalyst was compatible with a continuous flow setup capable of running for five consecutive days before deactivation was observed.

It was demonstrated for the first time, with our protocol, that various functional groups is tolerated in the asymmetric Michael addition reaction of malonates to aliphatic nitroalkenes, including sensitive groups. Additionally, an unprecedented tandem reaction between malonates and an alkyne pendant nitroalkene affording an enantioenriched *exo*-methylenecyclopentane was discovered. The system could easily be scaled up to multigram-scale both in batch and in flow. Lastly, to underline the relevance of the reaction in medicinal chemistry, the protocol was used to prepare the blockbuster drug Pregabalin.

2.9 Outlook – POPs

This project demonstrates that some organometallic complexes can be immobilized in polystyrene without losing activity or selectivity. To further improve the work, investigations towards improving the stability, especially within the continuous flow setup, should be the focus. However, before moving further one should consider if porous organic polymers have potential in the chemical industry?

Within asymmetric catalysis in academia, it is common that papers include a preparation of an enantiomerically enriched pharmaceutical utilizing the novel catalytic system. Some of these catalytic systems, as the one presented in this chapter, is suitable for immobilization. While this sound ideal for the pharmaceutical industry, very few non-hydrogenation reactions deliver *ee*'s exceeding 99%. Consequently, recrystallization would be required to reach satisfactory enantiomeric excess. Thus, synthetic routes where enzymes or hydrogenations can be implemented to deliver the stereogenic control remains preferred. In the case of Pregabalin, examples of both enzymatic and hydrogenation routes exists, providing up to 99.8% *ee* and 97.4% *ee*, respectively (without recrystallization).^{[28][29]}

While non-hydrogenation asymmetric catalysis is not yet relevant for pharmaceuticals, it could be relevant in other areas where enantiomeric excess is crucial albeit lower standards are acceptable, as the fragrance and flavour industry.

With catalytic asymmetric hydrogenation reactions favoured in the synthesis of chiral pharmaceuticals, typically based on expensive metals (Ir and Rh) in combination with expensive chiral ligands, these systems should be ideal for POPs.^{[30][31]} However, one should consider that they often are extremely efficient capable of reaching TONs around 10^5 in single runs. At this time, immobilizing strategies, including porous organic polymers, struggle to maintain the activities of such efficient systems. Another issue concerning recycling of catalysts is related to the quality of the product. With deactivation of the catalyst, changes in the impurity profiles might occur, potentially leading to batches that does not meet the correct specifications.^[32–34]

The future of porous organic polymers in the chemical industry remains unresolved. While I am skeptical about its potential in a batch setting where it introduces an increased complexity to the operation, it could play a key role in the expanding of continuous flow process within the fine chemical industry. However, the continuous advancement in catalysis with more earth-abundant metals, like nickel, might promote POPs. The transition towards earth-abundant metals in combination with complex ligands might change focus of reusing the metal towards reusing the ligands, as they become, relative to the metal, increasingly valuable. In this regard, POPs are excellent candidates as the ligands are covalently attached thus preventing ligand “leaching”.

2.10 References

- [1] M. B. Buendia, S. Kegnaes, S. Kramer, *Adv. Synth. Catal.* **2020**, 362, 5506.
- [2] H. Li, Y. Wang, L. Tang, F. Wu, X. Liu, C. Guo, B. M. Foxman, L. Deng, *Angew. Chem., Int. Ed.* **2004**, 44, 105–108.
- [3] T. Tsubogo, H. Oyamada, S. Kobayashi, *Nature* **2015**, 520, 329–332.
- [4] J. Ji, D. M. Barnes, J. Zhang, S. A. King, S. J. Wittenberger, H. E. Morton, *J. Am. Chem. Soc.* **1999**, 10215–10216.
- [5] M. Watanabe, A. Ikagawa, H. Wang, K. Murata, T. Ikariya, *J. Am. Chem. Soc.* **2004**, 11148–11149.
- [6] D. A. Evans, D. Seidel, *J. Am. Chem. Soc.* **2005**, 127, 9958–9959.
- [7] T. Okino, Y. Hoashi, Y. Takemoto, *J. Am. Chem. Soc.* **2003**, 125, 12672–12673.
- [8] T. Okino, Y. Hoashi, T. Furukawa, X. Xu, Y. Takemoto, *J. Am. Chem. Soc.* **2005**, 127, 119–125.
- [9] M. Terada, H. Ube, Y. Yaguchi, *J. Am. Chem. Soc.* **2006**, 128, 1454–1455.
- [10] H. Li, Y. Wang, L. Tang, L. Deng, *J. Am. Chem. Soc.* **2004**, 126, 9906–9907.
- [11] J. Ye, D. J. Dixon, P. S. Hynes, *Chem. Commun.* **2005**, 4481–4483.
- [12] T. Tsubogo, Y. Yamashita, S. Kobayashi, *Chem. - A Eur. J.* **2012**, 18, 13624–13628.
- [13] K. Liu, R. Jin, T. Cheng, X. Xu, F. Gao, G. Liu, H. Li, *Chem. - A Eur. J.* **2012**, 18, 15546–15553.
- [14] D. Bissessar, T. Achard, S. Bellemin-Laponnaz, *Adv. Synth. Catal.* **2016**, 358, 1982–1988.
- [15] H. Ishitani, K. Kanai, W. J. Yoo, T. Yoshida, S. Kobayashi, *Angew. Chem., Int. Ed.* **2019**, 58, 13313–13317.
- [16] K. A. Fredriksen, T. E. Kristensen, T. Hansen, *Beilstein J. Org. Chem.* **2012**, 8, 1126–1133.
- [17] M. S. Ullah, S. Itsuno, *ACS Omega* **2018**, 3, 4573–4582.
- [18] I. Billault, R. Launez, M. Scherrmann, *RSC Adv.* **2015**, 5, 29386–29390.
- [19] X. Xu, T. Cheng, X. Liu, J. Xu, R. Jin, G. Liu, *ACS Catal.* **2014**, 4, 2137–2142.
- [20] A. M. Goldys, M. G. Núñez, D. J. Dixon, *Org. Lett.* **2014**, 16, 6294–6297.
- [21] T. Wang, Y. Lyu, K. Xiong, W. Wang, H. Zhang, Z. Zhan, Z. Jiang, Y. Ding, *Chinese J. Catal.* **2017**, 38, 890–898.
- [22] A. Cornejo, J. M. Fraile, J. I. García, M. J. Gil, S. V Luis, V. Martínez-Merino, J. A. Mayoral, *J. Org. Chem.* **2005**, 70, 5536–5544.
- [23] H.-J. Nie, J. Yao, Y.-W. Zhong, *J. Org. Chem.* **2011**, 76, 4771–4775.
- [24] D. A. Evans, S. Mito, D. Seidel, *J. Am. Chem. Soc.* **2007**, 129, 11583–11592.
- [25] T. Iwai, T. Harada, H. Shimada, K. Asano, M. Sawamura, *ACS Catal.* **2017**, 7, 1681–1692.
- [26] D. Hack, M. Blümel, P. Chauhan, A. R. Philipps, D. Enders, *Chem. Soc. Rev.* **2015**, 44, 6059–6093.

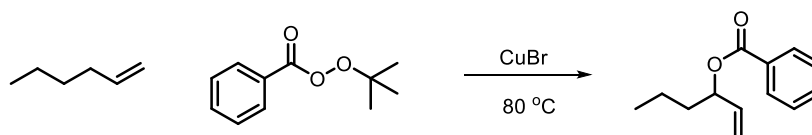
- [27] D. Hack, A. B. Dürr, K. Deckers, P. Chauhan, N. Seling, L. Rübenach, L. Mertens, G. Raabe, F. Schoenebeck, D. Enders, *Angew. Chem., Int. Ed.* **2016**, *55*, 1797–1800.
- [28] C. A. Martinez, S. Hu, Y. Dumond, J. Tao, P. Kelleher, L. Tully, *Org. Process Res. Dev.* **2008**, *12*, 392–398.
- [29] M. J. Burk, P. D. de Koning, T. M. Grote, M. S. Hoekstra, G. Hoge, R. A. Jennings, W. S. Kissel, T. V. Le, I. C. Lennon, T. A. Mulhern, J. A. Ramsden, R. A. Wade, *J. Org. Chem.* **2003**, *68*, 5731–5734.
- [30] C. S. Shultz, S. W. Krska, *Acc. Chem. Res.* **2007**, *40*, 1320–1326.
- [31] N. B. Johnson, I. C. Lennon, P. H. Moran, J. A. Ramsden, *Acc. Chem. Res.* **2007**, *40*, 1291–1299.
- [32] B. Pugin, H. U. Blaser, “*Immobilized Complexes for Enantioselective Catalysis: The Industrial Perspective*” *Heterogenized Homogeneous Catalysts for Fine Chemicals Production*, Springer, **2010**.
- [33] B. Pugin, H.-U. Blaser, *Adv. Synth. Catal.* **2006**, *348*, 1743–1751.
- [34] S. Hübner, J. G. de Vries, V. Farina, *Adv. Synth. Catal.* **2016**, *358*, 3–25.

3) Copper-Catalyzed Alkynylation of Benzylic C-H bonds with Alkynyl Boronic Esters

This chapter describes the work carried out to develop a methodology for the direct alkynylation of benzylic C-H bonds. The work was carried out in collaboration with Jan-George J. Balin (former Master student) and Mette E. Andersen (former Master student) and was published in "Synlett".^[1]

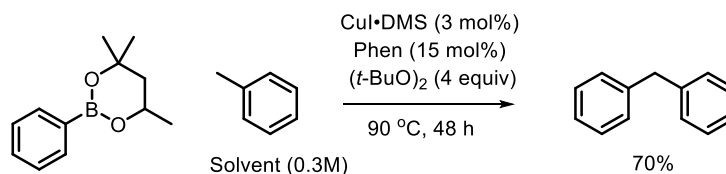
3.1 Background

Kharasch and Sosnovsky reported, in 1958, one of the first copper-catalyzed direct C(sp³)-H functionalizations. They found that *t*-butyl perbenzoate reacts with terminal alkenes to selectively give the branched allylic benzoates in presence of CuBr (Scheme 3.01).^[2]



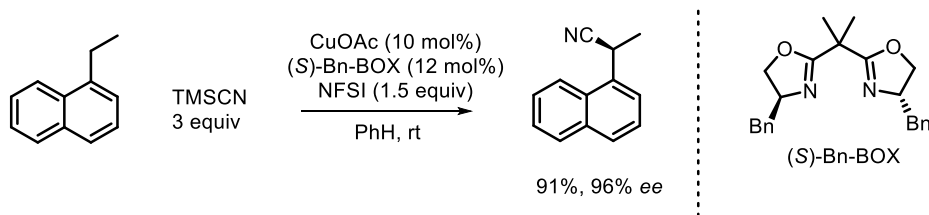
Scheme 3.01. The Kharasch-Sosnovsky reaction discovered in 1958.^[2]

This reaction have indisputably been source of inspiration for the multitude of copper-catalyzed C-H functionalization reactions, generally, consisting of a weak C-H bond, typically benzylic, a nucleophile and a peroxide oxidant, typically di-*tert*-butyl peroxide.^[3–6] Various reactions have been reported using heteroatomic nucleophiles but it was not until 2017, that Stahl and co-workers developed a C-C forming protocol by coupling aryl boronic esters with toluene (Scheme 3.02).^[7]



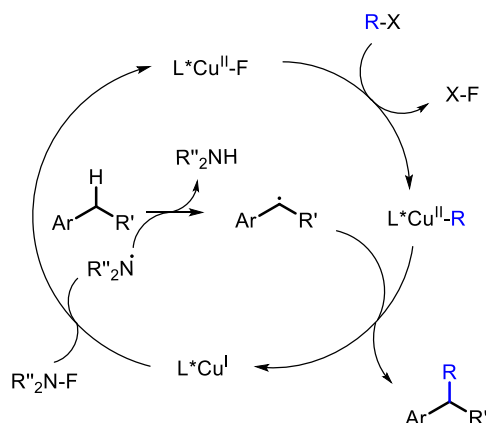
Scheme 3.02. Coupling of toluene with aryl boronic esters by Stahl et al.^[7]

Unfortunately, the use of *tert*-butyl-peroxides necessitates the use of high temperatures to facilitate the homolysis process. This constitutes a major drawback for reactions where a higher degree of selectivity is required, as is the case for enantioselective synthesis. The implementation of a much more reactive reagent, *N*-fluorobenzenesulfonimide (NFSI), have allowed for much more benign conditions, paving the way for copper-catalyzed enantioselective functionalization of benzylic C-H bonds. This was manifested in 2016 by the seminal work of Stahl and Liu et al. on copper catalyzed enantioselective cyanation of benzylic C-H bonds (Scheme 3.03).^[8]



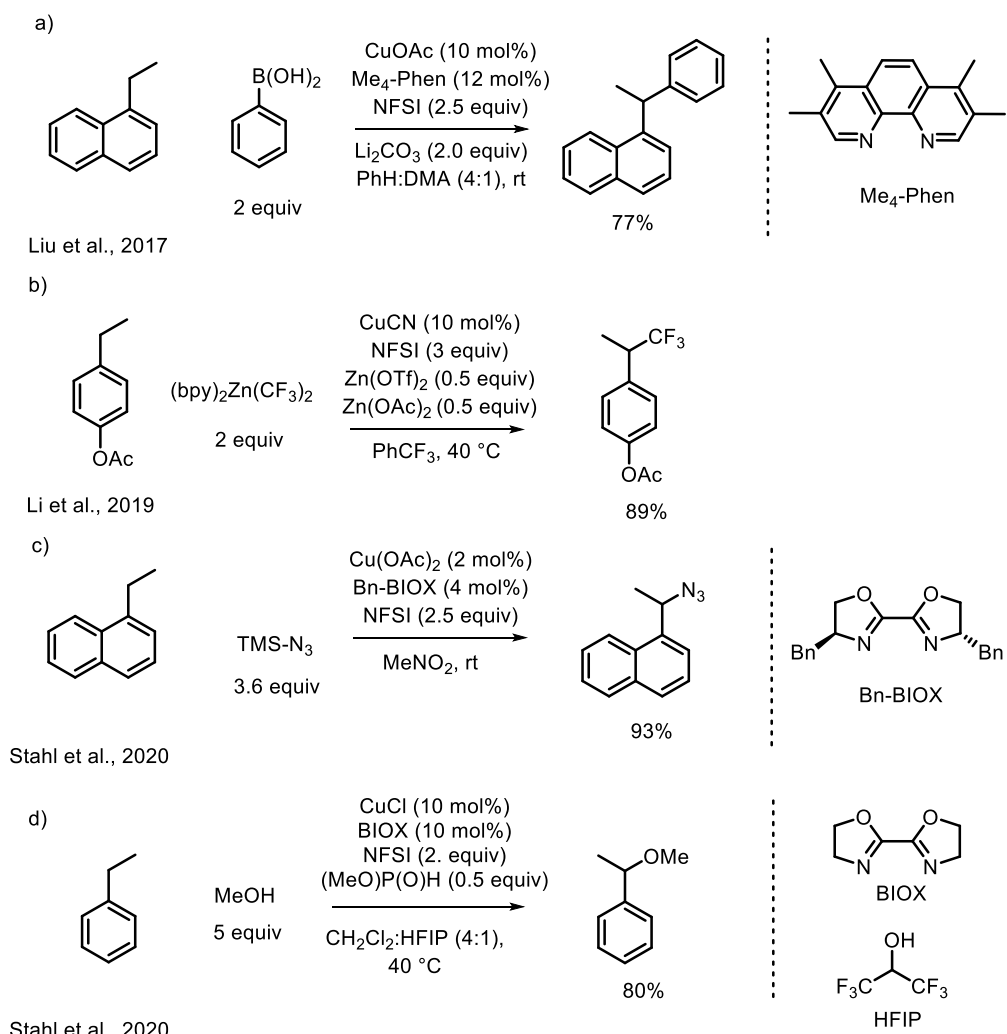
Scheme 3.03. Enantioselective cyanation of benzylic C-H bonds by Stahl and Liu et al.^[8]

The process is believed to go through a radical relay mechanism. Initially, NFSI oxidizes the copper(I) source yielding the corresponding copper(II) fluoride and the amine radical. The amine radical is capable of abstracting a hydrogen from a weak C-H bond. Concurrently, a nucleophile can attach to copper via transmetalation or substitution and subsequently the Cu(II) species can trap the benzylic radical to deliver the product while reforming the Cu(I) species (Scheme 3.04).



Scheme 3.04. Radical relay mechanism.

Since Stahl and Liu's report in 2016, the protocol have rapidly been expanded to efficiently allow a multitude of functionalizations. Already the year after (2017) Liu and co-workers published an arylation protocol, based on a similar protocol, utilizing aryl boronic acids as the nucleophilic coupling partner (Scheme 3.05a).^[9] This procedure was later improved to be enantioselective, affording the enantioenriched benzylic arylation products in good enantiomeric excess (up to 96% ee).^[10] In 2019, Li and co-workers published a protocol for the direct benzylic C-H trifluoromethylation (Scheme 3.05b). The introduction of a trifluoromethyl group is of special interest in agrochemicals and pharmaceuticals due to its privileged properties in permeability and metabolic stability.^[11] In 2020, Stahl and co-workers reported a protocol for the direct benzylic C-H azidation, the method proved very selective for benzylic C-H bonds over other weak C-H bonds (Scheme 3.05c). Despite the use of a chiral ligand (Bn-BIOX), no enantioselectivity was observed.^[12] Same year, Stahl and co-workers developed an alkoxylation protocol, providing high yields for a broad range of substrates, including a range of biological active compounds (Scheme 3.05d).^[13] Additionally, various protocols without nucleophiles, using NFSI as either fluorination reagent or sulfonimidation reagent have been published.^[14–17]



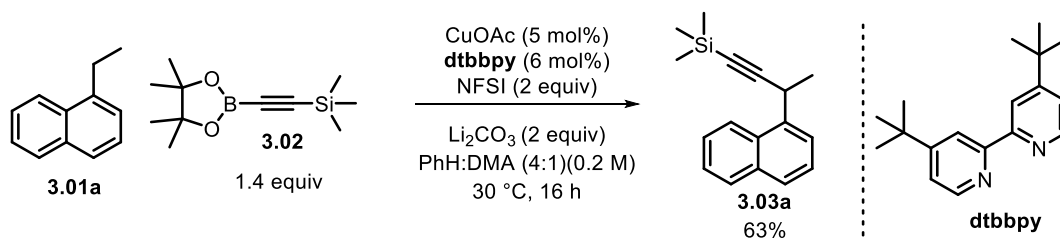
Scheme 3.05. Illustration of previous work in copper-catalyzed radical relay reactions.^[9,11–13]

Inspired by the previous work, we hypothesized that with a similar approach it should be possible to use alkynyl boronic esters as the nucleophilic coupling partner. This would be a powerful transformation due to the versatility of the alkyne motif.

3.2 Project Initiation

Initially, 2-phenyl-1-ethynyl boronic acid pinacol ester was used as the nucleophilic coupling partner, however, after a comprehensive screening results remained unsatisfactory (yields not surpassing 35%). Despite the initial results did not inspire hope, it was decided to change the alkyne source.

Gratifyingly, when exchanging the nucleophilic coupling partner to (trimethylsilyl) ethynyl) boronic acid pinacol ester (**3.02**) good yields were observed (Scheme 3.06). Using conditions similar to what Liu and co-workers used in their initial arylation work; the desired silylethynyl product (**3.03a**) was obtained in 63% isolated yield.^[9]

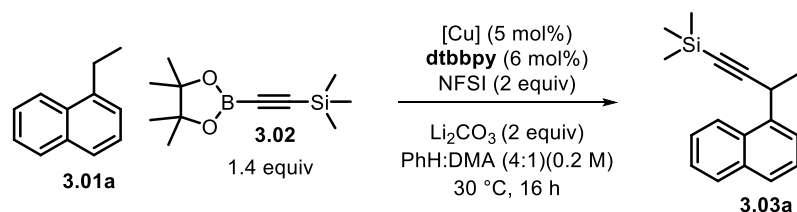


Scheme 3.06. Alkynylation of 1-ethyl-naphthalene. Adapted from Kramer et al.^[1]

3.3 Optimization

Initially, the copper source was screened. In the latest reports of copper catalyzed radical relay both Cu(I) and Cu(II) species have been reported as the catalyst. Accordingly, some Cu(II) species were included, but as CuOAc outperformed Cu(OAc)₂ (65% vs. 58%), Cu(I) species appeared marginally better (Table 3.01, entries 1-2). Additionally, various copper counter ions were tested, but acetate remained the best choice (Table 3.01, entry 2-8). While CuOAc was the best choice, the type of copper source did not appear crucial as most copper species furnished the product in similar yields. Notably, the catalyst loading could be reduced to just 2.5 mol% without any noteworthy reduction in yield (Table 3.01, entry 9), however, increasing the CuOAc loading to 10 mol% did not result in more product formation (Table 3.01, entry 10). A control experiment revealed that copper is crucial for the reaction (Table 3.01, entry 11)

Table 3.01 Evaluation of copper source.

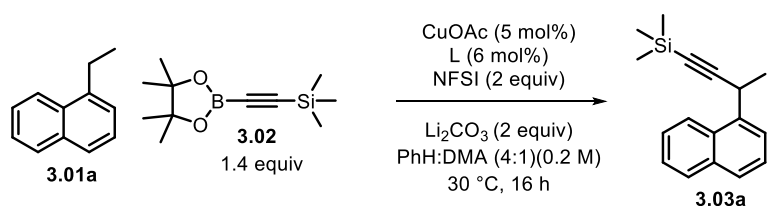
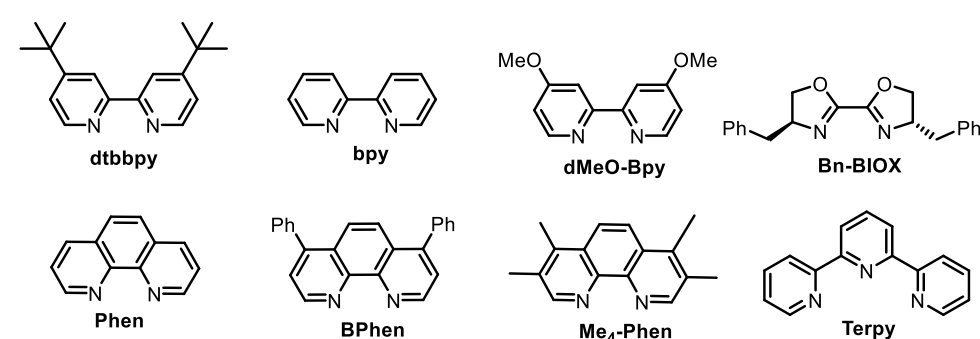


Entry	Copper source	Yield [%] ^[a]
1	CuOAc	65
2	Cu(OAc) ₂	58
3	Cu(OTf) ₂	56
4	CuI·DMS	52
5	CuBr·DMS	51
6	CuCl	53
7	Cu(acac) ₂	47
8	CuSO ₄ ·4H ₂ O	51
9	CuOAc ^[b]	63
10	CuOAc ^[c]	62
11	No Cu ^[d]	6

Reaction conditions: **3.01a** (0.20 mmol), **3.02** (0.28 mmol), Cu (5.0 mol%), **dtbbpy** (6.0 mol%), NFSI (0.40 mmol), Li₂CO₃ (0.40 mmol), PhH:DMA(4:1, 2 mL), 30°C, under argon for 16 hours. [a] Based on ¹H NMR relative to internal standard. [b] 2.5 mol% CuOAc and 3% **dtbbpy**. [c] 10 mol% CuOAc and 12 mol% **dtbbpy**. [d] No **dtbbpy** either.

A ligand screen revealed that a bidentate nitrogen based ligand was crucial for the reaction (Table 3.02, entries 1-7). The tridentate ligand, **Terpy**, only performed marginally better than having no ligand, 26% yield vs. 23% yield (Table 3.02, entries 8-9). Ligands in the bipyridine and in the phenanthroline families performed similarly, but the common ligand, **dtbbpy**, remained the best choice.

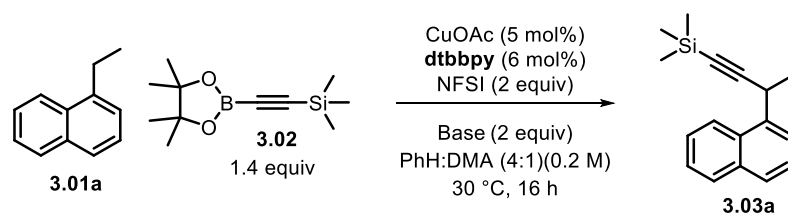
Table 3.02 Evaluation of ligand effect.

		
		
Entry	Ligand	Yield [%] ^[a]
1	dtbbpy	65
2	Bpy	51
3	dMeO-Bpy	52
4	Bn-BIOX	61
5	Phen	52
6	Bphen	64
7	Me ₄ -Phen	60
8	Terpy	26
9	No Ligand	23

Reaction conditions: **3.01a** (0.20 mmol), **3.02** (0.28 mmol), CuOAc (5.0 mol%), ligand (6.0 mol%), NFSI (0.40 mmol), Li₂CO₃ (0.40 mmol), PhH:DMA (4:1, 2 mL), 30 °C, under argon for 16 hours. [a] Based on ¹H NMR relative to internal standard.

For this type of chemistry alkali carbonates seems to be essential. Liu and co-workers found, that for their arylation of benzylic C-H bonds Li₂CO₃ were superior (besides alkali metal carbonates, hydroxides, *tert*-butoxides and flourides were tested).^{[9][10]} Accordingly, a base screen was carried out which consistently with the previous studies found that Li₂CO₃ was the best choice (Table 3.03, entries 1-5).

Table 3.03 Evaluation of bases.

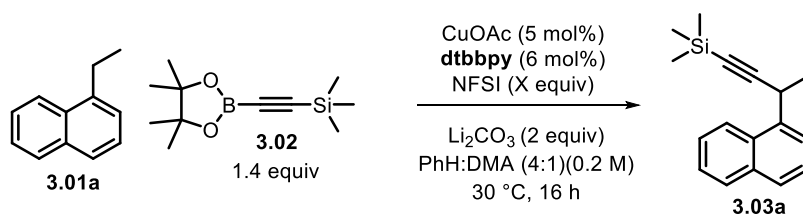


Entry	Base	Yield [%] ^[a]
1	Li ₂ CO ₃	65
2	Na ₂ CO ₃	58
3	K ₂ CO ₃	54
4	Cs ₂ CO ₃	39
5	No base	21

Reaction conditions: **3.01a** (0.20 mmol), **3.02** (0.28 mmol), CuOAc (5.0 mol%), ligand (6.0 mol%), NFSI (0.40 mmol), base (0.40 mmol), PhH:DMA (4:1, 2 mL), 30 °C, under argon for 16 hours. [a] Based on ¹H NMR relative to internal standard.

Next, it was evaluated if increasing the amount of NFSI could further promote the reaction. Incrementally increasing the equivalents of NFSI from two to four did not have any noteworthy effect (Table 3.04, entries 1-4). However, presence of NFSI is crucial for the reaction to occur (Table 3.04, entry 5). Additionally, increasing the equivalents of **3.02** to two equivalents also did not have any impact.

Table 3.04. Evaluation of NFSI equivalence.

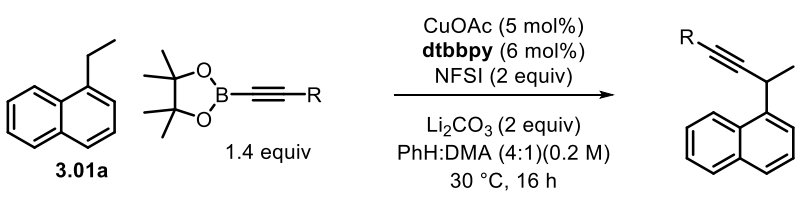


Entry	Equiv NFSI	Yield [%] ^[a]
1	2	65
2	2.5	67
3	3	65
4	4	66
5	No NFSI	0

Reaction conditions: **3.01a** (0.20 mmol), **3.02** (0.28 mmol), CuOAc (5.0 mol%), dtbbpy (6.0 mol%), NFSI (x mmol), Li₂CO₃ (0.40 mmol), PhH:DMA (4:1, 2 mL), 30 °C, under argon for 16 hours. [a] Based on ¹H NMR relative to internal standard.

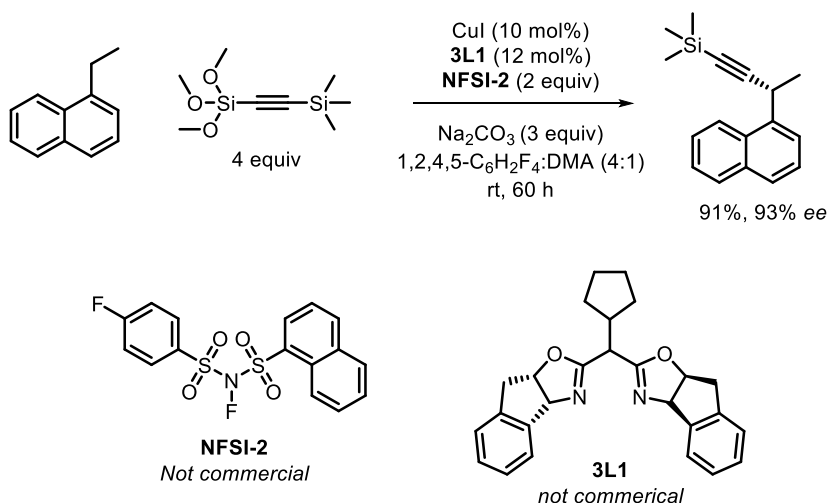
Lastly, an investigation of the nucleophilic partner was carried out. Most silyl groups furnished the desired product in good yield, the *tert*-butyl dimethyl silyl group provided the product in essentially identical yields (Table 3.05, entries 1-2), whereas the other silyl groups slightly reduced the yield (Table 3.05, entries 3-5). However, when changing the silyl group to either a phenyl or a *n*-propyl group the yield was significantly reduced (Table 3.05, entries 6-7). It is not clear why aryl and alkyl substituted alkynyl boronic esters perform poorly. Luckily, the use of silyl substituted alkynyl boronic ester presents an advantage as they allow for easy access of terminal alkynes.

Table 3.05 Evaluation of alkyne nucleophiles.

		
Entry	R	Yield [%] ^[a]
1	TMS	65
2	TBDMS	64
3	TIPS	57
4	DMPS	54
5	TES	58
6	Ph	33
7	<i>n</i> -Pr	17

Reaction conditions: **3.01a** (0.20 mmol), alkynylboronic ester (0.28 mmol), CuOAc (5.0 mol%), **dtbbpy** (6.0 mol%), NFSI (0.40 mmol), Li₂CO₃ (0.40 mmol), PhH:DMA(4:1, 2 mL), 30°C, under argon for 16 hours. [a] Based on ¹H NMR relative to internal standard. Adapted from Kramer et al.^[1]

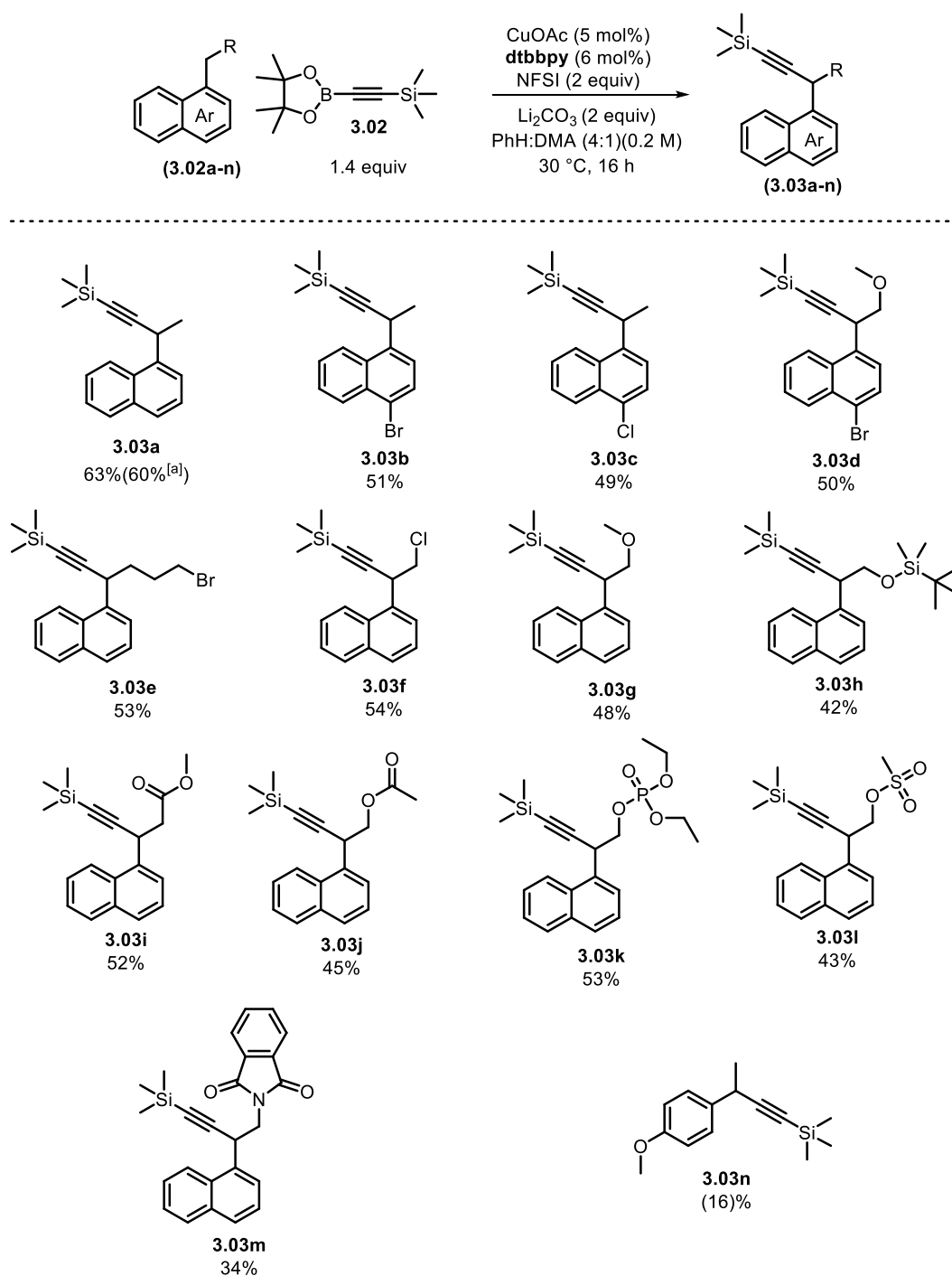
During the course of the project Liu and co-workers published their work on essentially the same reaction (Scheme 3.07). Although a slightly different nucleophile was used, they obtain same product in high yields and even high enantioselectivity.^[18] As the paper by Liu and co-workers had shattered the novelty of the project, it was decided to expedite the project and focus on finishing a small scope.



Scheme 3.07. Liu's report on enantioselective alkynylation of benzylic C-H bonds.^[18]

3.4 Scope

To evaluate the robustness of the protocol a small scope focusing on functional group tolerance was carried out (Scheme 3.08). Gratifyingly, various functional groups were tolerated, albeit with a slight yield erosion. The functional groups include an aryl chloride (**3.03c**), aryl bromides (**3.03b** and **3.03d**), an alkyl bromide (**3.03e**), an alkyl chloride (**3.03f**), a methoxy ether (**3.03g**), a silyl ether (**3.03h**), esters (**3.03i**-**3.03j**), a diethyl phosphonate ester (**3.03k**), a primary methansulfonate (**3.03l**) and a phthalimide-protected amine (**3.03m**). The tolerance towards these sensitive functional groups illustrated the mildness of the reaction conditions. Unfortunately, the protocol was limited to 1-alkyl naphthalenes as the benzylic C-H source. 4-Ethylanisole only furnished the product in 16% (NMR yield), similarly, 2-ethyl naphthalenes were also inactive. However, the reaction could be scaled five times (1 mmol) without any noteworthy changes, **3.03a** was isolated in 60% yield.

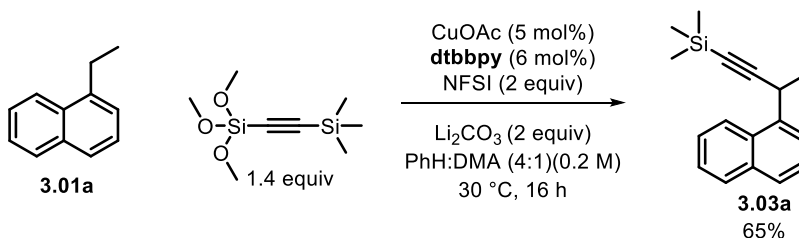


Scheme 3.08. Scope of C-H source in the benzylic C-H alkylation. Reaction conditions: C-H source (0.20 mmol), **3.02** (0.28 mmol), CuOAc (5.0 mol%), **dtbbpy** (6.0 mol%), NFSI (0.40 mmol), Li₂CO₃ (0.40 mmol), PhH:DMA (4:1, 2 mL), 30 °C, under argon for 16 hours. Isolated yields. [a] The reaction carried out in 1 mmol scale, everything scaled 5 times (carried out in 20 mL vial). Adapted from Kramer et al.^[1]

3.5 Investigation of the Reaction Mechanism

Comparison with Liu's protocol

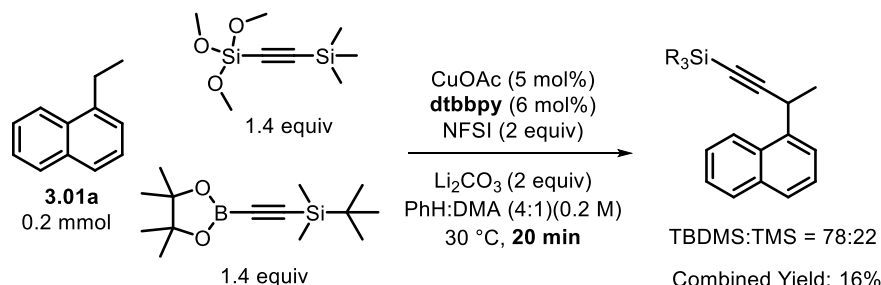
The main difference between the protocol developed by Liu et al. and our protocol was the nucleophile. Accordingly, we decided test their nucleophile under our conditions. Carrying out an experiment with our standard conditions with their trimethoxysilyl nucleophile furnished the desired product in essentially same yield 65% isolated (vs. 63%)(Scheme 3.09).



Scheme 3.09. Alkynylation of 1-ethyl naphthalene using Liu's trimethoxysilyl nucleophile under our reaction conditions. Adapted from Kramer et al.^[1]

Besides using four equivalents nucleophile to achieve high product formation, they also rely on custom-made reagents and ligand, **NFSI-2** and **3L1** in combination with 1,2,4,5 C₆H₂F₄ (Scheme 3.07).^[18] Manipulation of chiral ligands and synthesis of NFSI-type reagents are costly endeavors in addition to the use of 1,2,4,5 C₆H₂F₄, which is an extremely expensive solvent (51 €/mL for 1,2,4,5 C₆H₂F₄ and 0.1 €/mL for PhH (Sigma-Aldrich)). Overall, while Liu and co-workers protocol is very impressive, it is not easy to utilize by others. Contrarily, our protocol can be carried out solely with commercial reagents providing the desired products in synthetic useful yields, (**3.02** is not commercially available – but the TBDMS alkynyl boronic ester is) nicely complementing Liu and co-workers protocol.

When investigating the relative reactivity of the two nucleophiles we found the boronic ester were far more reactive (Scheme 3.10). In order to tell the products apart we used the TBDMS boronic ester nucleophile as it provided the same yield as the TMS (Table 3.05, entries 1 and 2). After 20 minutes, 78% of the formed product came from the boronic ester, while only 22% originated from the trimethoxysilyl nucleophile. Assuming both nucleophiles follow same mechanism, it appears as the transmetalation occurs much faster with the boronic esters.

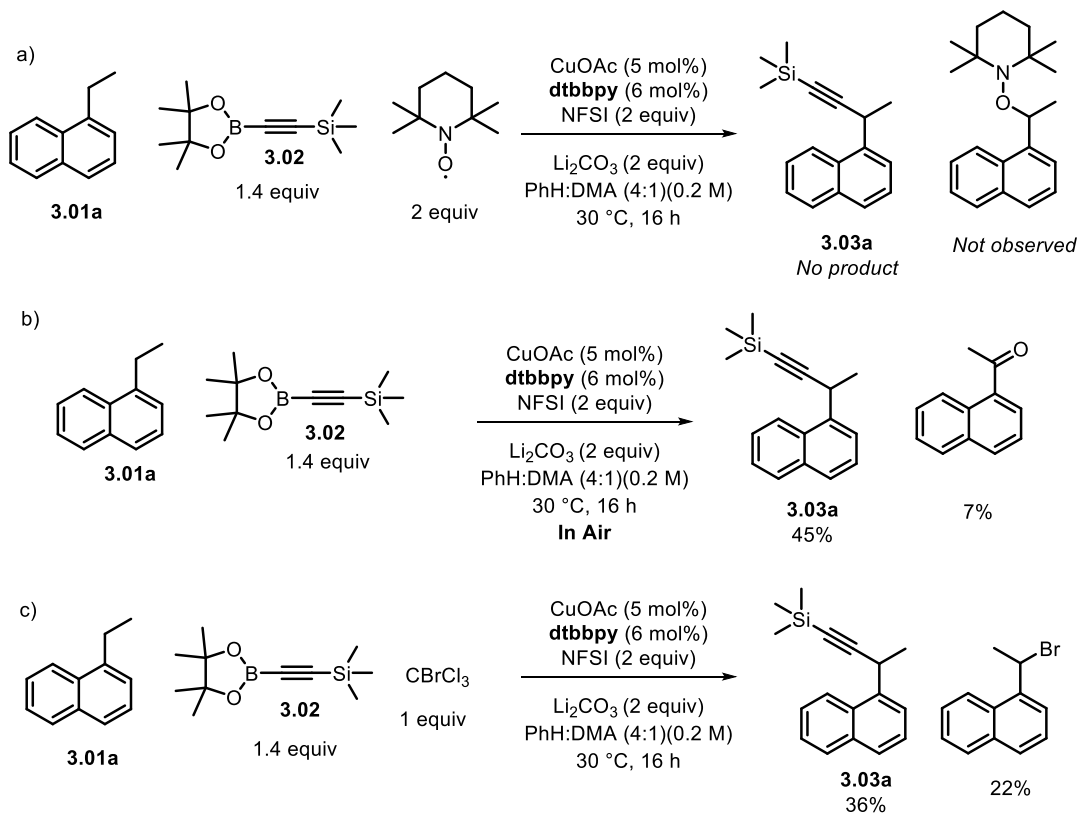


Scheme 3.10. Nucleophile competition in the alkynylation of 1-ethyl naphthalene. Adapted from Kramer et al.^[1]

The Presence of Radicals

As the reaction was believed to proceed via a radical relay process, radical intermediates should be present in the reaction and the addition of radical scavengers should inhibit the reaction. When carrying

out the standard reaction with two equivalents of the radical scavenger, (2,2,6,6-tetramethylpiperidin-1-yl)oxy (TEMPO), no product was observed. Unfortunately, it was not possible to detect the presence of the **3.01a**-TEMPO adduct (Scheme 3.11a). Carrying out the reaction in air, led to a reduction in yield (45% vs. 63%), additionally a ketone species was observed which could arise from the oxygen trapping of a benzylic radical (Scheme 3.11b). Lastly, an experiment containing 1 equiv of bromocarbontrichloride was conducted, which resulted in 22% bromination at the benzylic position (Scheme 3.11c). These experiments all suggest that radical intermediates are present in the reaction.



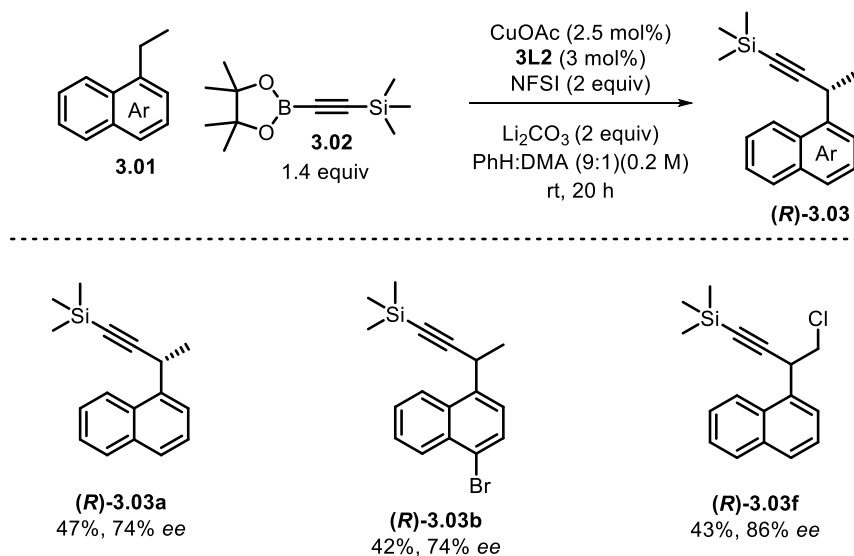
Scheme 3.11. Radical scavenging experiments; TEMPO (a), air (b) and bromocarbontrichloride (c). Adapted from Kramer et al.^[1]

Lastly, we developed an enantioselective procedure, focusing on commercially available reagents. By exchanging the racemic ligand for a BOX ligand, **3L2**, resembling the one used by Liu and co-workers the product was obtained in 68% ee and 47% yield (¹H NMR)(Table 3.06, entry 1). While increasing the catalyst loading slightly increased the ee it decreased the yield (Table 3.06, entry 3). However, reducing the polarity of the solvent by altering the ratio between benzene and DMA significantly increased the ee (from 68% to 76% ee) (Table 3.06, entries 1 and 4). Exchanging benzene for hexafluorobenzene, a cheap alternative to 1,2,4,5-C₆H₂F₄, further increased the enantioselectivity to 85% ee, however, it also severely reduced the yield (Table 3.06, entry 5). Finally, it was found that the catalyst loading could be reduced to solely 2.5 mol% furnishing the product in 48% yield and 78% ee. Again, this result cannot compete with the protocol developed by Liu et al., but stands out, as a cheap more convenient method. To ensure generality of the protocol, three enantioenriched products were synthesized using this protocol (Scheme 3.12).

Table 3.06. Development of an enantioselective protocol.

Entry	Modifications	Yield [%] ^[a]	Enantiomeric Excess [%] ^[b]
1	None	47	68
2	5 h	45	68
3	10% Cu, 12% 3L2 , 5 h	40	70
4	PhH:DMA (9:1)	41	76
5	PhF ₆ :DMA (9:1)	19	85
6	2.5% Cu, 3% 3L2 , PhH:DMA (9:1)	48	78

Reaction conditions: 3.01a (0.20 mmol), 3.02 (0.28 mmol), CuOAc (5.0 mol%), 3L2 (6.0 mol%), NFSI (0.40 mmol), base (0.40 mmol), PhH:DMA(4:1, 2 mL), rt, under argon for 16 hours. [a] Based on ¹H NMR relative to internal standard [b] Enantiomeric excess determined by chiral GC-FID.

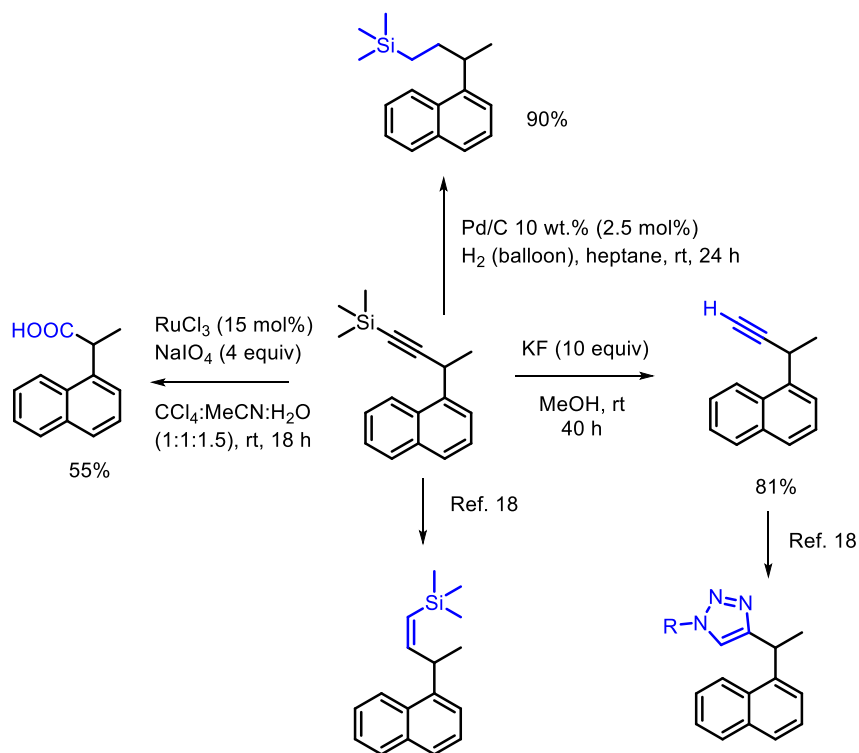


Scheme 3.12. Scope of 1-ethyl naphthalenes in the enantioselective benzylic C-H alkynylation. Adapted from Kramer et al.^[1]

The unambiguous enantioinduction caused by the chiral ligand suggest that the C-C bond formation occurs in close proximity to copper. This observation in combination with the presence of radical intermediates are both consistent with the radical relay mechanism illustrated in Scheme 3.04.

3.6 Applications

The addition of the TMS protected alkyne is an attractive reaction as it is a highly useful functional group that can undergo a multitude of different transformations (Scheme 3.13). It can directly be reduced to either an alkene TMS or an aliphatic TMS or oxidized to a carboxylic acid. The TMS group can easily be removed affording the terminal alkyne. Terminal alkynes are routinely used in copper catalyzed click chemistry with azides, used as nucleophiles in combination with a base, and used in Sonogashira-type cross-coupling reactions.^[19–22]



Scheme 3.13. Product derivatisations. Adapted from Kramer et al.^[1]

3.7 *Conclusion and Outlook*

In this work, we have developed a benign protocol for the direct alkynylation of benzylic C-H bonds using alkynyl boronic esters. The method relies on commercial reagents, low catalyst loading and near-stoichiometric substrate ratios. This is the first example of benzylic C-H alkynylations using alkynyl boronic esters as the nucleophile in the copper-catalyzed radical relay reaction. A substrate scope revealed that 1-alkyl naphthalenes with various functional groups and alkynyl boronic esters bearing terminal silyl groups were well tolerated. Additionally, the trimethoxysilyl alkyne species explored by Liu and co-workers could be utilized in our protocol providing identical reaction outcome, however, it was found that the boronic esters reacted much faster. Lastly, we have demonstrated that when employing chiral ligands the enantioenriched product, 74-86% *ee*, is afforded at room temperature.

Although this project will remain within the shadow of Liu's work, I believe it presents a more approachable methodology. The development of new convenient protocols is an important task towards a more efficient chemical industry. To further improve this work, expanding the scope of C-H substrates to (alkyl-benzenes) benzylic substrates would be extremely valuable as these are much more abundant motifs in the fine chemical industry.

3.8 References

- [1] M. B. Buendia, J.-G. J. Balin, M. E. Andersen, Z. Lian, S. Kramer, *Synlett* **2021**, 32, A-E.
- [2] M. S. Kharasch, G. Sosnovsky, *J. Am. Chem. Soc.* **1958**, 80, 756.
- [3] A. L. García-Cabeza, R. Marín-Barrios, F. J. Moreno-Dorado, M. J. Ortega, G. M. Massanet, F. M. Guerra, *Org. Lett.* **2014**, 16, 1598–1601.
- [4] H.-T. Zeng, J.-M. Huang, *Org. Lett.* **2015**, 17, 4276–4279.
- [5] D. A. Powell, H. Fan, *J. Org. Chem.* **2010**, 75, 2726–2729.
- [6] S. Kramer, *Org. Lett.* **2019**, 21, 65–69.
- [7] A. Vasilopoulos, S. L. Zultanski, S. S. Stahl, *J. Am. Chem. Soc.* **2017**, 139, 7705–7708.
- [8] W. Zhang, F. Wang, S. D. McCann, D. Wang, P. Chen, S. S. Stahl, G. Liu, *Science* **2016**, 353, 1014–1018.
- [9] W. Zhang, P. Chen, G. Liu, *J. Am. Chem. Soc.* **2017**, 139, 7709–7712.
- [10] W. Zhang, L. Wu, P. Chen, G. Liu, *Angew. Chem., Int. Ed.* **2019**, 131, 6491–6495.
- [11] H. Xiao, Z. Liu, H. Shen, B. Zhang, L. Zhu, C. Li, *Chem* **2019**, 5, 940–949.
- [12] S.-E. Suh, S.-J. Chen, M. Mandal, I. A. Guzei, C. J. Cramer, S. S. Stahl, *J. Am. Chem. Soc.* **2020**, 142, 11388–11393.
- [13] H. Hu, S.-J. Chen, M. Mandal, S. M. Pratik, J. A. Buss, S. W. Krska, C. J. Cramer, S. S. Stahl, *Nat. Catal.* **2020**, 3, 358–367.
- [14] Z. Ni, Q. Zhang, T. Xiong, Y. Zheng, Y. Li, H. Zhang, J. Zhang, Q. Liu, *Angew. Chem., Int. Ed.* **2012**, 51, 1244–1247.
- [15] T. Kawakami, K. Murakami, K. Itami, *J. Am. Chem. Soc.* **2015**, 137, 2460–2463.
- [16] J. A. Buss, A. Vasilopoulos, D. L. Golden, S. S. Stahl, *Org. Lett.* **2020**, 22, 5749–5752.
- [17] A. Vasilopoulos, D. L. Golden, J. A. Buss, S. S. Stahl, *Org. Lett.* **2020**, 22, 5753–5757.
- [18] L. Fu, Z. Zhang, P. Chen, Z. Lin, G. Liu, *J. Am. Chem. Soc.* **2020**, 142, 12493–12500.
- [19] B. A. Martek, M. Gazvoda, D. Urankar, J. Košmrlj, *Org. Lett.* **2020**, 22, 4938–4943.
- [20] T. Hundertmark, A. F. Littke, S. L. Buchwald, G. C. Fu, *Org. Lett.* **2000**, 2, 1729–1731.
- [21] S. Neumann, M. Biewend, S. Rana, W. H. Binder, *Macromol. Rapid Commun.* **2020**, 41, 1900359.
- [22] J. Clayden, N. Greeves, S. Warren, *Organic Chemistry*, Oxford University Press, **2012**.

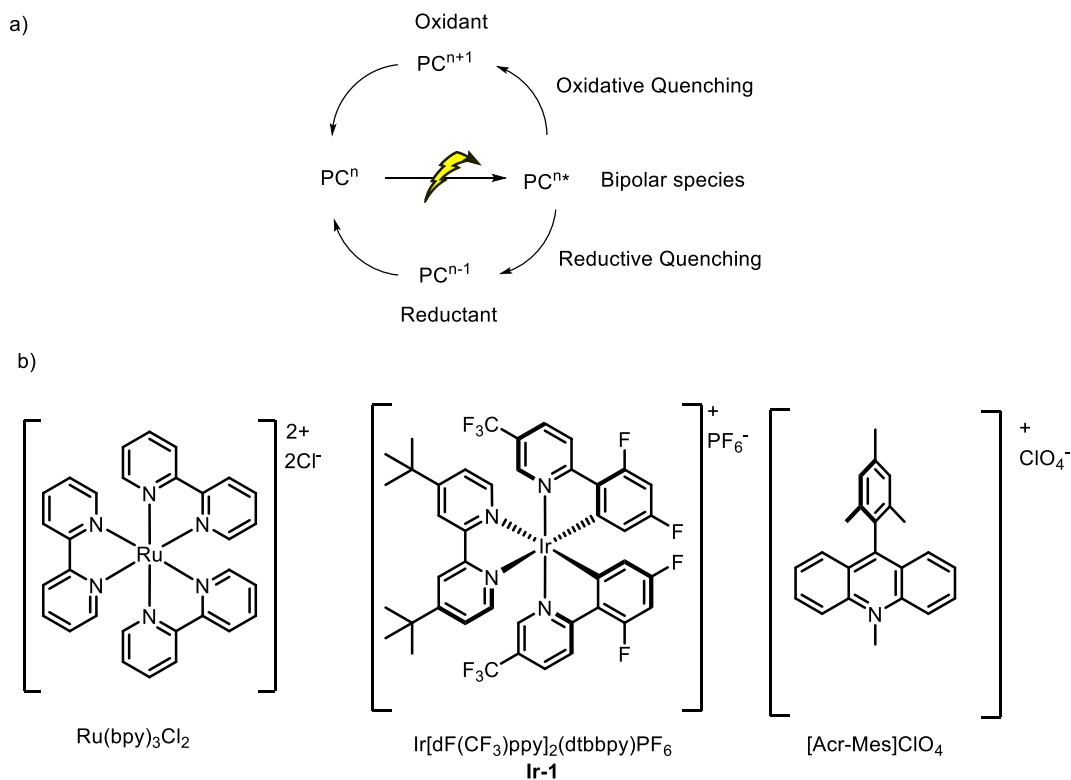
4) Combined Nickel- and Photoredox-Catalyzed Direct C-H Allylic Alkylation

While at external stay in ICIQ, Tarragona, Spain with Prof. Ruben Martin I was introduced to the combination of photoredox and transition metal catalysis. I proposed a new project utilizing combined photoredox and nickel catalysis to functionalize allylic C-H bonds, the project is described in this chapter. While the idea was developed at ICIQ the majority of the work was carried out at DTU.

4.1. Introduction to Photoredox Catalysis in Organic Chemistry

The concept of molecules harnessing visible light to promote its redox properties have been studied for almost 85 years since the synthesis of $\text{Ru}(\text{bpy})_3\text{Cl}_2$ was first reported.^[1] Since then, such molecules have been studied by physicists and inorganic chemists for its application within photovoltaic cells, water splitting and energy storage.^[2-4] But within the last decade the use of photocatalysts within synthetic organic chemistry have sparked great interest.

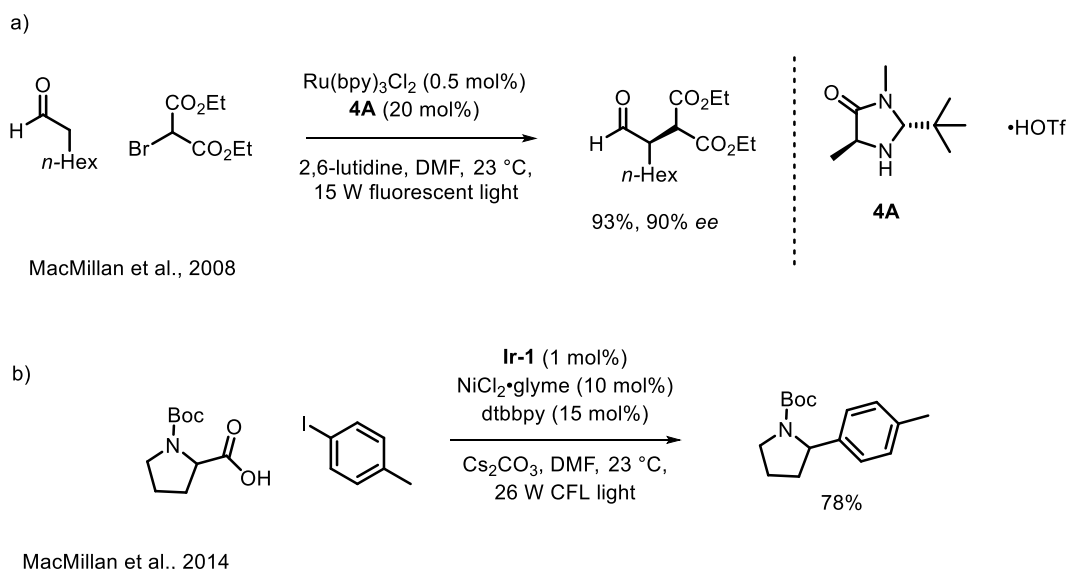
The principle of photocatalysts are based on an efficient visible-light induced formation of a long-lived excited state. This means that when a photocatalyst is excited, it mainly, through intersystem crossing, forms a long-lived triplet state, rather than going back to its ground state through fluorescence. For most of the Ru and Ir based photocatalysts the nature of the triplet state is bipolar, meaning that these species can undergo single electron oxidation or reduction. These processes are called oxidative or reductive quenching (Scheme 4.01a).^[5]



Scheme 4.01. a) The cycles of photoredox catalysts. b) Three common photoredox catalysts.

One of the first examples beautifully merging photoredox catalysis with organocatalysis came in 2008 when Nicewicz and MacMillan disclosed a protocol for a direct asymmetric alkylation of aldehydes. The excited photocatalyst $\text{Ru}(\text{bpy})_3^{2+*}$, oxidizes an organocatalyst-substrate intermediate, resulting in a $\text{Ru}(\text{bpy})_3^+$ species which can reduce an alkyl halide species to form an electron-deficient alkyl radical (Scheme 4.02a).^[6]

Six years later MacMillan in collaboration with Doyle and co-workers published the first work on combined nickel and photoredox chemistry. In here, they demonstrated the decarboxylative cross-coupling of amino-acids with aryl halides. The photocatalyst is responsible for carrying out the decarboxylation to form an alkyl radical, which can combine with a nickel(II) species and subsequently undergo reductive elimination to form the desired product and a nickel(I) species, the reduced photocatalyst reduces the nickel(I) species to nickel(0), reforming both active catalysts simultaneously (Scheme 4.02b).^[7] The merger of nickel and photoredox chemistry have seen a rapid development since its birth in 2014, which this chapter is a testimony to.



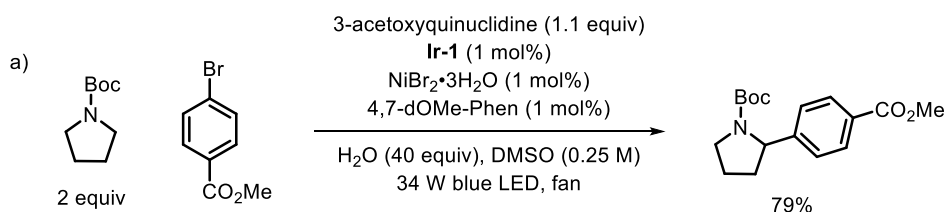
Scheme 4.02. a) The merger of photoredox and organocatalysis.^[6] b) The merger of nickel- and photoredox-catalysis.^[7]

4.2. Background

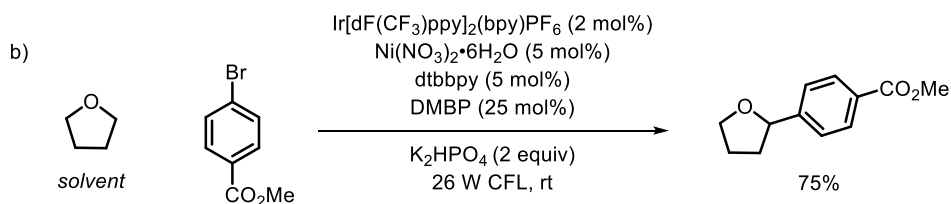
In recent years, combined photoredox and nickel catalysis has emerged as a powerful tool to forge C-C bonds directly from weak C-H bonds. One of the first examples appeared in 2016 when MacMillan and co-workers developed a protocol utilizing a tertiary amine hydrogen atom transfer (HAT) catalyst, a photocatalyst and a nickel catalyst to efficiently couple (hetero)aryl bromides with α -amino and α -oxy $\text{C}(\text{sp}^3)\text{-H}$ bonds (Scheme 4.03a).^[8]

Same year, Molander and co-workers developed a protocol, coupling aryl bromides with α -heteroatom (N, O, S) $\text{C}(\text{sp}^3)\text{-H}$ bonds (Scheme 4.03b).^[9] Doyle and co-workers reported a similar account utilizing aryl chlorides as coupling partners in addition to a system coupling *N*-phenylpyrrolidone and aryl iodides (Scheme 4.03c-d).^{[10][11]} Molander's and Doyle's systems used the C-H source as solvent and they found

that the reaction took place without the presence of a HAT catalyst.^{[9][10]} A year later, in 2017, MacMillan and co-workers further extended the protocol to include aliphatic bromides as coupling partners.^[12]



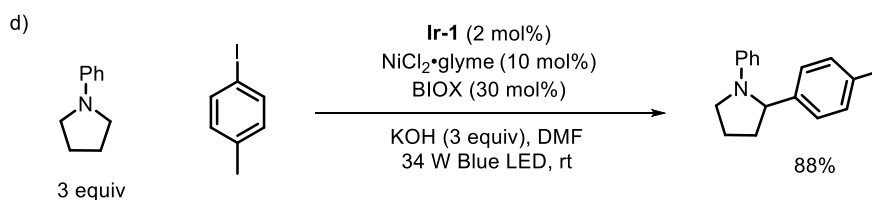
MacMillan et al., 2016



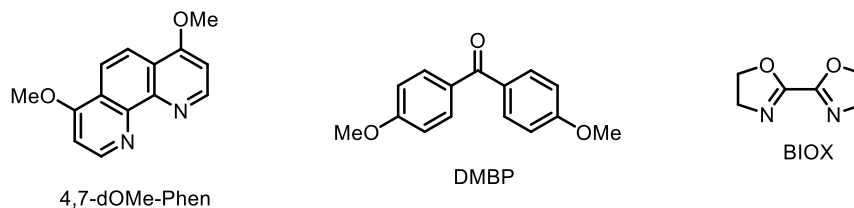
Molander et al., 2016



Doyle et al., 2016



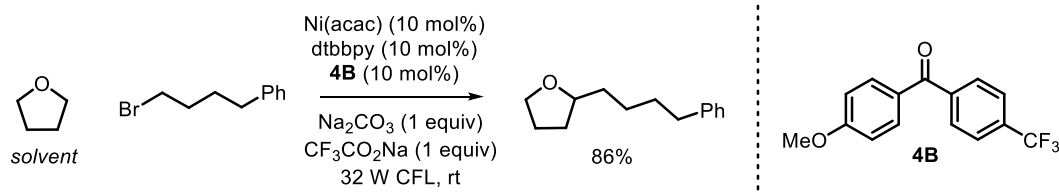
Doyle et al., 2016



Scheme 4.03. Previous work on nickel photocatalyzed direct C-H arylation.

In 2018, Martin and co-workers developed a system utilizing a diaryl ketone photosensitizer essentially functioning as both photoredox catalyst and HAT catalyst.^[13] Additionally, they were able to extend the

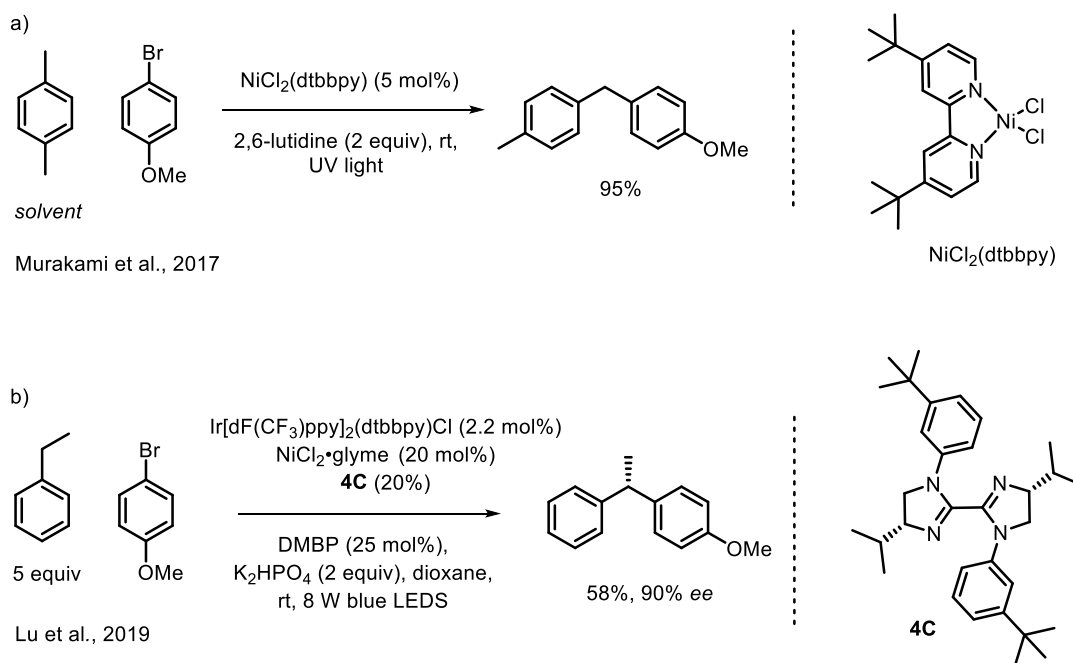
protocol to alkylations via aliphatic bromides (Scheme 4.04). Subsequently, Hashmi and co-workers developed a similar system with benzaldehyde as photosensitizer.^[14] In 2020 König and co-workers developed a system for coupling of THF at the α -oxy C-H bond and aliphatic bromides without the presence of a HAT catalyst. The system was limited to THF as C-H coupling partner and required it as solvent.^[15]



Martin et al., 2018

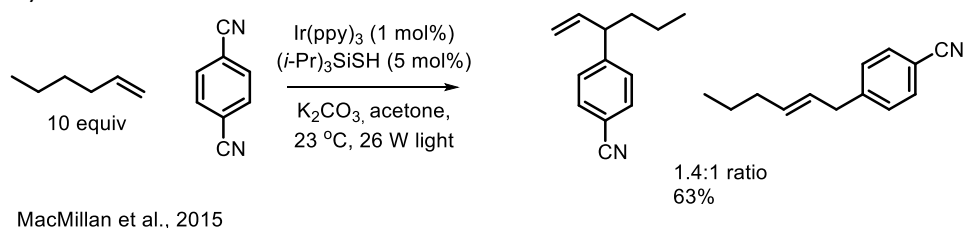
Scheme 4.04. Example of combined nickel- and photoredox-catalyzed direct C-H alkylation.

After the initial wave of research mainly focusing on the direct functionalization of C-H bonds in THF-like molecules the expansion to other molecules containing weak C-H bonds have commenced. In 2017 Murakami showed that benzylic C-H bonds could be directly arylated in the presence of nickel and UV light without the need for a photocatalyst (Scheme 4.05a).^[16] Two years later, Lu and co-workers developed an enantioselective protocol. They were able achieve couplings in good yields and enantioselectivities (80-92% *ee*) (Scheme 4.05b).^[17] At the time, the best example of enantioselective synthesis employing nickel photoredox catalysis only provided 54% *ee*, highlighting the novelty of their work.^[13]



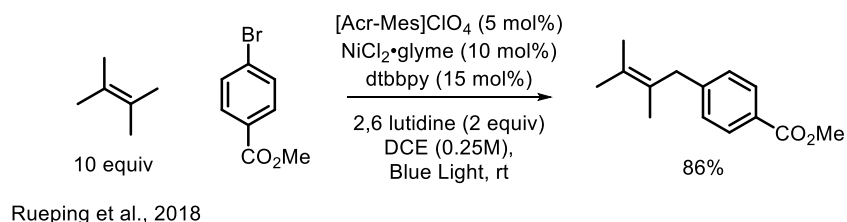
Scheme 4.05. Previous work on nickel photocatalyzed C-H arylation of benzylic substrates.

Another type of compounds containing C(sp³)-H bonds with similar bond dissociation energy (BDE) to benzylic and α-heteroatom (N, O, S) C(sp³)-H bonds are allylic C-H bonds. The first example of photocatalyzed allylic C-H arylation came in 2015, where MacMillan and co-workers developed a protocol for allylic arylation of alkenes utilizing cyanoarenes and a combination of a photocatalyst and a thiol-based organocatalyst.^[18] While this was impressive at the time, it has some drawbacks. The use of activated cyanoarenes presents a much more limited coupling partner, compared to aryl bromides. More crucial, the arylation of linear terminal alkenes provided no selectivity in regard to branched/linear arylation (Scheme 4.06).



Scheme 4.06. First example of photocatalyzed direct arylation of allylic C-H bonds.

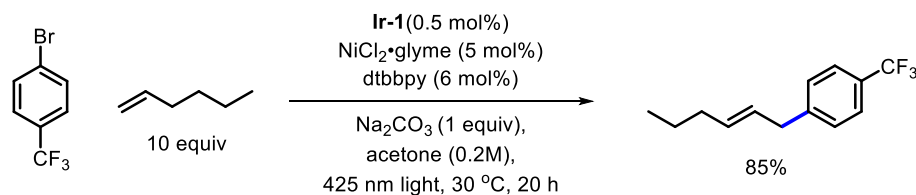
In 2018, Rueping and co-workers developed a combined nickel -and photoredox-catalyzed protocol for the direct arylation of allylic C-H bonds. However, the types of alkenes were limited to either tri or tetra substituted alkenes (Scheme 4.07).^[19]



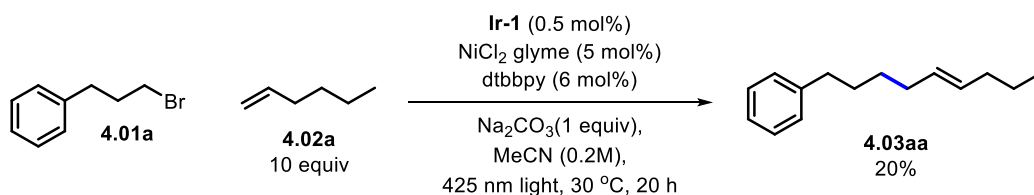
Scheme 4.07. Example of combined nickel- and photoredox-catalyzed direct arylation of allylic C-H bonds.

With precedence for nickel affording the linear product in allylic alkylations and its capability to carry out the allylic C-H arylation we envisioned a selective arylation of terminal alkenes should be possible and potentially even selective allylic alkylations.^{[20][21]}

We began our investigation with 1-hexene and 4-bromobenzotrifluoride. Gratifyingly, within a few rounds of optimization reactions, conditions providing the linear product in 85% yield (^1H NMR) was identified (Scheme 4.08).

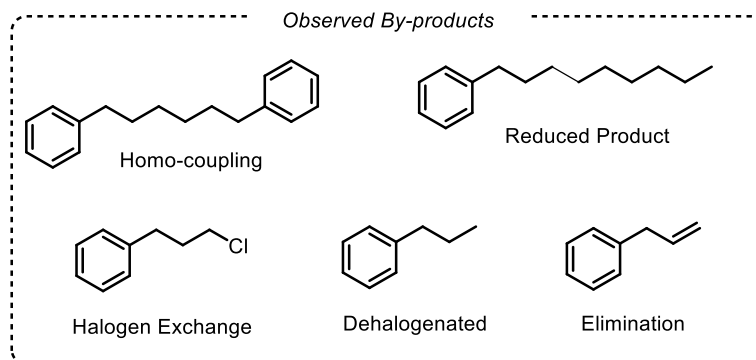


While the reaction offers some novelty over Rueping and MacMillans protocols in regard to utilizing mono substituted alkenes and selectively obtaining the linear products; the swift optimization prompted us to investigate the much more challenging alkylation.



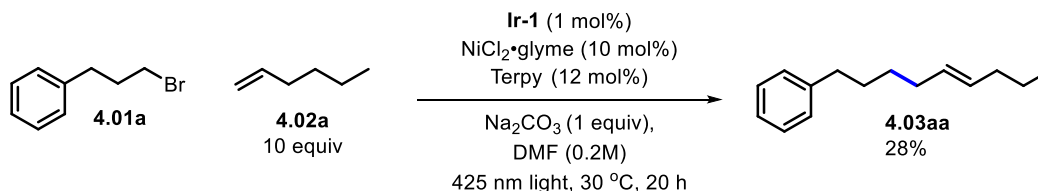
Using similar conditions in acetonitrile and **4.01a** as alkyl bromide afforded the alkylation product **4.03aa** in approximate 20% yield (uncalibrated GC) (Scheme 4.09). While this result was not impressive, it illustrated the plausibility of such a transformation.

From the initial experiment, a multitude of by-products were observed (Scheme 4.10). The main by-product being the homo-coupling, however, the reduced product was especially troublesome as the reduced product overlapped with the product both in GC and in ^1H NMR making it extremely difficult to distinguish the product from the reduced product.



Luckily, it was found that changing the ligand from a bidentate to a tridentate ligand such as Terpy suppressed the formation of the reduced product without compromising activity. With the simple

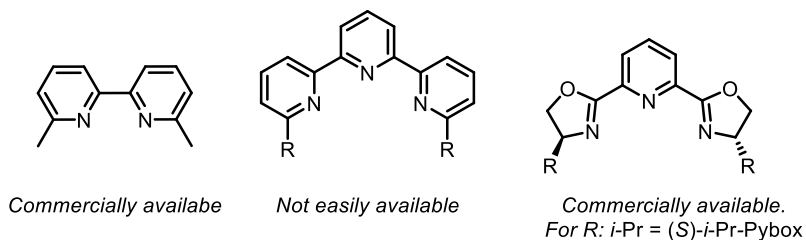
solution, no further investigation into the mechanistic origin of this species was undertaken. At this stage, yields were still poor, just below 30% with conversions around 80% (Scheme 4.11).



Scheme 4.11. First reaction conditions that did not lead to the reduced product.

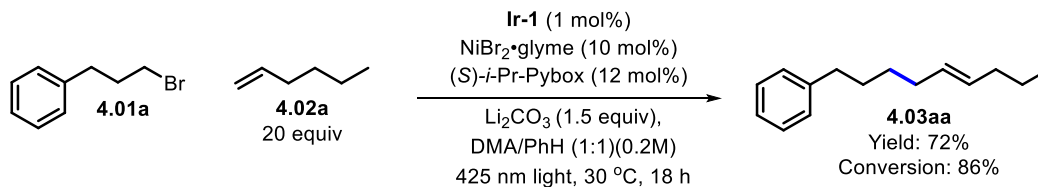
While struggling with pushing the yields it was realized that 1-hexene and DMF is not miscible, suggesting that despite having 10 equivalents of alkene present, the available amount of 1-hexene was probably much lower. It was hypothesized that if the reaction media could be modified to be miscible with 1-hexene without losing the solvating strength of DMF, this would be highly beneficial for the reaction. This was achieved by changing the solvent to a 1:1 mixture of DMF and benzene. This almost doubled the yield, affording **4.03aa** in 52% yield (calibrated GC).

The last remaining challenge was to address the selectivity, with conversion reaching 100%, the main by-product, the homo-coupling of **4.01a** accounted for approximately 40%. Early in the optimization a range of ligands had been tested, it was discovered that with 6,6'-dimethyl-2,2'-bipyridine as ligand no homo-coupling was observed. This inspired the idea, that introducing sterically bulk near the coordination site might aid suppressing the homo coupling. Unfortunately, terpyridines with substituents at the 6 position are not readily available; neither commercially nor synthetically.



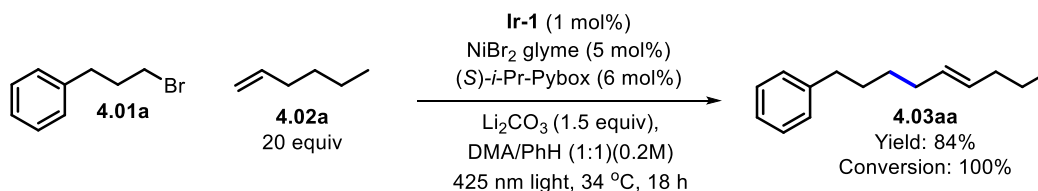
Scheme 4.12. Illustration of ligands suppressing the homo-coupling formation.

However, a ligand family commonly encountered in asymmetric copper and nickel catalysis; the Pybox family resembles a terpyridine with alkyl groups at the 6 and 6'' position (Scheme 4.12). At first sight, it seems excessive to use a chiral ligand for a reaction that cannot yield a chiral product, however, (*S*)-*i*-Pr-Pybox is cheaper than terpyridine (49 €/250 mg. vs. 67 €/250 mg (Sigma-Aldrich)).^[22] Gratifyingly, utilizing (*S*)-*i*-Pr-Pybox completely suppressed the formation of the homo-coupling by-product (Scheme 4.13).



Scheme 4.13. Conditions suppressing both the reduced by-product and the homo-coupling by-product.

At this stage yields were around 70%, when reaction were run at approximately 30 °C, removing the air cooling increased the temperature of the reactions to approximately 34 °C (temperature measured after the reaction) allowing the reaction to reach full conversion. Reducing the nickel loading from 10 mol% to 5 mol% resulted in a further improvement, providing the product in 84% yield (calibrated GC yield) (Scheme 4.14). This protocol was deemed satisfactory, but before concluding the optimization a few variations to the final conditions were carried out (Table 4.01).

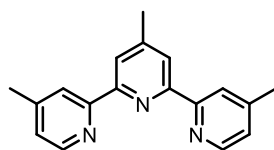


Scheme 4.14. Final optimized conditions.

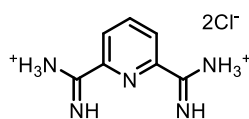
Table 4.01. Variations from conditions in Scheme 4.14.

Entry	Variation from conditions in Scheme 4.14	Conversion	Yield ^[a]
1	None	100%	84%(81%)
2	2.0% NiBr ₂ glyme and 2.4% Ligand	90%	65%
3	3.0% NiBr ₂ glyme and 3.6% Ligand	100%	83%
4	10% NiBr ₂ glyme and 12% Ligand	100%	77%
5	dtbbpy as Ligand	70%	36%
6	3Me-Terpy as Ligand	100%	69%
7	PyBCAM as Ligand	100%	52%
8	Na ₂ CO ₃ instead of Li ₂ CO ₃	100%	71%
9	K ₂ CO ₃ instead of Li ₂ CO ₃	80%	12%
10	NiBr ₂ instead of NiBr ₂ ·glyme	100%	81%
11	NiCl ₂ glyme instead of NiBr ₂ ·glyme	100%	41%
12	NiI ₂ instead of NiBr ₂ ·glyme	100%	70%
13	DMA instead of DMA:PhH	100%	64%
14	PhH instead of DMA:PhH	0%	0%
15	No Ligand	60%	31%
16	No Nickel	0%	0%
17	No Light	0%	0%
18	No PC	0%	0%
19	No Base	10%	10%
20	Under Air	72%	58%

Reaction conditions: **4.01a** (0.1 mmol), **4.02a** (2.0 mmol), NiBr₂·glyme (5 mol%), (S)-i-Pr-Pybox (6 mol%), **Ir-1** (1 mol%), Li₂CO₃ (0.15 mmol), DMA (0.25 mL), PhH (0.25 mL) at 34 °C for 18 h. [a] Yield determined by calibrated GC, parenthesis = isolated yields.



3Me-Terpy

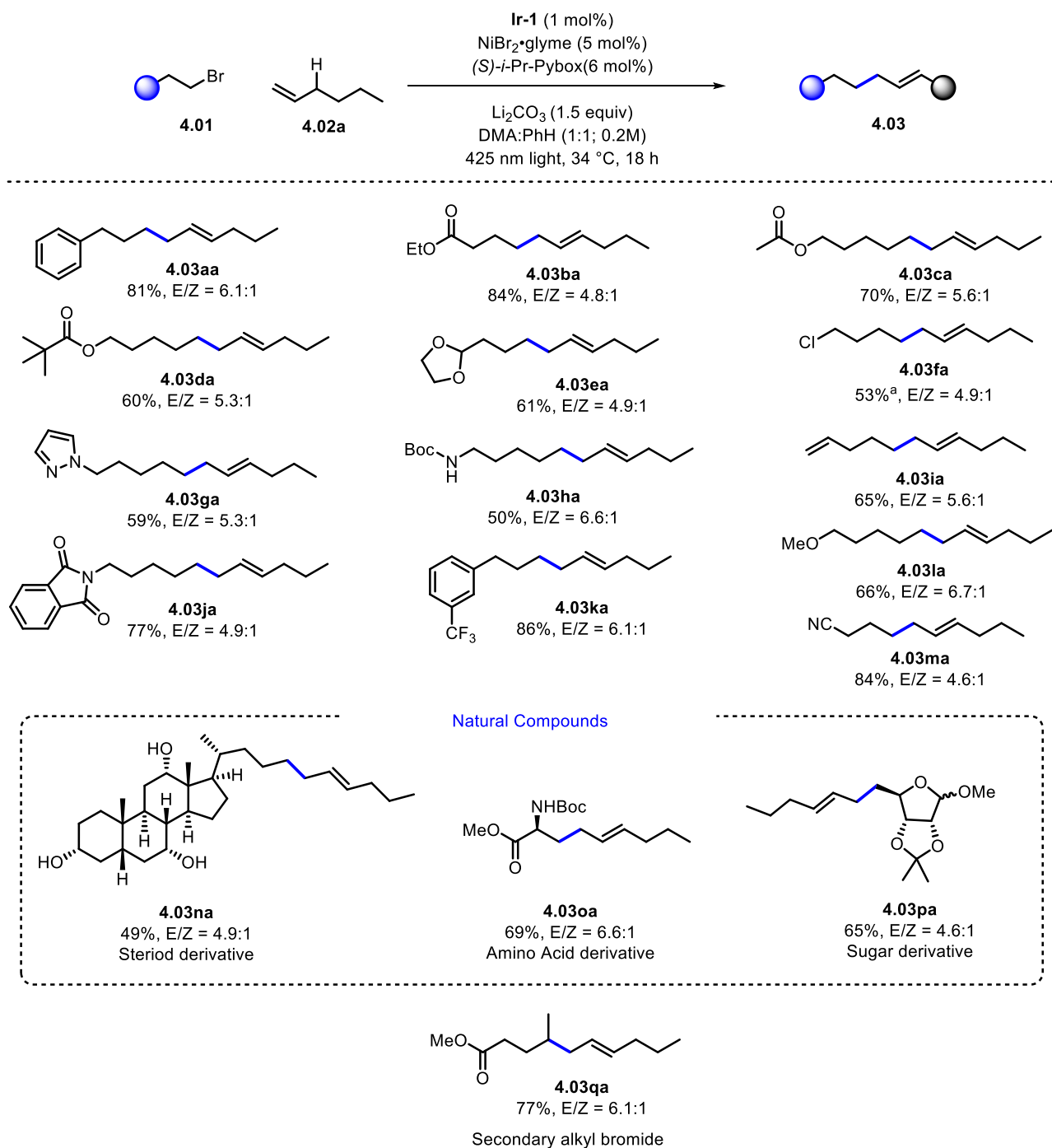


PyBCAM

The catalyst loading of the reaction could be reduced to 3 mol% without any significant change, however, going below 3 mol% diminished yield and conversion. During the optimization, it was found that inorganic carbonates are crucial for the reaction. Lithium carbonate can be exchanged for sodium carbonate with a slight yield reduction; however, potassium carbonate was ineffective. Albeit, it should be noted, that the particle size and homogeneity of the inorganic bases plays a part as this has an effect on the light scattering within the reaction. The control experiments revealed that light, photocatalyst and nickel are all crucial for the reaction.

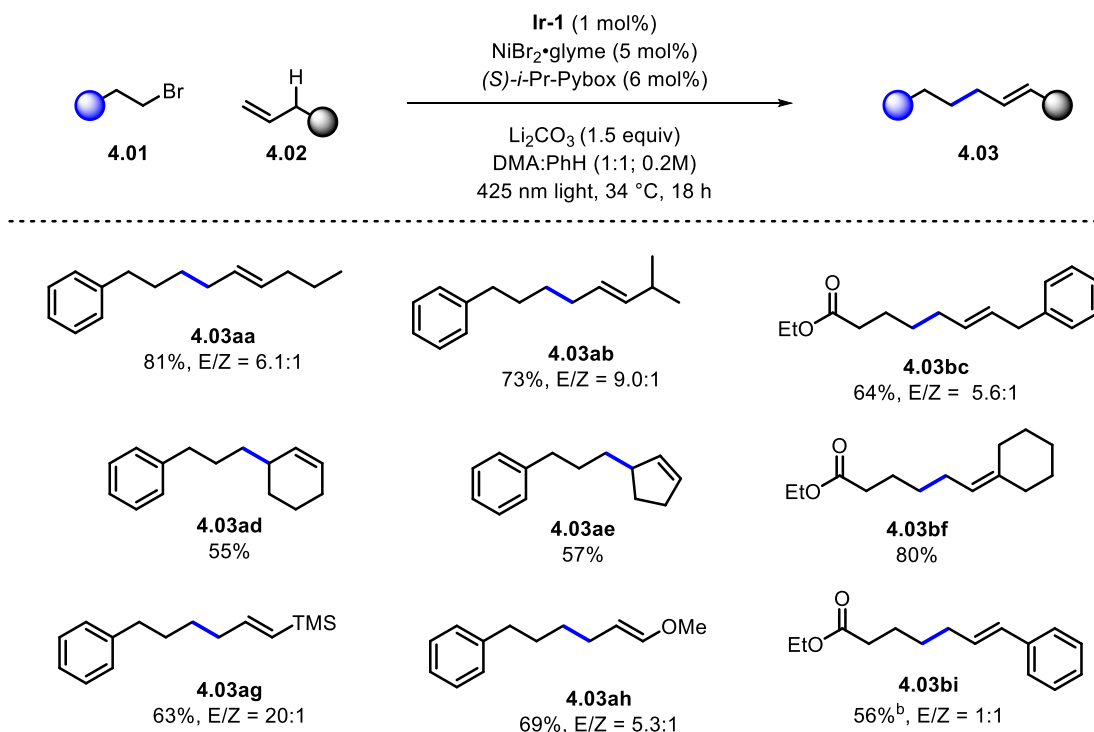
4.4. Scope

To investigate the scope of the protocol the tolerance towards functional groups were evaluated. Gratifyingly, a range of functionalities were tolerated providing moderate to good yields of the desired products. The functionalities included esters (**4.03ba-4.03da**), a protected aldehyde (**4.03ea**), an alkyl chloride (**4.03fa**), a pyrazole (**4.03ga**), a boc-amine (**4.03ha**), a terminal alkene (**4.03ia**), a phthalimide (**4.03ja**), a methoxy ether (**4.03la**) and a nitrile (**4.03ma**). Additionally, three densely functionalized natural compound derivatives were tolerated; a cholic acid derivative containing three secondary alcohols (**4.03na**), an amino acid (**4.03oa**) and a protected D-Ribose derivative (**4.03pa**). Lastly, it was found that the protocol could even be extended to a secondary alkyl bromide (**4.03qa**) (Scheme 4.15).



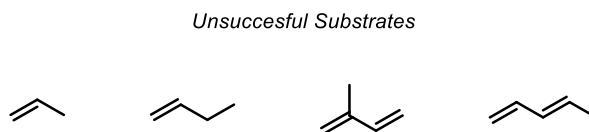
Scheme 4.15. Scope of alkyl bromides. Reaction conditions: **4.01** (0.3 mmol), **4.02a** (6.0 mmol), **NiBr₂·glyme** (5 mol%), (*S*)-*i*-Pr-Pybox (6 mol%), **Ir-1** (1 mol%), Li_2CO_3 (0.45 mmol), DMA (0.75 mL), PhH (0.75 mL) at 34 °C for 18 h. [a] **NiBr₂·glyme** (3 mol%), (*S*)-*i*-Pr-Pybox (3.6 mol%), additionally 5% of the corresponding bromide was co-isolated.

The scope of alkenes was also investigated; however, since the protocol employs alkenes in excess, alkenes containing functional groups were mostly omitted. Most carbon skeletons were tolerated (**4.03aa-4.03bf**), although a small decrease in yield were observed. Interestingly no isomerization of **4.03bc** to the more stable styrene product was observed. Notably, using substrates with a functional group at the allylic position leads to the corresponding vinyl functional group. A vinyl-TMS (**4.03ag**), a vinyl methyl ether (**4.03ah**) and a styrene (**4.03bi**) were obtained (Scheme 4.16).



Scheme 4.16. Scope of alkenes. Reaction conditions: **4.01** (0.3 mmol), **4.02** (6.0 mmol), $\text{NiBr}_2\cdot\text{glyme}$ (5 mol%), $(S)\text{-i-Pr-Pybox}$ (6 mol%), **Ir-1** (1 mol%), Li_2CO_3 (0.45 mmol), DMA (0.75 mL), PhH (0.75 mL) at 34 °C for 18 h. [b] 42 h reaction.

Unfortunately, the protocol did not prove efficient for short olefins which are cheap and abundant from the petrochemical industry: propene, 1-butene, isoprene and piperidine all failed to give the desired product in useful yields (Scheme 4.17).



Scheme 4.17. Unsuccessful alkene substrates

4.5. Discussion

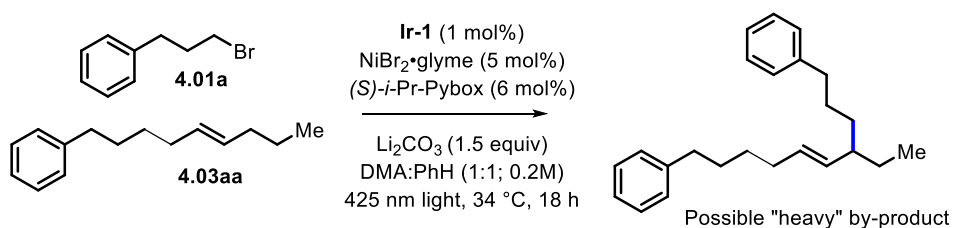
While the reaction provides the desired product in high yields, it requires twenty equivalents of alkene. Unfortunately, when reducing the amount of 1-hexene the yield quickly diminished. Reducing the amount of alkene by five equivalents approximately reduced yield by 15% where yield drops from 84 to 69% with 15 equivalents and from 69 to 56% with 10 equivalents (Table 4.02 entries 1-3). This trend did however not continue past 20 equivalents, adding five more equivalents of alkene only improved the yield with 5% (Table 4.02, entry 4).

Table 4.02. Effect of 1-hexene equivalents.

Entry	1-Hexene equiv	Conversion	Yield ^[a]
1	10	100%	56%
2	15	100%	69%
3	20	100%	84%
4	25	100%	89%

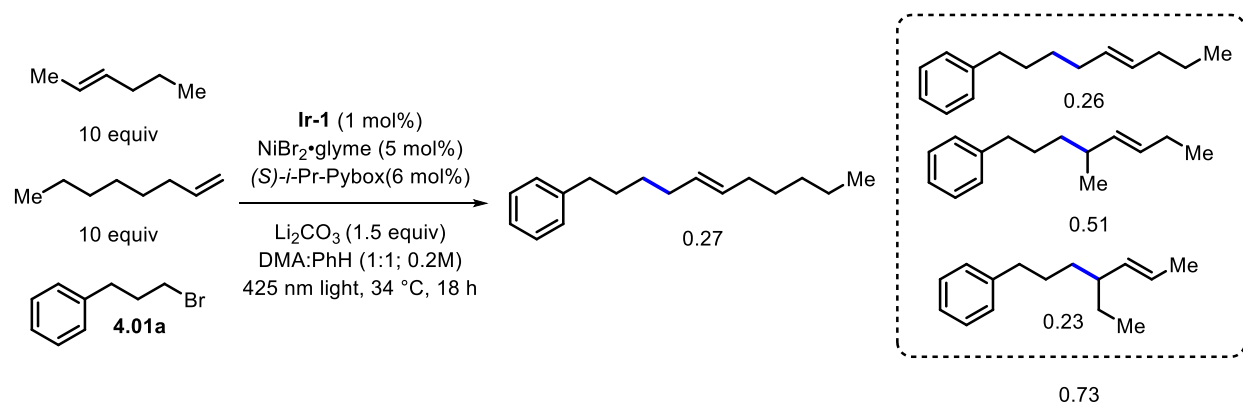
Reaction conditions: **4.01a** (0.1 mmol), **4.02a** (*x* mmol), NiBr₂·glyme (5 mol%), (*S*)-*i*-Pr-Pybox (6 mol%), **Ir-1** (1 mol%), Li₂CO₃ (0.15 mmol), DMA (0.25 mL), PhH (0.25 mL) at 34 °C for 18 h. [a] Yield determined by calibrated GC.

When reducing the amount of 1-hexene full conversion remains, however, no other species were found in the GC. Considering that the product of the reaction is also an alkene, the product might start competing with 1-hexene consequently leading to heavier by-products (Scheme 4.18). Thus, the excess amount of alkene might protect the product via a concentration effect.



Scheme 4.18. Possible reaction between **4.01a** and **4.03aa**.

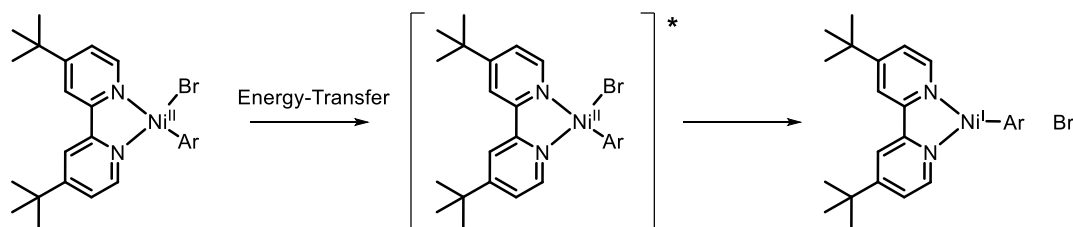
To investigate the hypothesis a competition experiment between *trans*-2-hexene and 1-octene was undertaken. The outcome of the reaction showed that 73% of the product originated from *trans*-2-hexene and the remaining 27% from 1-octene suggesting that *trans*-2-hexene was 2.7 times more reactive than 1-octene. A control experiment between 1-hexene and 1-octene showed that they reacted with the same rate. The increased reactivity of *trans*-2-hexene can be rationalized when evaluating the stability of the formed radical, 2-hexene can form two secondary allylic radicals and a terminal alkene can form a primary and a secondary allylic radical. However, the sterical hindrance around the radical is presumably important for nickel's ability to catch it. Which could be a reason for the unsymmetrical formation of the branched products, with twice the amount of product originated from the least hindered radical (Scheme 4.19).



Scheme 4.19. Competition experiment between 1-octene and 2-hexene.

Role of the photocatalyst

The need for a photocatalyst in the reaction is indisputable. However, the photocatalyst's mode of action is not necessarily trivial. In most examples, the photocatalyst acts as single-electron transfer (SET) species, but in some cases it is hypothesized to function as a triplet-energy transfer reagent; in Rueping and co-workers allylic arylation they hypothesized that the photocatalyst functioned as a triplet-energy transfer reagent. Subsequent to the energy transfer, the excited nickel complex can undergo homolysis of bromide to yield a nickel(I) species and a bromine radical (Scheme 4.20). The nickel-halide homolysis have previously been disclosed by Murakami and co-workers even without the presence of photocatalyst.^[16]



Scheme 4.20. A potential energy-transfer pathway to form of bromine radical.

To investigate the role of the photocatalyst we tried a series of different photocatalysts with different triplet-energies and redox potentials (Table 4.03). No trend with regard to triplet-energy alone was observed, however, the photocatalysts with a reduction potential of more than 1 V and an oxidation potential of less than -1V (within the reductive quenching pathway) provided the product in significant yields.

Although these findings are not conclusive, they suggest the photocatalyst plays a role as a redox SET species. The initial reductive quenching of the photocatalyst is hypothesized to occur through oxidation of a bromide ion (initially a nickel counter-anion). The bromide radical should be able to abstract an allylic hydrogen (BDE of H-Br is 366 kJ/mol and BDE of allylic 1-pentene C-H is 345 kJ/mol).^[23] Subsequently, the Ir(II) species could reduce a Ni(I) species, which would be consistent with the redox potentials $E_{1/2}^{\text{red}}(\text{Ni}^{\text{II}}/\text{Ni}^{\text{I}}) = -1.2\text{V}$ versus SCE in DMF and in agreement with most of the literature.^[8,10,12,17]

Table 4.03. Investigation of photocatalysts.

PC	Reductive Quenching		Oxidative Quenching		E_nT (kJ/mol)	Yield
	$E^{\text{red}}(\text{V})$	$E^{\text{ox}}(\text{V})$	$E^{\text{ox}}(\text{V})$	$E^{\text{red}}(\text{V})$		
Ir-1	+1.21	-1.37	-0.89	+1.69	259	84%
<i>Ir(dFppy)₂dtbbpy(PF₆)</i>	+1.1	-1.4	-0.93	+1.63	234	73%
<i>4-CzIPN</i>	+1.35	-1.21	-1.04	+1.52	222	38%
<i>Ir(dFppy)₃</i>	+0.76	-2.01	-1.46	+1.29	265	0%
<i>Ru(bpy)₃(PF₆)₂</i>	+0.77	-1.33	-0.81	+1.29	196	0%
<i>10-Me-Mes-Acr (ClO₄)</i>	+2.06	-0.57	N/A	N/A	188	0%
<i>[Ir(ppy)₂(dtbbpy)]PF₆</i>	+0.66	-1.51	-0.96	+1.21	205	7%

Reaction conditions: **4.01a** (0.1 mmol), **4.02a** (2.0 mmol), NiBr₂·glyme (5 mol%), (*S*)-*i*-Pr-Pybox (6 mol%), PC (1 mol%), Li₂CO₃ (0.15 mmol), DMA (0.25 mL), PhH (0.25 mL) at 34 °C for 18 h. [a] Yield determined by calibrated GC.

Quenching studies

In order to support the hypothesis that bromide ions were responsible for quenching of the photocatalyst, we conducted a quenching experiment. In here the phosphorescence of the photocatalyst is measured. Addition of substrates that quench the photocatalyst via different pathways (redox pathways) results in a reduced phosphorescence signal.

As expected did **4.02a** or **4.01a** not result in any quenching. This is in accordance with the redox potentials; oxidation potential of 1-hexene is approximately +2.8V vs. SCE in MeCN and $E^*(E/E^-)=+1.21\text{V}$ for **Ir-1** (Figure 4.01).^[24] The reduction potential of alkyl halides is approximately -1.2V vs. SCE in DMF and $E^*(E/E^+)= -0.89\text{V}$ for **Ir-1** (Figure 4.02).^[25] In contrast, but consistent with our hypothesis Br^- quenches the photocatalyst, indicating that the **Ir-1** undergoes a reductive quenching (Figure 4.03).

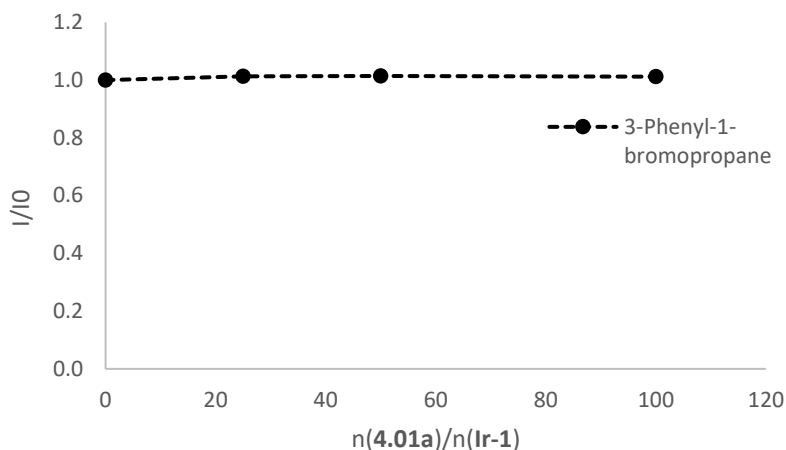


Figure 4.01. Quenching of **Ir-1** with **4.01a**.

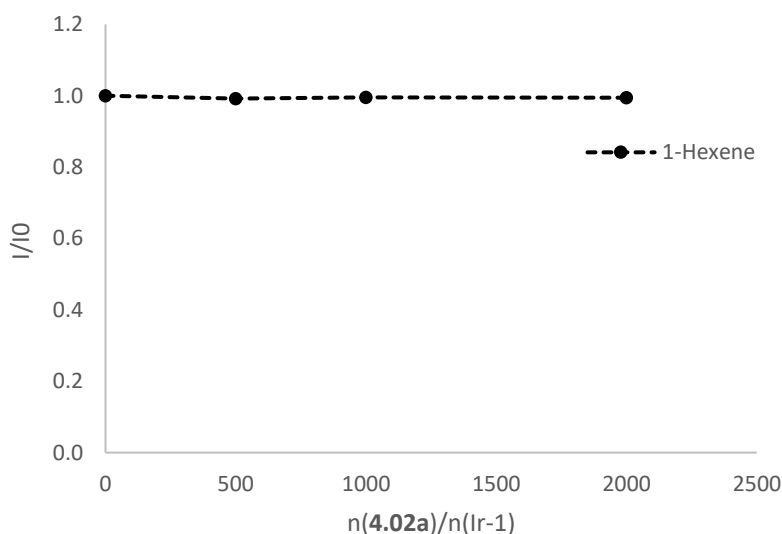


Figure 4.02. Quenching of **Ir-1** with **4.02a**.

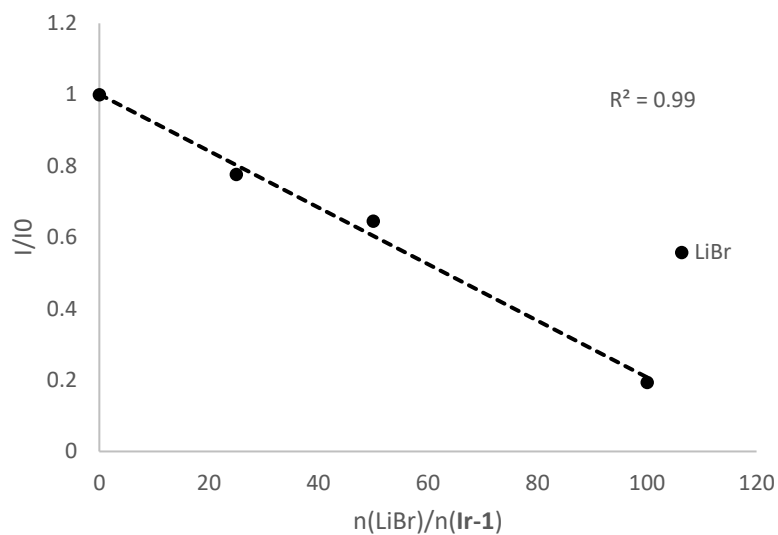
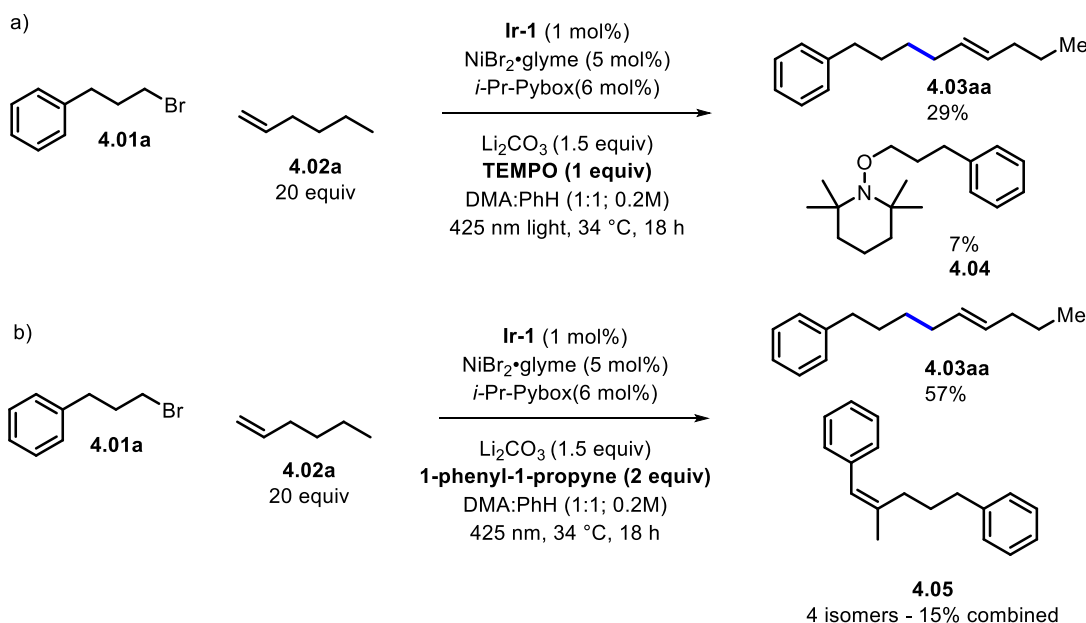


Figure 4.03. Quenching of Ir-1 with LiBr.

While the bromide ions do not originate from LiBr in the reaction, most of the bromide ions should after a few catalytic cycles be present as LiBr. Furthermore, nickel complexes with tridentate ligands typically leads to square planar complexes with counter anions, meaning that bromide ions are available even prior to the first catalytic cycle.^{[26][27]}

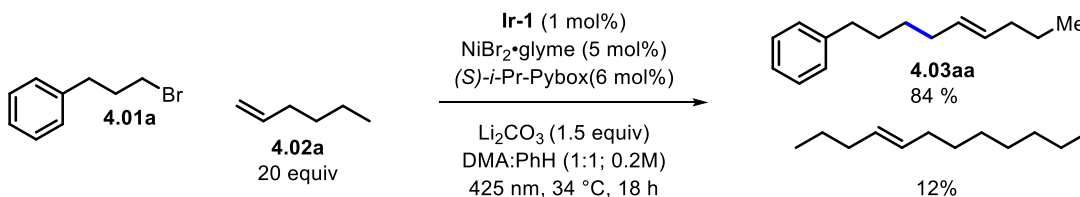
Radical Quenching

As the reaction was believed to occur via a radical pathway, the presence of radicals were investigated. Addition of one equivalent of TEMPO to a standard reaction severely inhibited the reaction, only 29% product vs. 84% (calibrated GC) was obtained. Unfortunately, no bromide or 1-hexene TEMPO-adducts were observed. A TEMPO-**4.01a** adduct **4.04** (7% by uncalibrated GC) was observed. While the inhibition of the reaction indicates that the reaction proceeds via radicals, the TEMPO-adduct also suggest that the oxidative addition occurs via a radical pathway (Scheme 4.21a). However, **4.04** could also form from a SET oxidation of TEMPO followed by a S_N^2 reaction. Consequently, the experiment does not reveal the presence of bromine or allylic radicals.



Scheme 4.21. Radical trapping experiments. a) with TEMPO. b) with 1-phenyl-1-propyne.

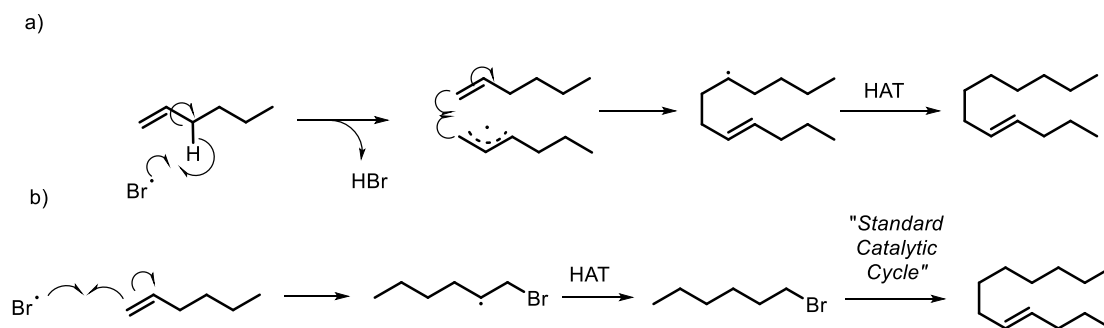
Lu and co-workers found that with the addition of 1-phenyl-1-propyne to a similar protocol they were able to catch a bromine radical.^[17] Unfortunately, when carrying out a standard experiment in the presence of two equivalents 1-phenyl-1-propyne we were not able to catch a bromine radical. The experiment essentially revealed the same as the TEMPO experiment, as the yield was diminished and a **4.01a** adduct was identified (**4.05**) (Scheme 4.21b).



Scheme 4.22. Observation of dodecene by-product from a standard reaction.

The main (and only observed) by-product from the standard reaction was dodecene (unknown isomer), typically, around 12% (uncalibrated GC) (Scheme 4.22). We hypothesized this could be formed in two ways, one involving addition of the allylic radical species to 1-hexene which after HAT from either solvent or another hexene would lead to a dodecene species (Scheme 4.23a). Another possibility could be

addition of the bromine radical to 1-hexene, which after HAT yields 1-bromohexene, which via the standard catalytic pathways would lead to a dodecene species (Scheme 4.23b). Of the two routes, the latter seems more probable. This can be rationalized by comparing the addition step. The addition of the nucleophilic allylic radical to hexene, forming a new nucleophilic radical, should be less favorable than addition of the electrophilic bromine radical to hexene. Speculation on favorability of the HAT step is tricky as the hydrogen source could originate from both solvent and 1-hexene. Although this is mere speculation, it hints at the presence of bromine and/or allylic radicals.



Scheme 4.23. Possible mechanistic routes to dodecene.

Based on previous studies and these mechanistic findings we propose the mechanism outlined in Scheme 4.24. Initially in-situ activation of the precatalyst **4.06A** can form the proposed active Ni(0) species **4.06B**. The Ni(0) species could undergo oxidative addition of **4.01a** furnishing the Ni(II) species **4.06C**. Concurrently, the excited Ir-1^{III*} species could oxidize a bromide counter-ion forming a bromine radical, which undergoes HAT with **4.02a** forming HBr and an allylic radical. The Ni(II) species **4.06D** could intercept the allylic radical forming the Ni(III) species **4.06E**. Through reductive elimination of **4.06E** the product would be liberated forming the Ni(I) species **4.06F**. Reduction of **4.06F** via Ir-1^{II} reforms both catalysts, **4.06B** and Ir-1.



Time Study

An initial time study revealed that the rate of the reaction proceeds in a linear fashion, at least until 8 hours and 48% yield (Figure 4.04). Although, this does not provide any conclusive information about the reaction it does provide some information. The lack of an induction period suggest that the initial activation of **4.06A** is not a slow step relative to the reaction. Additionally, the linearity might indicate the oxidative addition step is not rate-determining as one would expect a decay in reaction rate with dropping substrate concentration. Similarly, oxidation of bromide does not seem to be the rate-determining step as one would then expect the rate to increase as the reaction progressed and LiBr concentration increase. However, these two effects could also cancel out each other.

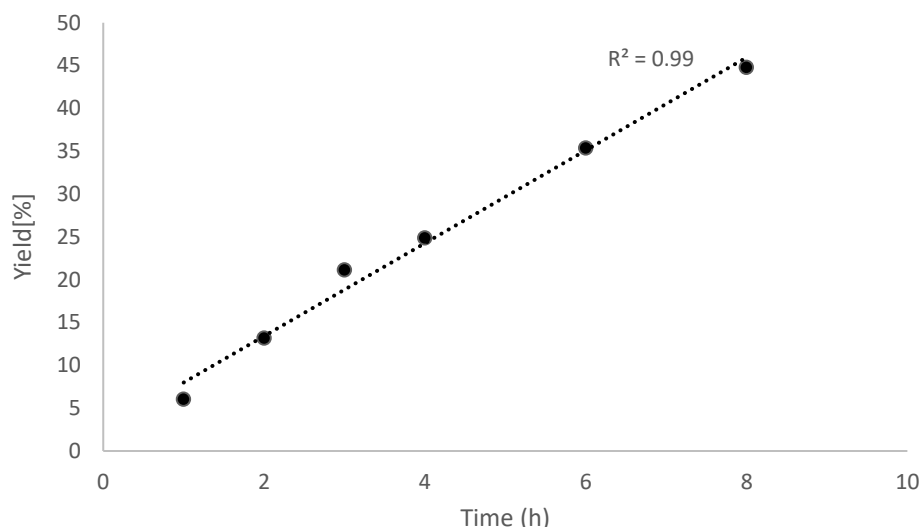
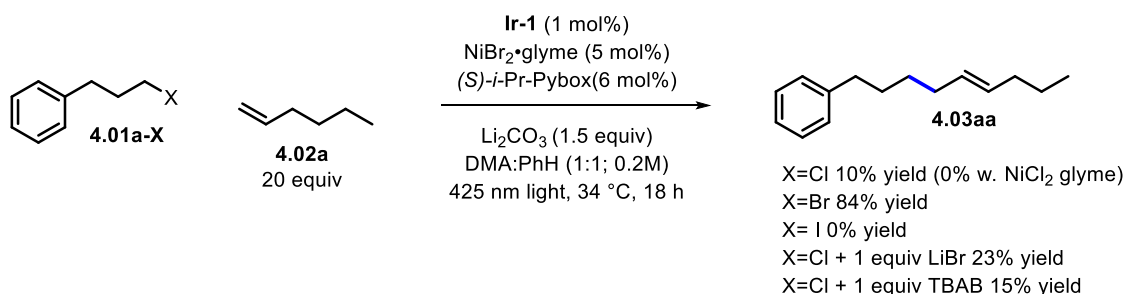


Figure 4.04. Kinetic profile of the standard reaction.

Halide Effect

Carrying out the standard reaction with the corresponding alkyl chloride **4.01a-Cl** or iodide **4.01a-I** resulted in little to no product formation (Scheme 4.25). The inability of alkyl iodides to carry out the reaction might seem puzzling at first, as the oxidative addition of alkyl iodides are typically facile. Additionally, oxidation of iodide is much more facile than oxidation of bromide.^{[28][29]} However, considering the mismatch of BDE (BDE of H-I: 298 kJ/mol vs. allylic 1-pentene C-H is 345 kJ/mol) HAT from iodide should a priori not occur and consequently no reaction should occur.^[13] As this is the case, it supports the proposed mechanism involving HAT from a bromine radical, and it is consistent with systems following a similar mechanism.^{[17][10]} In case of the alkyl chloride, it is less surprising that the reaction does not occur, as alkyl chlorides do not readily undergo oxidative addition and chloride is not easily oxidized.^{[28][29]}

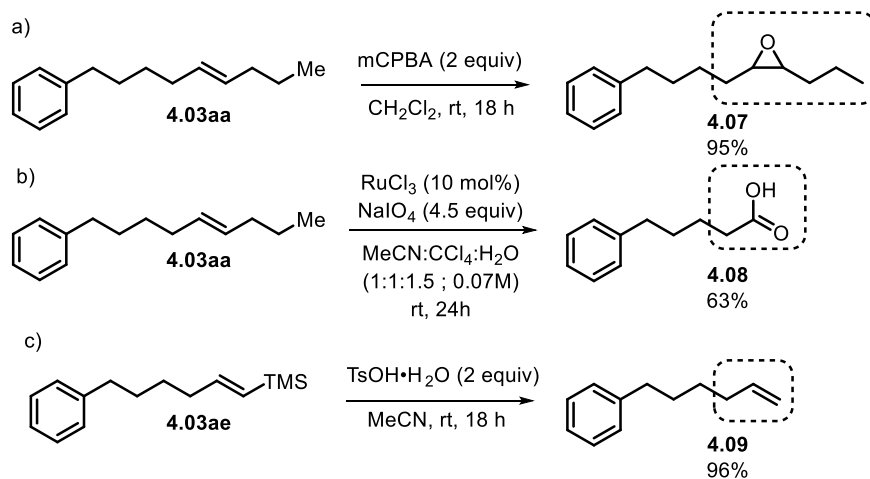
As the initial experiment with **4.01a-Cl** provided 10% product and coincidentally, the same amount of bromide is present from the nickel precursor, we speculated that by adding bromide additives the protocol could be extended to alkyl chlorides. Unfortunately our conditions did not seem to facilitate halide exchange efficiently. Adding one equivalent of LiBr only increased the yield to 23% and TBAB only to 15% (Scheme 4.25).



Scheme 4.25. Effect of alkyl halides and different halide additives.

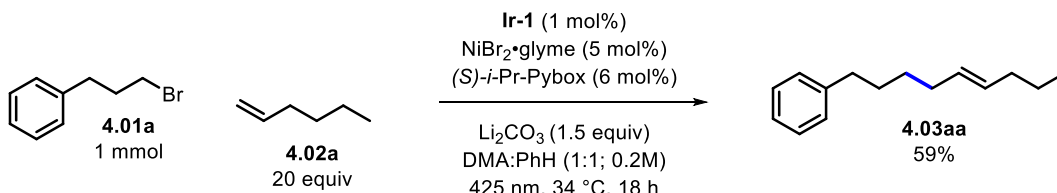
Post Modifications

The reaction presents a new way to forge a bond between two C(sp³); the only sign of the reaction is an alkene in the α -position of the new carbon. This presents an advantage as the alkene moiety can be further functionalized. **4.03aa** smoothly undergoes epoxidation by treating it with mCPBA at room temperature to yield **4.07** (Scheme 4.26a). Alkenes can also undergo catalytic oxidative cleavage using a combination of RuCl₃ and NaIO₄ effectively adding a CH₂COOH moiety to an alkyl halide yielding **4.08** (from **4.03aa**) (Scheme 4.26b). The use of allyltrimethylsilane as the alkene source yields terminal vinyl trimethylsilanes **4.03ae**. The TMS group is smoothly removed by addition of *p*-toluenesulfonic acid in MeCN furnishing a terminal alkene **4.09** (Scheme 4.26c).



Scheme 4.26. Product derivatisations: Reaction conditions: a) **4.03aa** (0.15 mmol), mCPBA (0.3 mmol) in CH₂Cl₂ (2 mL) at rt for 18 h. b) **4.03aa** (0.15 mmol), NaIO₄ (0.68 mmol), RuCl₃ (10 mol%) in MeCN/CCl₄/H₂O (1:1:1.5, 2.1 mL) at rt for 24 h. c) **4.03ae** (0.1 mmol), TsOH·H₂O (0.2 mmol) in MeCN (2 mL) at rt for 18 h. Dotted line indicates what the bromide in **4.01a** effectively have been substituted with.

Scaling up the standard reaction from 0.3 mmol to 1 mmol resulted in some yield erosion. As 59% isolated yield was obtained (compared to 81%) (Scheme 4.27). The reaction is sensitive to the amount of light available. This became evident during the optimization process, where we found the position of the reaction relative to the light source had a significant effect. When scaling the reaction the surface area to volume diminishes, due to change in vial diameter, and consequently the reaction receives less light, which could explain the slight decrease in yield.



Scheme 4.27. 1 mmol scale reaction.

4.6. Conclusion and Perspective

In summary, we have developed a protocol for the direct alkylation of allylic C(sp³)-H bonds by alkyl bromides. The protocol is simple and proceeds with excellent selectivity towards the linear product. The work presents the first example of direct allylic C(sp³)-H alkylation using alkyl bromides and terminal olefins. A substrate scope investigation revealed that various functional groups were tolerated, even densely functionalized ones. Although the study was focused on primary alkyl bromides one example of a secondary alkyl bromide shows the protocol can even be extended to secondary alkyl bromides. Various olefins could be employed including alkenes resulting in vinyl-functionalized products. Preliminary mechanistic experiments suggest that the photocatalyst acts by SET with a catalytic cycle intertwined with the cycle of nickel.

The cross-coupling of two C(sp³) is a powerful tool for the junction of two functionalized moieties. Previous C(sp³) cross-couplings have mainly relied on transition metal catalyzed couplings between alkyl halides and organometallic nucleophiles. However, the use of alkyl organometallic nucleophiles presents many drawbacks, e.g. stability issues and functional group tolerance challenges. The combination of transition metal and photoredox chemistry enables otherwise impossible transformations, this project is an example hereof.

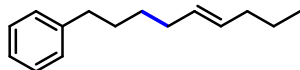
4.7. Experimental

General Information

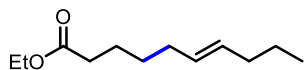
^1H NMR and ^{13}C NMR spectra were recorded on a Bruker Ascend 400 spectrometer. The chemical shifts are reported in ppm relative to solvent residual peak.^[30] The peak patterns are indicated as follows: s, singlet; d, doublet; t, triplet; q, quartet; m, multiplet; dd, doublet of doublets; dt, doublet of triplets; dq, doublet of quartets; qd, quartet of doublets; tt, triplet of triplets; ddd, doublet if doublets of doublets; ddt, doublet of doublets of triplets; dtd, doublet of triplets of doublets. Mass spectrometry was performed on either a Waters AQUITY UPLC system equipped with PDA and SQD2 electrospray (ESI) MS detector or by GC-MS/FID analysis on an Agilent 7890A GC equipped with an HP-5 column and a 5975C VLMSD with triple-axis detector (EI). Column chromatography was performed on silica gel 60 (40–63 μm). Anhydrous solvents were obtained from the solvent purification system Puresolv MD-7. All commercial solvents, reagents, nickel sources, and ligands were used as received without further purification. Quenching experiments was performed on a PerkinElmer fluorescence spectrometer LS55.

Direct C-H Allylic Alkylation - General Procedure A:

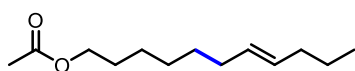
Inside an argon-filled glovebox, a 4 mL vial was charged with **Ir-1** (3.4 mg, 0.0030 mmol; 1.0 mol%), $\text{NiBr}_2\cdot\text{glyme}$ (4.5 mg, 0.015 mmol; 5.0 mol%), (*S*)-*i*-Pr-Pybox (5.4 mg, 0.018 mmol; 6.0 mol%) and Li_2CO_3 (33 mg, 0.45 mmol; 1.5 equiv). Subsequently, a stir bar followed by DMA (0.75 mL, anhydrous) and benzene (0.75 mL) were added. The vial was sealed with a Teflon-lined screw cap and taken out of the glovebox. Outside the glovebox the vial was stirred for 5 minutes prior to addition of alkene **2** (6.0 mmol, 20 equiv) and alkyl bromide **1** (0.30 mmol, 1.0 equiv) via syringes, respectively (in case of solid substrates, these were added inside the glovebox prior to addition of solvents). The reaction was placed in front of an 18W 425 nm LED lamp and stirred for 18 hours. After 18 hours the reactions were directly purified by column chromatography yielding the desired product. E/Z ratio was determined of the isolated product via GC-FID, ^1H NMR or ^{13}C NMR. To ensure reliable quantification results with ^{13}C NMR, inverse-gated ^{13}C NMR experiments of **4.03aa** and GC-FID quantification of the corresponding epoxide (**4.08**) were evaluated, as they both provided the same E/Z ratio as determined by standard ^{13}C NMR, determination of E/Z ratio was deemed adequate with ^{13}C NMR.



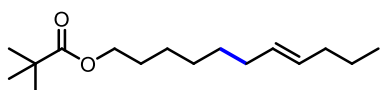
(E)-Non-5-en-1-ylbenzene (4.03aa). The title compound was prepared according to General Procedure A from 1-bromo-3-phenylpropane and 1-hexene. The reaction was purified by column chromatography (pentane) furnishing **4.03aa** as a colorless oil in 81% yield (49.2 mg). ^1H NMR (400 MHz, Chloroform- d) δ 7.35 – 7.27 (m, 2H), 7.24 – 7.17 (m, 3H), 5.49 – 5.36 (m, 2H), 2.64 (t, J = 7.7 Hz, 2H), 2.14 – 1.95 (m, 4H), 1.72 – 1.60 (m, 2H), 1.48 – 1.35 (m, 4H), 0.92 (t, J = 7.3 Hz, 3H). ^{13}C NMR (101 MHz, Chloroform- d) δ 142.8, 130.4, 130.2, 129.9 (minor (Z)), 129.8 (minor (Z)), 128.4, 128.2, 125.6, 35.9, 34.7, 32.5, 31.1 (minor (Z)), 31.0, 29.4 (minor (Z)), 29.3, 27.1 (minor (Z)), 22.9 (minor (Z)), 22.7, 13.8 (minor (Z)), 13.7. MS (EI) m/z (M^+) calcd for $\text{C}_{15}\text{H}_{22}$: 202, found 202. E/Z ratio determined by ^{13}C NMR to 6.1:1



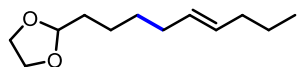
Ethyl (E)-dec-6-enoate (4.03ba). The title compound was prepared according to General Procedure A from ethyl-4-bromobutanoate and 1-hexene. The reaction was purified by column chromatography (5% Et₂O in pentane) furnishing **4.03ba** as a colorless oil in 84% yield (50.0 mg). ¹H NMR (400 MHz, Chloroform-d) δ 5.39 (dq, *J* = 15.2, 5.2 Hz, 2H), 4.14 (q, *J* = 7.1 Hz, 2H), 2.34 – 2.27 (m, 2H), 2.10 – 1.93 (m, 4H), 1.65 (p, *J* = 7.5 Hz, 2H), 1.44 – 1.34 (m, 4H), 1.27 (t, *J* = 7.1 Hz, 3H), 0.90 (t, *J* = 7.4 Hz, 3H). ¹³C NMR (101 MHz, Chloroform-d) δ 173.8, 130.7, 130.2 (minor (*Z*)), 129.8, 129.3 (minor (*Z*)), 60.2, 34.7, 34.3, 32.2, 29.3 (minor (*Z*)), 29.2 (minor (*Z*)), 29.1, 26.8 (minor (*Z*)), 24.6 (minor (*Z*)), 24.5, 22.8 (minor (*Z*)), 22.7, 14.3, 13.8 (minor (*Z*)), 13.7. MS (EI) *m/z* (*M*⁺) calcd for C₁₂H₂₂O₂: 198, found 198. E/*Z* ratio determined by ¹³C NMR to 4.8:1



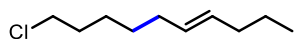
(E)-Undec-7-en-1-yl acetate (4.03ca). The title compound was prepared according to General Procedure A from 5-bromopentyl acetate and 1-hexene. The reaction was purified by column chromatography (5% Et₂O in pentane) furnishing **4.03ca** as a colorless oil in 70% yield (44.6 mg). ¹H NMR (400 MHz, Chloroform-d) δ 5.42 – 5.29 (m, 2H), 4.05 (t, *J* = 6.7 Hz, 2H), 2.04 (s, 3H), 2.02 – 1.92 (m, 4H), 1.65 – 1.56 (m, 2H), 1.39 – 1.27 (m, 8H), 0.88 (t, *J* = 7.4 Hz, 3H). ¹³C NMR (101 MHz, Chloroform-d) δ 171.2, 130.32, 130.29, 129.83 (minor (*Z*)), 129.80 (minor (*Z*)), 64.6, 34.7, 32.5, 29.6 (minor (*Z*)), 29.5, 29.3 (minor (*Z*)), 28.9 (minor (*Z*)), 28.7, 28.6, 27.1 (minor (*Z*)), 25.82 (minor (*Z*)), 25.77, 22.9 (minor (*Z*)), 22.7, 21.0, 13.8 (minor (*Z*)), 13.6. MS (EI) *m/z* (*M*⁺) calcd for C₁₃H₂₄O₂: 212, found 212. E/*Z* ratio determined by ¹³C NMR to 5.6:1



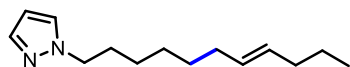
(E)-Undec-7-en-1-yl pivalate (4.03da). The title compound was prepared according to General Procedure A from 5-bromopentyl pivalate and 1-hexene. The reaction was purified by column chromatography (2.5% Et₂O in pentane) furnishing **4.03da** as a colorless oil in 60% yield (45.8 mg). ¹H NMR (400 MHz, Chloroform-d) δ 5.46 – 5.33 (m, 2H), 4.06 (t, *J* = 6.6 Hz, 2H), 2.07 – 1.91 (m, 4H), 1.63 (q, *J* = 6.8 Hz, 2H), 1.44 – 1.29 (m, 8H), 1.22 (s, 9H), 0.90 (t, *J* = 7.4 Hz, 3H). ¹³C NMR (101 MHz, Chloroform-d) δ 178.6, 130.3, 129.8 (minor (*Z*)), 64.4, 38.7, 34.7, 32.5, 29.6 (minor (*Z*)), 29.5, 29.3 (minor (*Z*)), 28.9 (minor (*Z*)), 28.7, 28.6, 27.2, 27.1 (minor (*Z*)), 25.84 (minor (*Z*)), 25.79, 22.9 (minor (*Z*)), 22.7, 13.8 (minor (*Z*)), 13.7. MS (EI) *m/z* (*M*⁺) calcd for C₁₆H₃₀O₂: 254, found 254. E/*Z* ratio determined by ¹³C NMR to 5.3:1



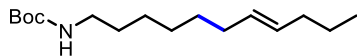
(E)-2-(Non-5-en-1-yl)-1,3-dioxolane (4.03ea). The title compound was prepared according to General Procedure A from 2-(3-bromopropyl)-1,3-dioxolane and 1-hexene. The reaction was purified by column chromatography (10% Et₂O in pentane) furnishing **4.03ea** as a colorless oil in 61% yield (39.3 mg). ¹H NMR (400 MHz, Chloroform-d) δ 5.45 – 5.36 (m, 2H), 4.86 (t, *J* = 4.8 Hz, 1H), 4.02 – 3.95 (m, 2H), 3.90 – 3.83 (m, 2H), 2.09 – 1.93 (m, 4H), 1.73 – 1.64 (m, 2H), 1.48 – 1.34 (m, 6H), 0.90 (t, *J* = 7.3 Hz, 3H). ¹³C NMR (101 MHz, Chloroform-d) δ 130.4, 130.1, 129.9 (minor (*Z*)), 129.6 (minor (*Z*)), 104.7, 64.8, 34.7, 33.83 (minor (*Z*)), 33.79, 32.5, 29.7 (minor (*Z*)), 29.6, 29.3 (minor (*Z*)), 27.1 (minor (*Z*)), 23.8 (minor (*Z*)), 23.6, 22.9 (minor (*Z*)), 22.7, 13.8 (minor (*Z*)), 13.7. MS (EI) *m/z* (*M*⁺) calcd for C₁₂H₂₂O₂: 198, found 198. E/*Z* ratio determined by ¹³C NMR to 4.9:1



(E)-10-Chlorodec-4-ene (4.03fa) The title compound was prepared according to General Procedure A from 1-bromo-5-chloropentane and 1-hexene. The reaction was purified by column chromatography (pentane) furnishing **4.03fa** as a colorless oil in 53% yield (27.8 mg) (additionally 5% of the bromide was co-isolated). ¹H NMR (400 MHz, Chloroform-d) δ 5.49 – 5.32 (m, 2H), 3.55 (t, *J* = 6.8 Hz, 1.7H), 3.43 (t, *J* = 6.9 Hz, 0.3H, from the corresponding bromide), 2.09 – 1.94 (m, 4H), 1.80 (p, *J* = 6.9 Hz, 2H), 1.50 – 1.33 (m, 6H), 0.91 (t, *J* = 7.4 Hz, 3H). ¹³C NMR (101 MHz, Chloroform-d) δ 130.6, 130.1 (minor (*Z*)), 130.0, 129.5 (minor (*Z*)), 45.1, 34.7, 32.5, 32.4, 29.3 (minor (*Z*)), 29.0 (minor (*Z*)), 28.9, 27.0 (minor (*Z*)), 26.5 (minor (*Z*)), 26.4, 22.9 (minor (*Z*)), 22.7, 13.8 (minor (*Z*)), 13.7. MS (EI) *m/z* (*M*⁺) calcd for C₁₀H₁₉Cl: 174, found 174. Minor (bromide): calcd for C₁₀H₁₉Br 218/220 found 218/220. E/*Z* ratio determined by ¹³C NMR to 4.9:1

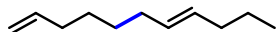


(E)-1-(1H-Pyrazol-1-yl)undec-7-en (4.03ga). The title compound was prepared according to General Procedure A from 1-(5-bromopentyl)-1H-pyrazole and 1-hexene. The reaction was purified by column chromatography (15% Et₂O in pentane) furnishing **4.03ga** as a colorless oil in 59% yield (39.0 mg). ¹H NMR (400 MHz, Chloroform-d) δ 7.49 (d, *J* = 1.7 Hz, 1H), 7.36 (d, *J* = 2.2 Hz, 1H), 6.22 (t, *J* = 2.1 Hz, 1H), 5.43 – 5.29 (m, 2H), 4.11 (t, *J* = 7.1 Hz, 2H), 2.02 – 1.90 (m, 4H), 1.85 (p, *J* = 7.2 Hz, 2H), 1.38 – 1.25 (m, 8H), 0.87 (t, *J* = 7.3 Hz, 3H). ¹³C NMR (101 MHz, Chloroform-d) δ 139.0, 130.4, 130.2, 129.9 (minor (*Z*)), 129.7 (minor (*Z*)), 128.8, 105.1, 52.1, 34.7, 32.4, 30.4, 29.5 (minor (*Z*)), 29.4, 29.3 (minor (*Z*)), 28.8 (minor (*Z*)), 28.6, 27.1 (minor (*Z*)), 26.54 (minor (*Z*)), 26.48, 22.9 (minor (*Z*)), 22.7, 13.8 (minor (*Z*)), 13.7. MS (EI) *m/z* (*M*⁺) calcd for C₁₄H₂₄N₂: 220, found 220. E/*Z* ratio determined by ¹³C NMR to 5.3:1

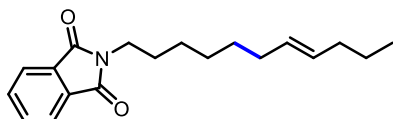


tert-Butyl (E)-undec-7-en-1-ylcarbamate (4.03ha). The title compound was prepared according to General Procedure A from *tert*-butyl (5-bromopentyl)carbamate and 1-hexene. The reaction was purified by column chromatography (20% EtOAc in hexane) furnishing **4.03ha** as a colorless oil in 50% (40.4 mg).

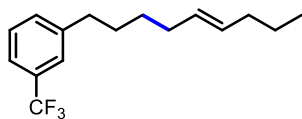
^1H NMR (400 MHz, Chloroform- d) δ 5.43 – 5.31 (m, 2H), 4.49 (s, 1H), 3.22 – 3.01 (m, 2H), 2.04 – 1.90 (m, 4H), 1.47 – 1.42 (m, 11H), 1.39 – 1.26 (m, 8H), 0.88 (t, J = 7.4 Hz, 3H). ^{13}C NMR (101 MHz, Chloroform- d) δ 156.0, 130.34, 130.28, 129.86 (minor (Z)), 129.80 (minor (Z)), 79.0, 40.6, 34.7, 32.5, 30.0, 29.6 (minor (Z)), 29.5, 29.3 (minor (Z)), 28.9 (minor (Z)), 28.8, 28.4, 27.1 (minor (Z)), 26.7, 22.9 (minor (Z)), 22.7, 13.8 (minor (Z)), 13.7. MS (EI) m/z (M^{+}) calcd for $\text{C}_{16}\text{H}_{31}\text{NO}_2$: 269, found 269. E/Z ratio determined by ^{13}C NMR to 6.6:1



(E)-Undeca-1,7-diene (4.03ia) The title compound was prepared according to General Procedure A from 1-bromo-pent-5-ene and 1-hexene. The reaction was purified by column chromatography (pentane) furnishing **4.03ia** as a colorless oil in 65% yield (29.7 mg). ^1H NMR (400 MHz, Chloroform- d) δ 5.81 (ddt, J = 16.9, 10.2, 6.6 Hz, 1H), 5.43 – 5.34 (m, 2H), 5.03 – 4.90 (m, 2H), 2.10 – 1.91 (m, 6H), 1.44 – 1.30 (m, 6H), 0.88 (t, J = 7.4 Hz, 3H). ^{13}C NMR (101 MHz, Chloroform- d) δ 139.1, 130.31, 130.30, 129.84 (minor (Z)), 129.8, 1 (minor (Z)) 114.2, 34.7, 33.7, 32.8 (minor (Z)), 32.4, 29.3 (minor (Z)), 29.2 (minor (Z)), 29.1, 28.5 (minor (Z)), 28.4, 27.0 (minor (Z)), 22.9 (minor (Z)), 22.7, 13.8 (minor (Z)), 13.7. MS (EI) m/z (M^{+}) calcd for $\text{C}_{11}\text{H}_{20}$: 152, found 152. E/Z ratio determined by ^{13}C NMR to 4.9:1

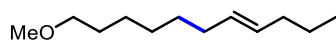


(E)-2-(Undec-8-en-1-yl)isoindoline-1,3-dione (4.03ja). The title compound was prepared according to General Procedure A from 2-(5-bromopentyl)isoindoline-1,3-dione and 1-hexene. The reaction was purified by column chromatography (20% Et_2O in pentane) furnishing **4.03ja** as a colorless oil in 77% yield (69.2 mg). ^1H NMR (400 MHz, Chloroform- d) δ 7.89 – 7.82 (m, 2H), 7.76 – 7.70 (m, 2H), 5.56 – 5.23 (m, 2H), 3.69 (t, J = 7.2 Hz, 2H), 2.05 – 1.92 (m, 4H), 1.72 – 1.65 (m, 2H), 1.42 – 1.31 (m, 8H), 0.89 (t, J = 7.3 Hz, 3H). ^{13}C NMR (101 MHz, Chloroform- d) δ 168.5, 133.8, 132.2, 130.30, 130.28, 129.82 (minor (Z)), 129.80 (minor (Z)), 123.1, 38.1, 34.7, 32.5, 29.6 (minor (Z)), 29.4, 29.3 (minor (Z)), 29.0 (minor (Z)), 28.8 (minor (Z)), 28.7, 28.6, 27.1 (minor (Z)), 26.7, 22.9 (minor (Z)), 22.7, 13.8 (minor (Z)), 13.7. MS (EI) m/z (M^{+}) calcd for $\text{C}_{19}\text{H}_{25}\text{NO}_2$: 299, found 299. E/Z ratio determined by ^{13}C NMR to 4.9:1

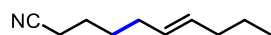


(E)-1-(Non-5-en-1-yl)-3-(trifluoromethyl)benzene (4.03ka). The title compound was prepared according to General Procedure A from 1-(3-bromopropyl)-3-(trifluoromethyl)benzene and 1-hexene. The reaction was purified by column chromatography (pentane) furnishing **4.03ka** as a colorless oil in 86% yield (69.7 mg). ^1H NMR (400 MHz, Chloroform- d) δ 7.50 – 7.33 (m, 4H), 5.49 – 5.35 (m, 2H), 2.74 – 2.64 (m, 2H), 2.12 – 1.95 (m, 4H), 1.66 (ddd, J = 15.5, 8.7, 6.9 Hz, 2H), 1.47 – 1.34 (m, 4H), 0.91 (t, J = 7.3 Hz, 3H). ^{13}C NMR (101 MHz, Chloroform- d) δ 143.63, 143.56 (minor (Z)), 131.79, 131.78, 130.7 (minor (Z)), 130.6, 130.4 (minor (Z)), 130.1 (minor (Z)), 130.0, 129.5 (minor (Z)), 128.6, 125.7 (minor (Z)), 125.0, 123.0 (minor (Z)), 122.5, 35.65 (minor (Z)), 35.62, 34.7, 32.3, 30.8 (minor (Z)), 30.7, 29.32 (minor (Z)), 29.26 (minor (Z)), 29.1,

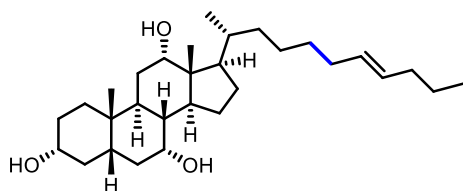
27.0 (minor (Z)), 22.9 (minor (Z)), 22.7, 13.8 (minor (Z)), 13.6. MS (EI) m/z (M^{+}) calcd for $C_{16}H_{21}F_3$: 270, found 270. E/Z ratio determined by ^{13}C NMR to 6.1:1



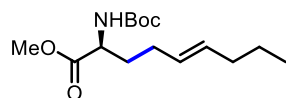
(E)-11-Methoxyundec-4-ene (4.03la). The title compound was prepared according to General Procedure A from 1-bromo-pent-5-ene and 1-hexene. The reaction was purified by column chromatography (10% Et₂O in pentane) furnishing **4.03la** as a colorless oil in 66% yield (36.5 mg). 1H NMR (400 MHz, Chloroform-d) δ 5.40 (m, 2H), 3.38 (t, J = 6.7 Hz, 2H), 3.35 (s, 3H), 2.08 – 1.92 (m, 4H), 1.58 (q, J = 6.8 Hz, 2H), 1.44 – 1.28 (m, 8H), 0.90 (t, J = 7.4 Hz, 3H). ^{13}C NMR (101 MHz, Chloroform-d) δ 130.4, 130.2, 130.0 (minor (Z)), 129.7 (minor (Z)), 72.9, 58.5, 34.7, 32.5, 29.7 (minor (Z)), 29.62, 29.57, 29.3 (minor (Z)), 29.2 (minor (Z)), 29.0, 27.2 (minor (Z)), 26.0, 22.9 (minor (Z)), 22.7, 13.8 (minor (Z)), 13.6. MS (EI) m/z (M^{+}) calcd for $C_{12}H_{24}O$: 184, found 184. E/Z ratio determined by ^{13}C NMR to 6.7:1



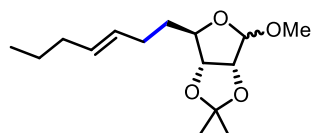
(E)-Dec-6-enenitrile (4.03ma). The title compound was prepared according to General Procedure A from 4-bromo-butyronitrile and 1-hexene. The reaction was purified by column chromatography (5% Et₂O in pentane) furnishing **4.03ma** as a colorless oil in 84% yield (38.1 mg). 1H NMR (400 MHz, Chloroform-d) δ 5.47 – 5.29 (m, 2H), 2.33 (t, J = 7.1 Hz, 2H), 2.11 – 1.92 (m, 4H), 1.70 – 1.61 (m, 2H), 1.56 – 1.47 (m, 2H), 1.41 – 1.31 (m, 2H), 0.88 (t, J = 7.4 Hz, 3H). ^{13}C NMR (101 MHz, Chloroform-d) δ 131.4, 130.9 (minor (Z)), 129.0, 128.4 (minor (Z)), 119.8, 34.6, 31.6, 29.3 (minor (Z)), 28.6 (minor (Z)), 28.4, 26.3 (minor (Z)), 24.9 (minor (Z)), 24.7, 22.8 (minor (Z)), 22.6, 17.1 (minor (Z)), 17.0, 13.8 (minor (Z)), 13.6. MS (EI) m/z (M^{+}) calcd for $C_{10}H_{17}N$: 151, found 151. E/Z ratio determined by ^{13}C NMR to 4.6:1



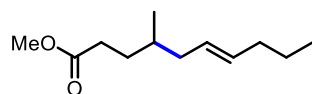
(3R,5S,7R,8R,9S,10S,12S,13R,14S,17R)-10,13-Dimethyl-17-((R,E)-undec-7-en-2-yl)hexadecahydro-1H-cyclopenta[a]phenanthrene-3,7,12-triol (4.03na). The title compound was prepared according to General Procedure A from (3R,5S,7R,8R,9S,10S,12S,13R,14S,17R)-17-((R)-5-bromopentan-2-yl)-10,13-dimethylhexadecahydro-1H-cyclopenta[a]phenanthrene-3,7,12-triol and 1-hexene. The reaction was purified by column chromatography (10-40% acetone in dichloromethane) furnishing **4.03na** as a colorless solid in 49% yield (67.7 mg). 1H NMR (400 MHz, Chloroform-d) δ 5.47 – 5.34 (m, 2H), 4.02 (s, 1H), 3.88 (s, 1H), 3.48 (q, J = 9.8, 8.2 Hz, 1H), 2.23 (ddd, J = 17.2, 10.9, 4.3 Hz, 2H), 2.08 – 1.02 (m, 30H), 0.99 (d, J = 6.6 Hz, 3H), 0.93 – 0.89 (m, 6H), 0.71 (s, 3H). ^{13}C NMR (101 MHz, Chloroform-d) δ 130.5, 130.2, 129.7 (minor (Z)), 73.1, 72.0, 68.4, 47.6, 46.5, 41.9, 41.5, 39.7, 39.6, 35.6, 35.5, 35.2, 34.7, 34.7, 34.5, 32.7, 30.5, 30.1, 28.2, 27.6, 26.6, 25.7, 23.2, 22.8, 22.5, 17.8, 13.7, 12.5. MS (ESI) m/z ($M+NH_4^{+}$) calcd for $C_{30}H_{53}O_3$: 478, found 478. E/Z ratio determined by ^{13}C NMR to 4.9:1



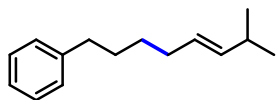
Methyl (S,E)-2-((tert-butoxycarbonyl)amino)non-5-enoate (4.03oa). The title compound was prepared according to General Procedure A from methyl (R)-3-bromo-2-((tert-butoxycarbonyl)amino)propanoate and 1-hexene. The reaction was purified by column chromatography (10% EtOAc in hexane) furnishing **4.03oa** as a brown solid in 69% yield (59.1 mg). ^1H NMR (400 MHz, Chloroform-d) δ 5.42 (m, 2H), 5.11 – 4.94 (m, 1H), 4.32 (m, 1H), 3.75 (s, 3H), 2.17 – 1.93 (m, 4H), 1.87 (p, J = 7.1, 6.4 Hz, 1H), 1.70 (dq, J = 13.8, 7.2, 6.7 Hz, 1H), 1.46 (s, 9H), 1.38 (q, J = 7.3 Hz, 2H), 0.90 (t, J = 7.2 Hz, 3H). ^{13}C NMR (101 MHz, Chloroform-d) δ 173.4, 155.3, 131.8, 131.3 (minor (Z)), 128.3, 127.8 (minor (Z)), 79.8, 53.1, 52.2, 34.6, 32.7 (minor (Z)), 32.6, 29.3 (minor (Z)), 28.4, 28.3, 23.1 (minor (Z)), 22.7 (minor (Z)), 22.6, 13.8 (minor (Z)), 13.6. MS (EI) m/z (M^+) calcd for $\text{C}_{15}\text{H}_{27}\text{NO}_4$: 285, found 285. E/Z ratio determined by ^{13}C NMR to 6.6:1



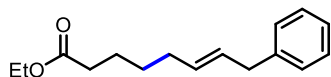
(3aR,4R,6aR)-4-((E)-Hept-3-en-1-yl)-6-methoxy-2,2-dimethyltetrahydrofuro[3,4-d][1,3]dioxole (4.03pa). The title compound was prepared according to General Procedure A from (3aS,4S,6aR)-4-(bromomethyl)-6-methoxy-2,2-dimethyltetrahydrofuro[3,4-d][1,3]dioxole and 1-hexene. The reaction was purified by column chromatography (10% Et₂O in pentane) furnishing **4.03pa** as a colorless oil in 65% yield (52.7 mg). ^1H NMR (400 MHz, Chloroform-d) δ 5.52 – 5.31 (m, 2H), 4.94 (s, 1H), 4.60 (d, J = 6.0 Hz, 1H), 4.53 (d, J = 6.0 Hz, 1H), 4.19 – 4.13 (m, 1H), 3.34 (s, 3H), 2.21 – 1.99 (m, 2H), 1.96 (m, 2H), 1.67 (dtd, J = 14.5, 8.8, 5.8 Hz, 1H), 1.60 – 1.51 (m, 1H), 1.48 (s, 3H), 1.36 (q, J = 7.4 Hz, 2H), 1.31 (s, 3H), 0.88 (t, J = 7.4 Hz, 3H). ^{13}C NMR (101 MHz, Chloroform-d) δ 131.2, 130.7 (minor (Z)), 129.0, 128.4 (minor (Z)), 112.2, 109.4, 86.6, 85.6, 84.2, 54.9, 35.1 (minor (Z)), 35.0, 34.7, 29.25 (minor (Z)), 29.21, 26.5, 25.05 (minor (Z)), 25.01, 24.1 (minor (Z)), 22.8 (minor (Z)), 22.6, 13.8 (minor (Z)), 13.7. MS (EI) m/z (M^+) calcd for $\text{C}_{15}\text{H}_{26}\text{O}_4$: 270, found 270. E/Z ratio determined by ^{13}C NMR to 4.6:1



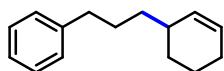
Methyl (E)-4-methyldec-6-enoate (4.03qa). The title compound was prepared according to General Procedure A from methyl 4-bromopentanoate and 1-hexene. The reaction was purified by column chromatography (5% Et₂O in pentane) furnishing **4.03qa** as a colorless oil in 77% yield (45.8 mg). ^1H NMR (400 MHz, Chloroform-d) δ 5.48 – 5.30 (m, 2H), 3.69 (s, 3H), 2.41 – 2.28 (m, 2H), 2.06 – 1.83 (m, 4H), 1.77 – 1.65 (m, 1H), 1.56 – 1.34 (m, 4H), 0.93 – 0.87 (m, 6H). ^{13}C NMR (101 MHz, Chloroform-d) δ 174.5, 132.0, 131.0 (minor (Z)), 128.2, 127.8 (minor (Z)), 51.5, 39.7, 36.6 (minor (Z)), 34.7, 34.2 (minor (Z)), 33.1 (minor (Z)), 32.8, 31.9, 31.6 (minor (Z)), 31.4, 26.9 (minor (Z)), 22.8 (minor (Z)), 22.7, 19.3 (minor (Z)), 19.1, 13.8 (minor (Z)), 13.6. MS (EI) m/z (M^+) calcd for $\text{C}_{12}\text{H}_{22}\text{O}_2$: 198, found 198. E/Z ratio determined by ^{13}C NMR to 6.1:1



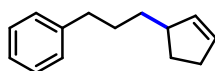
(E)-(7-Methyloct-5-en-1-yl)benzene (4.03ab) The title compound was prepared according to General Procedure A from methyl 1-bromo-3-phenylpropane and 5-methyl-pent-1-ene. The reaction was purified by column chromatography (pentane) furnishing **4.03ab** as a colorless oil in 73% yield (44.2 mg). ^1H NMR (400 MHz, Chloroform- d) δ 7.34 – 7.27 (m, 2H), 7.24 – 7.17 (m, 3H), 5.46 – 5.33 (m, 2H), 2.64 (t, J = 7.8 Hz, 2H), 2.31 – 2.21 (m, 1H), 2.13 – 2.01 (m, 2H), 1.70 – 1.60 (m, 2H), 1.44 (p, J = 7.5 Hz, 2H), 1.00 (d, J = 6.9 Hz, 6H). ^{13}C NMR (101 MHz, Chloroform- d) δ 142.8, 137.8, 137.7 (minor (Z)), 128.4, 128.2, 127.2 (minor (Z)), 126.9, 125.6, 35.9, 32.4, 31.1 (minor (Z)), 31.01, 30.97, 29.6 (minor (Z)), 29.3, 27.1 (minor (Z)), 26.5 (minor (Z)), 23.3 (minor (Z)), 22.7. MS (EI) m/z (M^+) calcd for $\text{C}_{15}\text{H}_{22}$: 202, found 202. E/Z ratio determined by GC-FID to 9.0:1



Ethyl (E)-8-phenyloct-6-enoate (4.03bc). The title compound was prepared according to General Procedure A from methyl ethyl-4-bromobutanoate and 4-phenylbut-1-ene. The reaction was purified by column chromatography (5% Et_2O in pentane) furnishing **4.03bc** as a colorless oil in 64% (47.3 mg). ^1H NMR (400 MHz, Chloroform- d) δ 7.34 – 7.27 (m, 2H), 7.25 – 7.16 (m, 3H), 5.66 – 5.45 (m, 2H), 4.15 (q, J = 7.2 Hz, 2H), 3.42 (d, J = 7.1 Hz, 0.3H, minor (Z)), 3.35 (d, J = 6.4 Hz, 1.7H), 2.32 (t, J = 7.6 Hz, 2H), 2.20 (q, J = 7.3 Hz, 0.3H, minor (Z)), 2.07 (q, J = 7.0 Hz, 1.7H), 1.74 – 1.62 (m, 2H), 1.44 (p, J = 7.6 Hz, 2H), 1.28 (t, J = 7.2 Hz, 3H). ^{13}C NMR (101 MHz, Chloroform- d) δ 173.8, 141.0, 131.4, 130.3 (minor (Z)), 129.2, 128.5, 128.3, 128.2 (minor (Z)), 125.9, 125.6 (minor (Z)), 60.2, 39.0, 35.9 (minor (Z)), 34.2, 33.5 (minor (Z)), 32.1, 29.1 (minor (Z)), 28.9, 26.9 (minor (Z)), 24.7 (minor (Z)), 24.5, 14.3. MS (EI) m/z (M^+) calcd for $\text{C}_{16}\text{H}_{22}\text{O}_2$: 246, found 246. E/Z ratio determined by ^1H NMR to 5.6:1

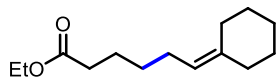


(3-(Cyclohex-2-en-1-yl)propyl)benzene (4.03ad). The title compound was prepared according to General Procedure A from methyl 1-bromo-3-phenylpropane and cyclohexene. The reaction was purified by column chromatography (pentane) furnishing **4.03ad** as a colorless oil in 55% yield (33.3 mg). ^1H NMR (400 MHz, Chloroform- d) δ 7.37 – 7.27 (m, 2H), 7.21 (d, J = 7.3 Hz, 3H), 5.72 – 5.55 (m, 2H), 2.64 (t, J = 7.8 Hz, 2H), 2.15 – 2.06 (m, 1H), 2.02 – 1.96 (m, 2H), 1.85 – 1.66 (m, 4H), 1.54 (m, 1H), 1.47 – 1.19 (m, 3H). ^{13}C NMR (101 MHz, Chloroform- d) δ 142.8, 132.1, 128.4, 128.2, 126.8, 125.6, 36.2, 36.1, 35.1, 29.1, 28.9, 25.4, 21.5. MS (EI) m/z (M^+) calcd for $\text{C}_{15}\text{H}_{20}$: 200, found 200.

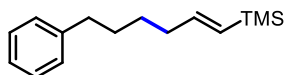


(3-(Cyclopent-2-en-1-yl)propyl)benzene (4.03ae). The title compound was prepared according to General Procedure A from methyl 1-bromo-3-phenylpropane and cyclopentene. The reaction was purified by

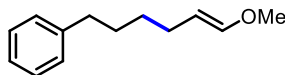
column chromatography (pentane) furnishing **4.03ae** as a colorless oil in 57% yield (32.1 mg). ^1H NMR (400 MHz, Chloroform- d) δ 7.34 – 7.27 (m, 2H), 7.21 (d, J = 7.3 Hz, 3H), 5.72 (m, 2H), 2.74 – 2.61 (m, 3H), 2.42 – 2.23 (m, 2H), 2.06 (dtd, J = 13.0, 8.4, 4.7 Hz, 1H), 1.73 – 1.64 (m, 2H), 1.53 – 1.28 (m, 3H). ^{13}C NMR (101 MHz, Chloroform- d) δ 142.8, 135.1, 130.2, 128.4, 128.2, 125.6, 45.5, 36.2, 35.8, 32.0, 29.9, 29.8. MS (EI) m/z (M^{+}) calcd for $\text{C}_{14}\text{H}_{18}$: 186, found 186.



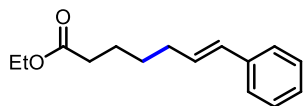
Ethyl 6-cyclohexylidenehexanoate (4.03bf). The title compound was prepared according to General Procedure A from methyl ethyl-4-bromobutanoate and vinylcyclohexane. The reaction was purified by column chromatography (5% Et_2O in pentane) furnishing **4.03bf** as a colorless oil in 80% yield (54.0 mg). ^1H NMR (400 MHz, Chloroform- d) δ 5.07 (td, J = 7.3, 1.4 Hz, 1H), 4.15 (q, J = 7.1 Hz, 2H), 2.31 (t, J = 7.6 Hz, 2H), 2.13 (t, J = 5.9 Hz, 2H), 2.08 (t, J = 5.6 Hz, 2H), 2.02 (q, J = 7.4 Hz, 2H), 1.65 (p, J = 7.5 Hz, 2H), 1.58 – 1.47 (m, 6H), 1.37 (p, J = 7.5 Hz, 2H), 1.30 – 1.25 (m, 3H). ^{13}C NMR (101 MHz, Chloroform- d) δ 173.9, 140.0, 120.8, 60.2, 37.2, 34.3, 29.6, 28.7, 27.8, 27.0, 26.6, 24.6, 14.3. MS (EI) m/z (M^{+}) calcd for $\text{C}_{14}\text{H}_{24}\text{O}_2$: 225, found 225.



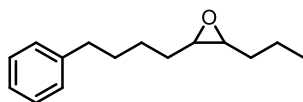
(E)-Trimethyl(6-phenylhex-1-en-1-yl)silane (4.03ag). The title compound was prepared according to General Procedure A from methyl 1-bromo-3-phenylpropane and allyltrimethylsilane. The reaction was purified by column chromatography (pentane) furnishing **4.03ag** as a colorless oil in 63% yield (43.8 mg). ^1H NMR (400 MHz, Chloroform- d) δ 7.20 – 7.14 (m, 2H), 7.10 – 7.05 (m, 3H), 5.90 (dt, J = 18.5, 6.2 Hz, 1H), 5.51 (dq, J = 18.5, 1.3 Hz, 1H), 2.51 (t, J = 7.7 Hz, 2H), 2.07 – 1.98 (m, 2H), 1.52 (tt, J = 9.2, 6.7 Hz, 2H), 1.34 (p, J = 7.5 Hz, 2H), -0.07 (s, 9H). ^{13}C NMR (101 MHz, Chloroform- d) δ 147.0, 142.7, 129.8, 128.4, 128.2, 125.6, 36.6, 35.8, 31.0, 28.3, -1.1. MS (EI) m/z (M^{+}) calcd for $\text{C}_{15}\text{H}_{24}\text{Si}$: 232, found 232. E/Z ratio determined by ^1H NMR to 20:1



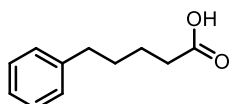
(E)-(6-Methoxyhex-5-en-1-yl)benzene (4.03ah) The title compound was prepared according to General Procedure A from methyl 1-bromo-3-phenylpropane and allyl methyl ether. The reaction was purified by column chromatography (10% Et_2O in pentane) furnishing **4.03ah** as a colorless oil in 69% yield (39.3 mg). ^1H NMR (400 MHz, Chloroform- d) δ 7.33 – 7.27 (m, 2H), 7.23 – 7.17 (m, 3H), 6.30 (dd, J = 12.6, 1.2 Hz, 0.84H), 5.90 (dq, J = 6.4, 1.3 Hz, 0.16H, minor (Z)), 4.74 (dt, J = 12.6, 7.3 Hz, 0.84H), 4.35 (q, J = 7.0 Hz, 0.16H, minor (Z)), 3.60 (s, 0.48H, minor (Z)), 3.52 (s, 2.52H), 2.63 (t, J = 7.7 Hz, 2H), 2.12 (qd, J = 7.4, 1.3 Hz, 0.32H, minor (Z)), 1.98 (q, J = 7.3 Hz, 1.68H), 1.65 (p, J = 7.6 Hz, 2H), 1.41 (p, J = 7.4 Hz, 2H). ^{13}C NMR (101 MHz, Chloroform- d) δ 147.1, 146.1 (minor (Z)), 142.7, 128.4, 128.2, 125.6 (minor (Z)), 125.5, 106.8 (minor (Z)), 102.9, 59.5 (minor (Z)), 55.9, 35.8, 31.1 (minor (Z)), 30.8, 30.4, 29.4 (minor (Z)), 27.6, 23.6 (minor (Z)). MS (EI) m/z (M^{+}) calcd for $\text{C}_{13}\text{H}_{18}\text{O}$: 190, found 190. E/Z ratio determined by ^1H NMR to 5.3:1



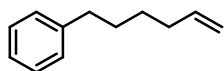
Ethyl (E)-7-phenylhept-6-enoate (4.03bi). The title compound was prepared according to General Procedure A, with the reaction time extended to 42 hours, from methyl ethyl-4-bromobutanoate and allylbenzene. The reaction was purified by column chromatography (5% Et₂O in pentane) furnishing **4.03bi** as a colorless oil in 56% yield (39.0 mg). ¹H NMR (400 MHz, Chloroform-d) δ 7.38 – 7.17 (m, 5H), 6.48 – 6.38 (m, 1H, (E & Z)), 6.23 (dt, *J* = 15.8, 6.9 Hz, 0.5H, (Z)), 5.67 (dt, *J* = 11.6, 7.2 Hz, 0.5H, (E)), 4.18 – 4.10 (m, 2H), 2.42 – 2.20 (m, 4H), 1.70 (m, 2H), 1.53 (m, 2H), 1.28 (m, 3H). ¹³C NMR (101 MHz, Chloroform-d) δ 173.70, 173.66, 137.6, 132.4, 130.4, 130.2, 129.2, 128.7, 128.5, 128.1, 126.9, 126.5, 125.9, 60.24, 60.22, 34.23, 34.20, 32.6, 29.4, 28.8, 28.2, 24.6, 24.5, 14.3. MS (EI) *m/z* (M⁺) calcd for C₁₅H₂₀O₂: 232, found 232. E/Z ratio determined by ¹H NMR to 1:1



2-(4-Phenylbutyl)-3-propyloxirane (4.08). To a 4 mL vial containing a stir bar, **4.01aa** (30.3 mg, 0.15 mmol; 1.0 equiv) and dichloromethane (2.0 mL) was added *meta*-chloroperoxybenzoic acid (51.8 mg, 0.30 mmol; 2.0 equiv). The reaction was stirred for 18 hours at room temperature. After 18 hours, the reaction was concentrated and purified by column chromatography (5% Et₂O in pentane) furnishing **4.08** as a colorless oil in 95% yield (31.1 mg). ¹H NMR (400 MHz, Chloroform-d) δ 7.29 (d, *J* = 7.3 Hz, 2H), 7.20 (d, *J* = 7.3 Hz, 3H), 2.94 (d, *J* = 4.8 Hz, 0.3H, minor (Z)), 2.74 – 2.60 (m, 3.7H), 1.70 (p, *J* = 8.4, 7.7 Hz, 2H), 1.61 – 1.41 (m, 8H), 1.07 – 0.89 (m, *J* = 7.1 Hz, 3H). ¹³C NMR (101 MHz, Chloroform-d) δ 142.4, 128.4, 128.3, 125.7, 58.7, 57.0, 35.9, 34.2, 32.0, 31.3, 29.9 (minor (Z)), 27.7 (minor (Z)), 26.3 (minor (Z)), 25.7, 19.9 (minor (Z)), 19.4, 14.1 (minor (Z)), 14.0. MS (EI) *m/z* (M⁺) calcd for C₁₅H₂₂O: 218, found 218. E/Z ratio determined by GC-FID to 6.1:1



5-Phenylpentanoic acid (4.09). To a 4 mL vial containing a stir bar, **4.01aa** (30.3 mg, 0.150 mmol; 1.00 equiv), acetonitrile (0.6 mL), tetrachloromethane (0.6 mL) and water (0.9 mL) was added RuCl₃ (3.10 mg, 0.0150 mmol; 10.0 mol%) and NaIO₄ (144 mg, 0.600 mmol, 4.50 equiv), respectively. The slurry was stirred for 24 hours at room temperature. After 24 hours, water (2.5 mL) was added and the mixture was extracted with dichloromethane (3x 2.5 mL), the combined organic phases were washed with brine (2.5 mL), concentrated and passed through a short silica plug (EtOAc). The solution was concentrated and sat. Na₂CO₃ (1.5 mL, aq.) was added, the solution was washed with Et₂O (2x 1.5 mL) and then acidified with HCl (37% aq.) before extracting the solution with Et₂O (3x 1.5 mL). The combined organic phases were concentrated to dryness to furnish **4.09** as colorless crystals in 63% yield (16.8 mg). ¹H NMR (400 MHz, Chloroform-d) δ 7.44 – 7.37 (m, 2H), 7.34 – 7.27 (m, 3H), 2.80 – 2.73 (m, 2H), 2.53 – 2.48 (m, 2H), 1.86 – 1.78 (m, 4H). ¹³C NMR (101 MHz, Chloroform-d) δ 179.6, 142.0, 128.4, 128.3, 125.8, 35.5, 33.8, 30.8, 24.3. MS (EI) *m/z* (M⁺) calcd for C₁₁H₁₄O₂: 178, found 178.



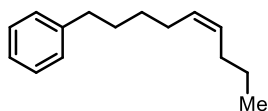
Hex-5-en-1-ylbenzene (4.10). To a 4 mL vial containing a stir bar, **4.03ae** (23.2 mg, 0.100 mmol; 1.00 equiv) and acetonitrile (0.5 mL) was added TsOH·H₂O (38.0 mg, 0.200 mmol; 2.00 equiv). The reaction was stirred for 18 hours at room temperature. After 18 hours, the reaction was directly purified by column chromatography (pentane) to give **4.10** as a colorless oil in 96% yield (15.4 mg). ¹H NMR (400 MHz, Chloroform-d) δ 7.36 – 7.25 (m, 2H), 7.24 – 7.16 (m, 3H), 5.84 (ddt, *J* = 16.9, 10.2, 6.7 Hz, 1H), 5.08 – 4.92 (m, 2H), 2.65 (t, *J* = 7.7 Hz, 2H), 2.12 (q, *J* = 7.1, 6.6 Hz, 2H), 1.67 (p, *J* = 7.4 Hz, 2H), 1.47 (p, *J* = 7.5 Hz, 2H). ¹³C NMR (101 MHz, Chloroform-d) δ 142.7, 138.9, 128.4, 128.3, 125.6, 114.4, 35.8, 33.7, 31.0, 28.6. MS (EI) *m/z* (*M*⁺) calcd for C₁₂H₁₆: 160, found 160.

Time Study.

A standard reaction according to General Procedure A with **4.01a** and **4.02a** was prepared. From this reaction 50 μL aliquots was taken out with a Hamilton syringe after 1, 2, 3, 4, 6 and 8 hours. To each aliquot was added 1 equiv of standard (1,3,5 trimethoxybenzene, 100 μL from a stock solution (0.067 mmol/mL)) and analyzed by GC-MS.

Quenching-Experiments

A Hellma® fluorescence cuvette containing a solution of **Ir-1** in 2.7 × 10⁻⁵ M in DMA:PhH (1:1) was capped with a Teflon cap and parafilm before flushing with N₂. The sample was excited at 425 nm and emission monitored at 477 nm. Appropriate amount of quencher in DMA:PhH(1:1) was added via a Hamilton syringe (5 μL pr. 25 equiv for **4.01a** and LiBr, **4.02a** was added neat), and measurements were continued until a stable measurements were obtained.



(Z)-non-5-en-1-ylbenzene (4.03aa-(Z)). An oven dried 100 mL round-bottom flask was charged with butyltriphenylphonium bromide (700 mg, 1.75 mmol; 1.0 equiv) and cooled to room temperature under vacuum. Subsequently, the flask was filled with nitrogen and THF (anhydrous; 15 mL); the slurry was then cooled to -25 °C and *n*-BuLi (1.75 mmol, 0.7 mL (2.5 M in hexanes); 1.0 equiv) was added dropwise. The reaction was stirred for 30 minutes at -25 °C then the cooling bath was removed and the solution was stirred for another 30 minutes. Then, the solution was cooled to -78 °C and 5-phenylpentanal (324 mg, 2.00 mmol, 1.2 equiv) was added dropwise, the solution was left to stir over night. Acetone (2 mL) was added, and the reaction was stirred for 10 minutes before filtering over celite with the aid of hexane. The mixture was concentrated before diluting with hexane (100 mL) and washing with brine (2x 100 mL), the organic phase was dried over MgSO₄, concentrated and purified by column chromatography (pentane) affording **4.03aa-(Z)** as a colorless oil in 30% yield (100 mg). ¹H NMR (400 MHz, Chloroform-d) δ 7.35 – 7.27 (m, 2H), 7.24 – 7.17 (m, 3H), 5.49 – 5.36 (m, 2H), 2.64 (t, *J* = 7.7 Hz, 2H), 2.14 – 1.95 (m, 4H), 1.72 – 1.60 (m, 2H), 1.48 – 1.35 (m, 4H), 0.92 (t, *J* = 7.3 Hz, 3H). ¹³C NMR (101 MHz, Chloroform-d) δ 142.8, 130.4, 130.2, 129.9, 129.8, 128.4 (minor (*E*)), 128.2 (minor (*E*)), 125.6, 35.9, 34.7 (minor (*E*)), 32.5 (minor (*E*)),

31.1, 31.0 (minor (*E*)), 29.4, 29.33, 29.30 (minor (*E*)), 27.1, 22.9, 22.7 (minor (*E*)), 13.7 (minor (*E*)). MS (EI) *m/z* (M^{+}) calcd for $C_{15}H_{22}$: 202, found 202.

4.8. References

- [1] F. H. Burstall, *J. Chem. Soc.* **1936**, 173–175.
- [2] A. J. Bard, M. A. Fox, *Acc. Chem. Res.* **1995**, *28*, 141–145.
- [3] B. O'Regan, M. Grätzel, *Nature* **1991**, *353*, 737–740.
- [4] H. B. Gray, A. W. Maverick, *Science* **1981**, *214*, 1201–1205.
- [5] J. J. Douglas, J. D. Nguyen, K. P. Cole, C. R. J. Stephenson, *Aldrichimica Acta* **2014**, *47*.
- [6] D. A. Nicewicz, D. W. C. MacMillan, *Science* **2008**, *322*, 77–80.
- [7] Z. Zuo, D. T. Ahneman, L. Chu, J. A. Terrett, A. G. Doyle, D. W. C. MacMillan, *Science* **2014**, *345*, 437–440.
- [8] M. H. Shaw, V. W. Shurtleff, J. A. Terrett, J. D. Cuthbertson, D. W. C. MacMillan, *Science* **2016**, *352*, 1304–1308.
- [9] D. R. Heitz, J. C. Tellis, G. A. Molander, *J. Am. Chem. Soc.* **2016**, *138*, 12715–12718.
- [10] B. J. Shields, A. G. Doyle, *J. Am. Chem. Soc.* **2016**, *138*, 12719–12722.
- [11] D. T. Ahneman, A. G. Doyle, *Chem. Sci.* **2016**, *7*, 7002–7006.
- [12] C. Le, Y. Liang, R. W. Evans, X. Li, D. W. C. MacMillan, *Nature* **2017**, *547*, 79–83.
- [13] Y. Shen, Y. Gu, R. Martin, *J. Am. Chem. Soc.* **2018**, *140*, 12200–12209.
- [14] L. Zhang, X. Si, Y. Yang, M. Zimmer, S. Witzel, K. Sekine, M. Rudolph, A. S. K. Hashmi, *Angew. Chem., Int. Ed.* **2019**, *58*, 1823–1827.
- [15] M. S. Santos, A. G. Corrêa, M. W. Paixão, B. König, *Adv. Synth. Catal.* **2020**, *362*, 2367–2372.
- [16] N. Ishida, Y. Masuda, N. Ishikawa, M. Murakami, *Asian J. Org. Chem.* **2017**, *6*, 669–672.
- [17] X. Cheng, H. Lu, Z. Lu, *Nat. Commun.* **2019**, *10*, 3549.
- [18] J. D. Cuthbertson, D. W. C. MacMillan, *Nature* **2015**, *519*, 74–77.
- [19] L. Huang, M. Rueping, *Angew. Chem., Int. Ed.* **2018**, *57*, 10333–10337.
- [20] R. Matsubara, T. F. Jamison, *J. Am. Chem. Soc.* **2010**, *132*, 6880–6881.
- [21] H. D. Srinivas, Q. Zhou, M. P. Watson, *Org. Lett.* **2014**, *16*, 3596–3599.
- [22] “Merck,” can be found under <https://www.sigmaaldrich.com/DK/en>, (accessed 15/07/2021).
- [23] S. L. Khursan, *React. Kinet. Catal. Lett.* **1997**, *61*, 91–95.
- [24] D. A. Nicewicz, D. S. Hamilton, *Synlett* **2014**, *25*, 1191–1196.
- [25] A. A. Isse, C. Y. Lin, M. L. Coote, A. Gennaro, *J. Phys. Chem. B* **2011**, *115*, 678–684.

- [26] N. D. Schley, G. C. Fu, *J. Am. Chem. Soc.* **2014**, *136*, 16588–16593.
- [27] J. Hou, W.-H. Sun, S. Zhang, H. Ma, Y. Deng, X. Lu, *Organometallics* **2006**, *25*, 236–244.
- [28] L. Troian-Gautier, M. D. Turlington, S. A. M. Wehlin, A. B. Maurer, M. D. Brady, W. B. Swords, G. J. Meyer, *Chem. Rev.* **2019**, *119*, 4628–4683.
- [29] J. F. Hartwig, “Chapter 7 Oxidative Addition of Polar Reagents” *Organotransition Metal Chemistry: From Bonding to Catalysis*, University Science Books, **2009**.
- [30] H. E. Gottlieb, V. Kotlyar, A. Nudelman, *J. Org. Chem.* **1997**, *62*, 7512–7515.

5) *Final Remarks*

In chapter two, a chiral nickel complex was incorporated into a POP. The POP, NiL1₂-POP, proved highly active and enantioselective in the asymmetric Michael addition of malonates to aliphatic nitroalkenes. For the first time it was demonstrated that various functional groups can be tolerated in the reaction. The POP was easily recycled and could even be applied in a continuous flow setup. Additionally, a novel tandem reaction, both steps catalyzed by NiL1₂-POP, was discovered.

In chapter three, a benzylic C-H alkynylation protocol was disclosed. The reaction represented the first direct coupling of alkynyl boronic esters and 1-alkyl naphthalenes. The reaction is catalyzed by copper, it proceeds under benign conditions and the C-H substrate is used as limiting reagent. Additionally, enantioenriched products were obtained when using chiral ligands.

In chapter four, a direct allylic C-H alkylation protocol was presented. By merging nickel- and photoredox-catalysis the direct allylic C-H alkylation between alkyl bromides and terminal olefins was achieved. The protocol proceeds under benign conditions and exclusively provides the linear product. The protocol was robust towards a multitude of functional groups and could even be extended to secondary alkyl bromides. The methodology represents the first direct allylic C-H alkylation using terminal olefins and alkyl bromides.

In summary, the first project demonstrates that homogeneous organometallic catalysts can be upgraded to heterogeneous catalysts without compromising activity or selectivity by incorporating them into polystyrene-based POPs. In the last two projects we have developed new C-C forging methods, in both cases a C(sp³)-H bond is directly turned into a C(sp³)-C(sp) or C(sp³)-C(sp³) bond respectively under benign conditions. These two projects illustrate the potential of earth-abundant transition metals in new C-C forming reactions.

6) Appendix

6.1 Publications

Publications relevant for this thesis:

- **M. B. Buendia**, S. Kegnæs, S. Kramer, *Adv. Synth. Catal.* **2020**, 362, 5506.
- **M. B. Buendia**, J.-G. J. Balin, M. E. Andersen, Z. Lian, S. Kramer, *Synlett* **2021**, 32, A-E.

Other publications:

- **M. B. Buendia**, A. E. Dugaard, A. Riisager, *Catal. Letters* **2021**, 151, 8–16.
- J. Himmelstrup, **M. B. Buendia**, X.-W. Sun, S. Kramer, *Chem. Commun.* **2019**, 55, 12988–12991.

6.2 Co-Author statements

Declaration of co-authorship at DTU

If a PhD thesis contains articles (i.e. published journal and conference articles, unpublished manuscripts, chapters, etc.) written in collaboration with other researchers, a co-author statement verifying the PhD student's contribution to each article should be made.

If an article is written in collaboration with three or less researchers (including the PhD student), all researchers must sign the statement. However, if an article has more than three authors the statement may be signed by a representative sample, cf. article 12, section 4 and 5 of the Ministerial Order No. 1039, 27 August 2013. A representative sample consists of minimum three authors, which is comprised of the first author, the corresponding author, the senior author, and 1-2 authors (preferably international/non-supervisor authors).

DTU has implemented the Danish Code of Conduct for Research Integrity, which states the following regarding attribution of authorship:

"Attribution of authorship should in general be based on criteria a-d adopted from the Vancouver guidelines¹, and all individuals who meet these criteria should be recognized as authors:




- a. Substantial contributions to the conception or design of the work, or the acquisition, analysis, or interpretation of data for the work, *and*
- b. drafting the work or revising it critically for important intellectual content, *and*
- c. final approval of the version to be published, *and*
- d. agreement to be accountable for all aspects of the work in ensuring that questions related to the accuracy or integrity of any part of the work are appropriately investigated and resolved."²

For more information regarding definition of co-authorship and examples of authorship conflicts, we refer to DTU Code of Conduct for Research Integrity (pp. 19-22).

¹ International Committee of Medical Journal Editors – Recommendations for the Conduct, Reporting, Editing, and Publication of Scholarly Work in Medical Journals, updated December 2016

² DTU Code of Conduct for Research Integrity (E-book p. 19)

Title of article		
A Nickel-Bisdiamine Porous Organic Polymer as Heterogeneous Chiral Catalyst for Asymmetric Michael Addition to Aliphatic Nitroalkenes		
Journal/conference		
Advanced Synthesis and Catalysis		
Author(s)		
Mikkel B. Buendia, Søren Kegnæs & Søren Kramer		
Name (capital letters) and signature of PhD student		
MIKKEL BURGGRAAF BUENDIA		
PhD student's date of birth		
30/07/1993		
Declaration of the PhD student's contribution		
<i>For each category in the table below, please specify the PhD student's contribution to the article as appropriate (please do not fill in with names or x's)</i>		
Category	Minor contribution to the work <i>(please specify the nature of the PhD student's contribution)</i>	Substantial contribution to the work <i>(please specify the nature of the PhD student's contribution)</i>
Formulation of the conceptual framework and/or planning of the design of the study including scientific questions		Contributed with relevant scientific input throughout the project and discussed the direction of the project with the other authors
Carrying out of experiments/data collection and analysis/interpretation of results		Carried out all of the experimental work
Writing of the article/revising the manuscript for intellectual content		Wrote the initial draft of the manuscript with a majority of the figures, schemes and tables. Contributed continuously with input and helped during revision of the draft
Signatures		

Date	Name	Title	Signature
10/07/2021	Mikkel Burggraaf Buendia	PhD Student	
12/07/2021	Søren Kegnæs	Professor	
12/07/2021	Søren Kramer	Assistant Professor	

By signing this declaration, co-authors permit the PhD student to reuse whole or parts of co-authored articles in their PhD thesis, under the condition that co-authors are acknowledged in connection with the reused text or figure.

It is **important** to note that it is the responsibility of the PhD student to obtain permission from the publisher to use the article in the PhD thesis³

Please note that by signing this declaration, co-authors permit the PhD student to reuse whole or parts of co-authored articles in their PhD thesis, under the condition that co-authors are acknowledged in connection with the reused text or figure.

³ Many journals will allow you to use only the post-print version of your article, meaning the accepted version of the article, without the publisher's final formatting. In the event that your article is submitted, but still under review, you should of course use the latest submitted version of your article in your thesis. Always remember to check your publisher's guidelines on reuse of published articles. Most journals, unless open access, have an embargo period on published articles, meaning that within this period you cannot freely use the article. Check your publisher's rules on this issue

Declaration of co-authorship at DTU

If a PhD thesis contains articles (i.e. published journal and conference articles, unpublished manuscripts, chapters, etc.) written in collaboration with other researchers, a co-author statement verifying the PhD student's contribution to each article should be made.

If an article is written in collaboration with three or less researchers (including the PhD student), all researchers must sign the statement. However, if an article has more than three authors the statement may be signed by a representative sample, cf. article 12, section 4 and 5 of the Ministerial Order No. 1039, 27 August 2013. A representative sample consists of minimum three authors, which is comprised of the first author, the corresponding author, the senior author, and 1-2 authors (preferably international/non-supervisor authors).

DTU has implemented the Danish Code of Conduct for Research Integrity, which states the following regarding attribution of authorship:

"Attribution of authorship should in general be based on criteria a-d adopted from the Vancouver guidelines⁴, and all individuals who meet these criteria should be recognized as authors:

- a. Substantial contributions to the conception or design of the work, or the acquisition, analysis, or interpretation of data for the work, *and*
- b. drafting the work or revising it critically for important intellectual content, *and*
- c. final approval of the version to be published, *and*
- d. agreement to be accountable for all aspects of the work in ensuring that questions related to the accuracy or integrity of any part of the work are appropriately investigated and resolved."⁵




For more information regarding definition of co-authorship and examples of authorship conflicts, we refer to DTU Code of Conduct for Research Integrity (pp. 19-22).

By signing this declaration, co-authors permit the PhD student to reuse whole or parts of co-authored articles in their PhD thesis, under the condition that co-authors are acknowledged in connection with the reused text or figure.

⁴ International Committee of Medical Journal Editors – Recommendations for the Conduct, Reporting, Editing, and Publication of Scholarly Work in Medical Journals, updated December 2016

⁵ DTU Code of Conduct for Research Integrity (E-book p. 19)

Title of article		
Copper-Catalyzed Alkynylation of Benzylic C–H Bonds with Alkynylboronic Esters		
Journal/conference		
Synlett		
Author(s)		
Mikkel B. Buendia, Jan-Georges J. Balin, Mette E. Andersen, Zhong Lian & Søren Kramer		
Name (capital letters) and signature of PhD student		
MIKKEL BURGGRAAF BUENDIA		
PhD student's date of birth		
30/07/93		
Declaration of the PhD student's contribution		
For each category in the table below, please specify the PhD student's contribution to the article as appropriate (please do not fill in with names or x's)		
Category	Minor contribution to the work (please specify the nature of the PhD student's contribution)	Substantial contribution to the work (please specify the nature of the PhD student's contribution)
Formulation of the conceptual framework and/or planning of the design of the study including scientific questions		Contributed with relevant scientific input throughout the project and discussed the direction of the project with the other authors
Carrying out of experiments/data collection and analysis/interpretation of results		Carried out synthesis of most substrates (or designed synthesis route) and carried out some catalytic reactions
Writing of the article/revising the manuscript for intellectual content	Contributed continuously with input and helped during revision of the draft	
Signatures		

Date	Name	Title	Signature
10/07/2021	Mikkel B. Buendia	PhD student	
12/07/2021	Søren Kramer	Assistant Professor	
12/07/21	Zhong Lian	Professor	

It is **important** to note that it is the responsibility of the PhD student to obtain permission from the publisher to use the article in the PhD thesis⁶

Please note that by signing this declaration, co-authors permit the PhD student to reuse whole or parts of co-authored articles in their PhD thesis, under the condition that co-authors are acknowledged in connection with the reused text or figure.

⁶ Many journals will allow you to use only the post-print version of your article, meaning the accepted version of the article, without the publisher's final formatting. In the event that your article is submitted, but still under review, you should of course use the latest submitted version of your article in your thesis. Always remember to check your publisher's guidelines on reuse of published articles. Most journals, unless open access, have an embargo period on published articles, meaning that within this period you cannot freely use the article. Check your publisher's rules on this issue.